UNIVERSIDAD NACIONAL DE INGENIERÍA

FACULTAD DE INGENIERIA MECÁNICA

TESIS

UNCERTAINTY QUANTIFICATION IN STRUCTURAL RESPONSES OF OFFSHORE MONOPILE WIND TURBINES

PARA OBTENER EL GRADO ACADÉMICO DE DOCTOR EN CIENCIAS CON MENCIÓN EN ENERGÉTICA

ELABORADO POR:

DAVID BARRETO LARA

ASESORES:

ARTURO JESÚS ORTEGA MALCA, PhD

MADJID KARIMIRAD, PhD

LIMA-PERU

2020

DEDICATORY

Dedicated to my mother and sister, Sonia and Dayhana, for their unconditional support throughout these years, and for being the fundamental supports in my academic and personal life, and in all that I am.

Also, I would like to dedicate this thesis to all those who supported me, in diverse ways, to achieve this personal goal.

ACKNOWLEDGEMENTS

I want to express my gratitude to the people and institutions that supported and guided me throughout this long process. First of all, I would like to thank **CONCYTEC** (Consejo Nacional de Ciencia, Tecnología e Innovación Tecnológica), which through its executing unit: **FONDECYT** (Fondo Nacional de Desarrollo Científico, Tecnológico y de Innovación Tecnológica) financed my doctoral research. I am also grateful for the funding received under contract reference number 174/2019 to perform a worthwhile research internship at Queen's University Belfast (QUB) which was very important for the achievement of this thesis.

I would also like to acknowledge my external advisor, **Dr Madjid Karimirad,** Senior Lecturer at Queen's University Belfast (United Kingdom), who has always provided helpful comments on my work and has guided me within the field of structural reliability of offshore wind turbines, as well as for hosting me at his institution to perform a valuable internship. Similarly, I also want to recognize the valuable contribution of my local advisor, **Dr Arturo Ortega**, Research Associate at The University of Edinburgh (United Kingdom), who accompanied and guided me during all these years of development of this thesis. I want to thank him for his valuable and useful advice and his encouragement in academic and personal aspects.

I want to especially acknowledge **Dr Jaime Luyo** and **Mrs Laura Parillo** for their continuous support during the development of the doctoral program, as well as their collaboration in the administrative affairs at UNI. Likewise, I would like to make a special recognition to **Dr Alberto Coronado**, who introduced me to the "Python" programming language and gave me his support in terms of computational resources for the simulations used for the development of chapter 2. I also want to acknowledge the High-Performance Computing (HPC) team of Queen's University Belfast for their support regarding resources and training in the use of their HPC cluster system.

Finally, I would like to thank my family, my doctoral colleagues, and everyone who has given me any kind of help during the development of this thesis.

TABLE OF CONTENTS

LIST OF FIGURES

LIST OF TABLES

RESUMEN

A nivel mundial existe un gran interés en la transición hacia fuentes de energías renovables. Esto es motivado por diversos factores como por ejemplo el calentamiento global, la inestabilidad de los precios del petróleo, la diversificación de la matriz energética, entre otros. En este escenario, la energía eólica juega un papel importante debido a su prometedor desempeño en comparación con las plantas de energía convencionales. Asimismo, existe un interés relativamente reciente en la explotación de los recursos eólicos en las zonas offshore. Aunque el costo de la generación de electricidad a partir de este tipo de energía ha ido disminuyendo gradualmente, en algunos casos sigue siendo comercialmente no competitivo con respecto a otras fuentes de energía.

Uno de los problemas relacionados con los altos costos de la energía eólica es la presencia de incertidumbres que afectan al proceso de diseño. Esto lleva a un exceso de conservadurismo, altos factores de seguridad y exceso de material en los diseños. Por lo tanto, la comprensión del impacto que estas incertidumbres pueden tener en las cargas/respuestas que rigen el diseño de las turbinas eólicas marítimas es crucial. Los proyectos de energía eólica offshore se basan principalmente en simulaciones por computadora que se alimentan de datos de campo. Sin embargo, estos modelos numéricos no son completamente ajustados a la realidad y los datos fiables no siempre están disponibles.

En la industria offshore, las condiciones ambientales, que están representadas por un gran número de parámetros, son aspectos muy importantes a tener en cuenta. Mientras que algunas de ellas se tratan como valores estocásticos, otras se consideran determinísticas y, por lo tanto, la existencia de incertidumbres en sus valores medidos/estimados es inevitable. Por otra parte, los modelos matemáticos que representan los fenómenos físicos son a menudo simplificados con el fin de atenuar los altos costos computacionales. Una situación que al mismo tiempo introduce nuevas fuentes de incertidumbre. Finalmente, el propio tratamiento estadístico de las condiciones estocásticas en el diseño estructural genera su correspondiente nivel de incertidumbre con respecto a las inferencias realizadas a partir de los datos de entrada.

En la presente investigación se exploran los efectos de los tres principales tipos de incertidumbre considerados en el ámbito del análisis de la confiabilidad de los sistemas estructurales: física, estadística y de modelo. Se estudian los efectos de la incertidumbre en los parámetros de las olas, la incertidumbre en el coeficiente de cizallamiento, la influencia de la duración de la simulación y los efectos de la flexibilidad del suelo en las respuestas dinámicas de una turbina eólica offshore monopilar.

Los resultados muestran que las respuestas dinámicas extremas en la base del monopilar están influenciadas por las variaciones de los parámetros de la ola y pueden modelarse mediante relaciones lineales y cuadráticas. También se descubrió que las respuestas extremas a largo plazo tienen baja sensibilidad a la incertidumbre del cizallamiento del viento. Por último, se observó que la duración de las simulaciones afecta moderadamente a las cargas extremas a largo plazo. También se encontró que la flexibilidad del suelo tiene un impacto limitado en las respuestas dinámicas.

Palabras Claves: Energía eólica, turbina eólica, tecnología offshore, confiabilidad estructural, cuantificación de incertidumbre

ABSTRACT

Worldwide there is a high interest in the transition to renewable energy sources. It is motivated by diverse concerns such as global warming, oil price volatility, diversification of the energy matrix, among others. In this scenario, wind energy plays an important role due to its promising performance compared to conventional power plants. There is also a relatively recent interest in exploiting wind resources in offshore areas. Although the cost of electricity generation from this type of energy has been gradually decreasing, in some cases it remains commercially uncompetitive concerning other energy sources.

One of the problems related to the high costs of wind energy is the presence of uncertainties that affect the design process. This leads to over-conservatism, high safety factors and excess of material in the designs. Therefore, the understanding of the impact that these uncertainties can have on the loads/responses that govern the design of offshore wind turbines is crucial. Offshore wind energy projects are mainly based on computer simulations that are fed by field data. However, the numerical models are not completely accurate and reliable data is not always available.

In the offshore industry, the environmental conditions, which are represented by a large number of parameters, are very important aspects to take into account. Whereas some of them are treated as stochastic values, some others are considered deterministic, and therefore the existence of uncertainties in their measured/estimated values is inevitable. On the other hand, mathematical models representing physical phenomena are often simplified to mitigate high computational costs. A situation that, at the same time, introduces new sources of uncertainty. Finally, the own statistical treatment of the stochastic conditions in the structural design generates its corresponding level of uncertainty due to the inferences made from the input data.

The present research explores the effects of the three main types of uncertainty considered in the field of reliability analysis of structural systems: physical, statistical and model. The effects of uncertainty in the wave parameters, uncertainty in the shear coefficient, the influence of the simulation length, and

effects of soil flexibility on the dynamic responses of a monopile offshore wind turbine are investigated.

The results show that the extreme dynamic responses at the base of the monopile are affected by variations in the wave parameters and they can be modelled by linear and quadratic relationships. It was also found that long-term extreme responses have low sensitivity to wind shear uncertainty. Finally, it was observed that the simulation length moderately affects long-term extreme loads. Also, it was found that soil flexibility has limited impact on the dynamic responses.

Keywords: Wind energy, wind turbine, offshore technology, structural reliability, uncertainty quantification.

CHAPTER I. METHODOLOGICAL ASPECTS OF THE RESEARCH

1.1 INTRODUCTION

In the last few decades, concern about environmental degradation due to global warming has grown significantly. Since carbon dioxide (CO_2) is one of the main greenhouse gas emissions, many governments have committed to migrating from a fossil fuel-based energy matrix to a renewable energy scheme. Therefore, the development of renewable energy technologies has received a great stimulus and now plays a key role in the fight against the effects of global warming. Among all the types of renewable energy sources, the one that attracts special interest is wind energy, with wind turbines as the most developed technology to exploit this resource. Today, there is a total installed capacity of 650 GW, with 60 GW installed in 2019 [1]. The Asia Pacific region concentrates 50.7% of these new installations, and particularly five nations dominate 70% of the wind energy market, see **Fig. 1.1**.

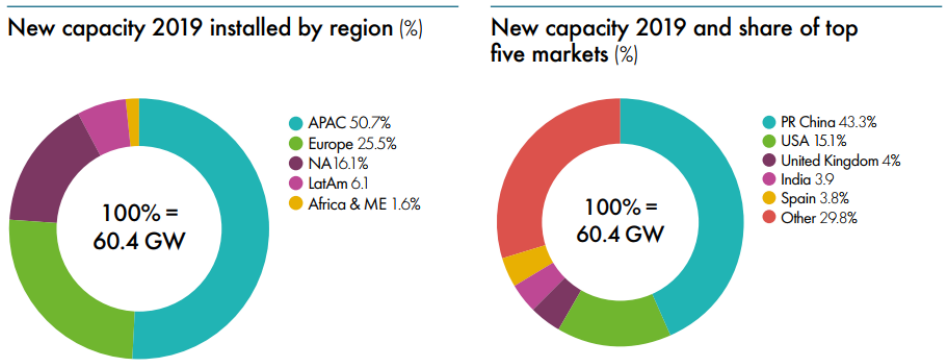

Figure 1.1: Market share of new wind power plants worldwide in 2019, segmented by region (left), segmented by country (right) [1].

In the early days of wind turbines development, they were installed on land because of the inherent facilities for extensive installation. However, a major problem with onshore locations is the high levels of roughness and wind shear, so it is necessary to install very high turbines to catch stronger winds. Then, in the

pursuit of new options to produce electricity from wind in a more effective manner, offshore sites began to be explored. The advantages at sea are considerable better regarding wind resource levels. The wind has a stable regime with stronger velocities and great vertical uniformity (low wind shear and surface roughness). These conditions allow getting stronger winds at low altitudes. However, offshore projects are more expensive; they are difficult to access and involve more risks. As a result, the market for offshore wind farms is still on the rise, but not yet at the level of development of onshore farms. In 2019, there was a total installed capacity of 650 GW of wind power plants, 95.5% (621 GW) corresponded to onshore installations, and only 4.5% (29.1 GW) were for offshore wind farms, see **Fig. 1.2**.

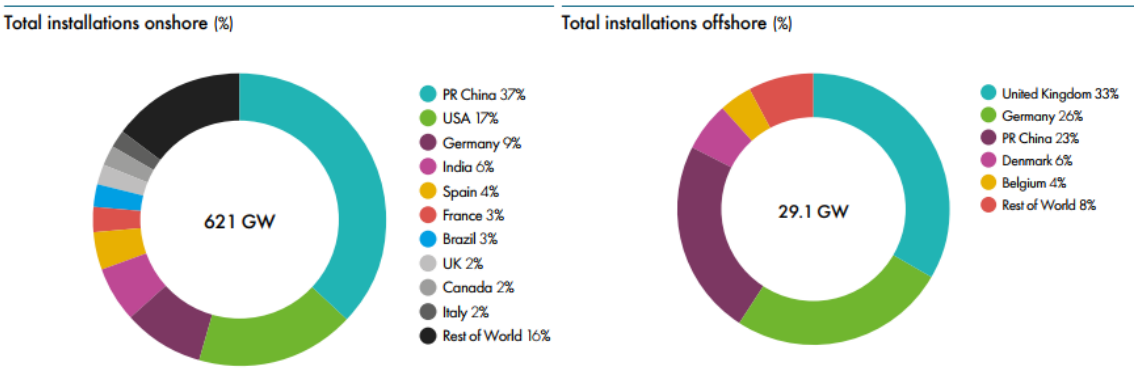

Figure 1.2: Total installed wind capacity worldwide onshore (left) and offshore (right) by 2019 [1].

The main cost drivers in an offshore installation are the individual power of the turbine to be installed, the distance from the coast, and the depth of the site where the project will be installed, see **Fig. 1.3** [2]. Hence, a perfect project is one that is not too far from the coast, with a shallow depth, and with the largest turbine available in the market. Currently, the individual turbine capacity has steadily grown over the last decade from 3 MW in 2009 to about 8 MW in 2019 [3], and wind turbines of 12 MW [4] and 14 MW [5] are already in the testing stage. The average depth for most projects has been moving from 5 m to nearly 35 m in 2019. Offshore wind energy projects have shown a tendency to move further away from the coast to find winds of better quality and currently, the average distance is already 60 km [3]. These parameters are important because they will define many aspects of the project, especially the type of foundation that will be needed.

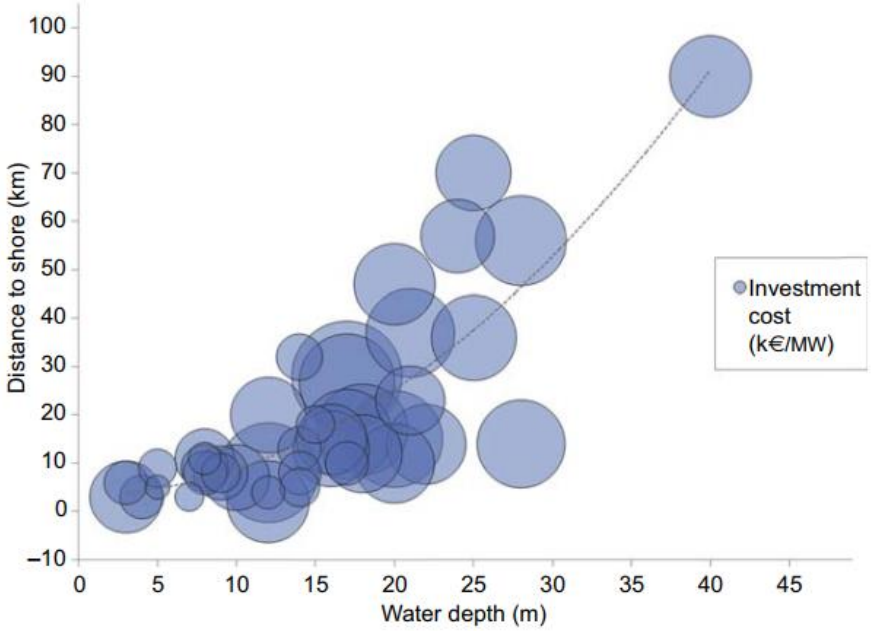

Figure 1.3: Relationship between the distance to the coastline, the sea depth and the specific investment cost of an offshore wind energy project [2].

Up to 2019, 80% (4258 units) of offshore projects have used a monopile foundation, see **Fig. 1.4**. The popularity of this type of substructure is based on the fact that it is the lowest relative cost foundation. A total of 25% of the total investment cost can be attributed to the foundation [6] then, the more economical this component is, there is more probability that the project will have a positive financial outcome.

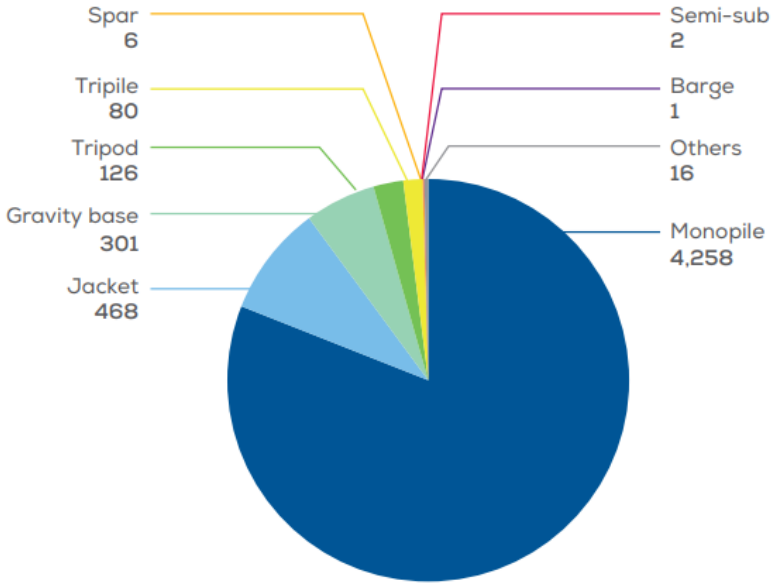

Figure 1.4: Number of offshore units installed by 2019 grouped by type of foundation used [3].

Considering the relatively early stage of development of offshore wind energy, there are still many uncertainties in the design phase of monopiles. This leads to the use of high safety factors and produces over-conservative designs. This situation is more relevant since there is a continuous trend to install larger turbines over theses substructures to benefit from economies of scale. Turbine manufacturers are continually pushing the established power and size limits, see **Fig. 1.5**. However, larger turbines require larger foundations, and in that context, uncertainties play a major role. Therefore, it becomes important to understand how the presence of uncertainties in different parameters of wind turbine design affects the design of support structures. In this way, it will possible to achieve structural optimization, and thus reduce the required investment cost without sacrificing safety and reliability.

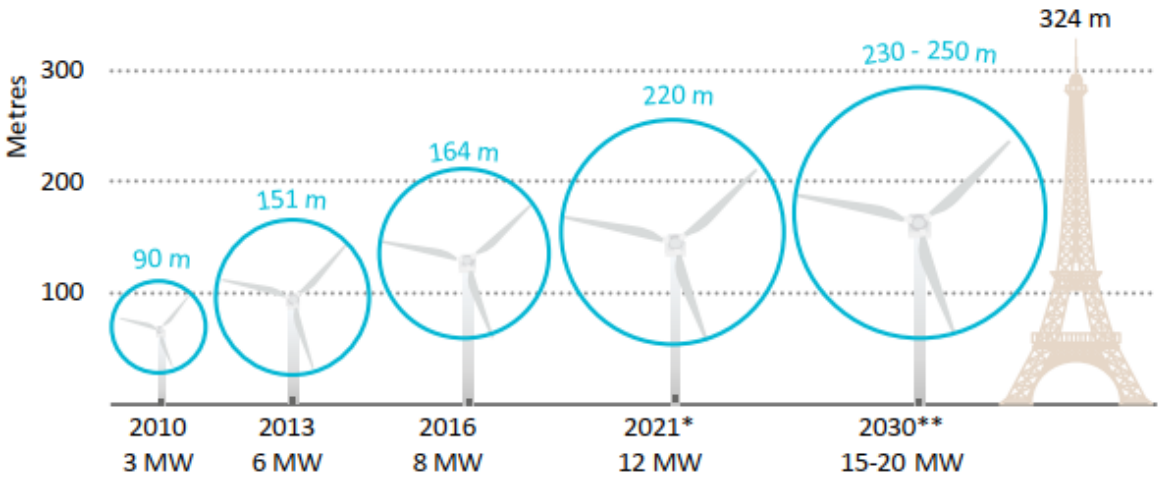

Figure 1.5: Trend in the development of offshore wind turbines [6].

1.2 THESIS OUTLINE

This research is organized as follows. In this chapter (chapter 1), the methodological aspects of the research are presented. The details of the research problem are stated and analysed. The general objective and specific objectives are then formulated. This is followed by a brief description of the work carried out through research articles. It also describes how these papers are interrelated to achieve the objectives. Later, the contributions generated from the work developed are analysed. The final parts of this chapter present the justification and importance of the research as well as the scope and limitations.

Chapters 2, 3 and 4 follow the same outline as the specific objectives. Chapter 2 explores the effect of uncertainty in wave parameters on the dynamic responses of a monopile wind turbine. The study is carried out considering two relevant operational wind speeds: the rated speed and the cut-out speed. Chapter 3 analyses the effect of a variable wind shear coefficient (WSC). A review of the literature is carried out, and the relationships between wind speed, wind shear and extreme long-term loads are formulated. For this purpose, the MECM method is used to avoid the well-known problem regarding the survival mechanism of the wind turbine.

In chapter 4, the last two specific objectives of this research work are addressed. A study of the impact of simulation length on the extrapolation of long-term loads is conducted. For such purpose, 10, 20 and 30 minutes simulations are made and their results are compared with one-hour simulations to establish the deviation levels. Besides, modelling uncertainty is explored by comparing long-term dynamic responses considering both rigid and flexible foundations. For this part of the research, only one-hour simulations were used.

The last part of this document presents a summary of the research and provides relevant conclusions from the work carried out, as well as recommendations for future work. This is followed by a list of the references that have been used. The thesis closes with the presentation of the main codes used in the execution of this research.

1.3 PROBLEM STATEMENT

In this section, the problem is presented from a global perspective. However, in each chapter, there is a more complete coverage of the state of the art related to the specific aspects studied in the present thesis. The main problems addressed in the present work are mainly based on the limitations identified in the work done by Robertson et al. [7]. These authors performed a sensitivity analysis to evaluate the effects of varying wind characteristics, and wind turbine properties on extreme and fatigue loads of a wind turbine. This study evaluated several wind turbine design parameters using the elementary effects (EE) method. The main objective of this method was mostly focused on ranking parameters based on their sensitivity level instead of providing accurate sensitivity indicators. The main

structural responses analysed were blade-root, tower-top, and tower-base moments as well as blade-tip displacements, electrical power, and moments at low-speed shaft main bearing. The main conclusions of that work showed that: a) Most ultimate responses showed high sensitivity to wind shear, except for tower-base moment and blade-root pitch-moment, b) Wind shear was among the top three contributors to fatigue load sensitivity for all the responses. Even this study provides useful and relevant insights; some limitations in the study were identified to be applicable in an offshore context:

a) Wave loading

The previously mentioned work was focused on an onshore wind turbine. However, in an offshore environment, the contribution of wave loads is important for the determination of dynamic responses and its influence on final statistical parameters is significant.

b) Conditionality of environmental parameters

For an onshore wind turbine, the main environmental variable is wind speed. This simplifies probabilistic analyses, but in the case of an offshore wind turbine, at least three environmental parameters must be considered, the wind speed, the wave height and the wave period. This adds complexities for a probabilistic-based analysis since it is necessary to consider multivariate probability distributions. Moreover, the range of values that these variables can take is limited since they are related to each other through joint probability distributions.

c) Effect of control actions

Many ordinary offshore structures have a monotonic relationship between the environmental variables and the load they support. In the case of wind turbines, there is a control system that governs the pitch angle. This makes the load experienced by the structure to decrease for high wind values. This control strategy generates nonlinearities in the behaviour of the entire system, and then determining long-term loads that meet a specified return period becomes challenging. In the analysis mentioned at the beginning of this section, only short-term responses were explored. However, the effects of control actions on long-term extreme responses are more

significant and it needs to be addressed by including more advanced methodologies.

d) Load probability distribution

In the paper taken as a reference for this thesis, the authors based their analysis for extreme loads on the average of the highest absolute maximum of the temporal response instead of a more accurate load probability distribution fitting procedure based on Extreme Value theory. These types of procedures are more exact and are recommended to well capture the stochastic behaviour for extreme response values.

e) Soil structure interaction

An important issue for an accurate prediction of ultimate loads for a wind turbine is the inclusion of the soil-structure interaction. Offshore wind turbines are often modelled as fixed to the seabed. This situation can lead to mispredictions in the natural frequencies of the tower and substructure as the modal shapes are not properly accounted for.

f) Simulation length

In the sensitivity analysis mentioned at the beginning of this section, the calculations were based on 10-minute simulations, which is correct in the case of onshore turbines to ensure the statistical independence of the results. However, there is a discussion (see chapter 4) whether this duration is sufficient in the case of offshore turbines under combined wave and wind loads. So, the problem related to statistical uncertainty when considering small durations is also considered in the present work.

The aforementioned points are identified as sources of uncertainty to the estimation of design loads for a monopile offshore wind turbine (OWT). Therefore, it is important to consider their effects and impact. The problems mentioned above will be addressed through the development of three research articles. In **section 1.3**, the research objectives are stated, and details on how these objectives are intended to be fulfilled through the papers will be given. **Section 1.4** presents the contributions made in this research and their relationship with the results obtained.

1.4 RESEARCH OBJECTIVES AND METHODOLOGY

The main research objective (RO) is established as:

- **RO:** Evaluate the influence of uncertainties in input parameters on the extreme responses of a monopile OWT.

To achieve this main objective, four specific objectives (SO) are defined:

- **SO1:** Investigate the effects of wave parameters uncertainty on the dynamic responses of a monopile OWT.
- **SO2:** Study the influence of wind shear uncertainty on the dynamic responses of a monopile OWT.
- **SO3:** Evaluate the impact of uncertainty in the simulation length on the dynamic response extrapolation process in a monopile OWT.
- **SO4:** Assess the effect of soil-structure interaction uncertainty on the dynamic responses of a monopile OWT.

1.4.1. PAPER 1: EFFECTS OF UNCERTAINTIES IN WAVE PARAMETERS

In this part of the research, the effects of progressive variations (uncertainties) of the wave parameters (i.e. significant wave height, spectral peak period) on the dynamic response of a Monopile Wind Turbine are analysed. Although attention is focused on waves, studies are carried out considering important wind speeds. Two operative conditions are considered: rated wind and cut-out wind speed. In each case, the 50-year environmental contour is plotted for a site located in the North Sea. Some sea states are selected from the environmental contour (base cases) and then derived cases with introduced uncertainties are generated. All the cases are simulated in FAST (NREL) using the NREL 5MW wind turbine. Then, the standard deviations of the resulting time series are compared against the values obtained in the base cases. The results for the dynamic responses at mudline (e.g. fore-aft shear force and fore-aft bending moment) are assessed as the most important parameters governing the design of the monopile. Details of the development of the aforementioned analysis are provided in chapter 2.

1.4.2. PAPER 2: INFLUENCE OF UNCERTAINTIES IN WIND SHEAR

In this stage of the research it is sought to study the relevance of an accurate selection of wind shear coefficient, and its influence on the probabilistic analysis of a bottom fixed OWT taking into account that considerable variations from recommended values may occur. Through the use of aero-hydro-servo-elastic simulations in FAST, the NREL 5MW wind turbine is subjected to varying wind shear conditions. The corresponding 50-yr long-term responses are calculated considering the Modified Environmental Contour Method (MECM) to take into account the influence of the wind turbine survival mode. The extreme values are fitted to a Gumbel distribution considering the Global Maxima Method (GMM). Finally, it is aimed to relate the uncertainty in a relevant input parameter (i.e. wind shear coefficient) with the uncertainties propagated to the output parameters (i.e. 50yr extrapolated long-term extreme responses). The development of this study is comprehensively presented in chapter 3.

1.4.3. PAPER 3: IMPACT OF SIMULATION LENGTH AND FLEXIBLE FOUNDATION

This part of the research is focused on the assessment of the effects of the statistical and modelling uncertainty on the estimation of long-term extreme responses in a bottom-fixed offshore wind turbine. The statistical uncertainty is addressed by evaluating the effects of simulation length on short-term and long-term extreme responses when statistical extrapolation is applied. To carry out this investigation, stochastic conditions are simulated for 10, 20 and 30-min. The results are later extrapolated to a 1-hr level. Finally, it is made a comparison against results obtained from 1hr simulations. In the same way, all results are extrapolated to a 50-year level and then compared to assess the differences obtained by using different simulation lengths. The second type of uncertainty, modelling uncertainty, is explored by contrasting the results obtained using a rigid soil model with a flexible model. To take into account the flexible behaviour of the soil, the improved apparent fixity method is considered. In this case, one-hour simulations are used. In both parts of this chapter, the MECM is employed for the estimation of 50yr long-term extreme responses. The specific details and the methodology employed in this study are developed extensively in Chapter 4.

1.4.4. CONNECTIONS AMONG THE PAPERS

The present thesis consists of the development of three papers that are related to the research objectives previously declared. First of all, the three papers deal with uncertainty quantification. The sources of uncertainties can be classified into three types: physical uncertainty, statistical uncertainty and model uncertainty. **Paper 1 (P1)** deals with the study of the physical uncertainty associated with wave parameters. **Paper 2 (P2)** addresses statistical uncertainty since it is necessary to use multiple stochastic realizations to have stable estimates of the coefficients of the adjusted distributions, and it is also associated with physical uncertainty since it evaluates multiple wind shear values. Finally, **paper 3 (P3)** focuses on the statistical uncertainty associated with simulation length and statistical independence. It also addresses model uncertainty as it considers the inclusion of soil-structure interaction. Although the work developed in the present research aims to cover the gaps described in section 1.2, these issues are addressed in an integrated way within the papers rather than in a problem-specific manner.

The relationship between the papers, the research objectives and the types of uncertainties they address can be seen in **Fig.1.6**. At the time of writing this thesis, the papers produced in the present research are in the following situation:

- **Paper 1:** Paper accepted and published [1] in the *"Proceedings of the International Conference on Offshore Mechanics and Arctic Engineering – OMAE 2019".* This is a publication of *"The American Society of Mechanical Engineers - ASME"* which is indexed in SCOPUS [2].
- **Paper 2:** Paper accepted for *"Proceedings of the International Conference on Offshore Mechanics and Arctic Engineering – OMAE 2020"* [3], to be published and indexed in SCOPUS.
- **Paper 3:** Paper to be submitted to OMAE 2021.

[1] https://doi.org/10.1115/OMAE2019-95390
[2] https://www.scopus.com/sourceid/91440
[3] https://event.asme.org/OMAE

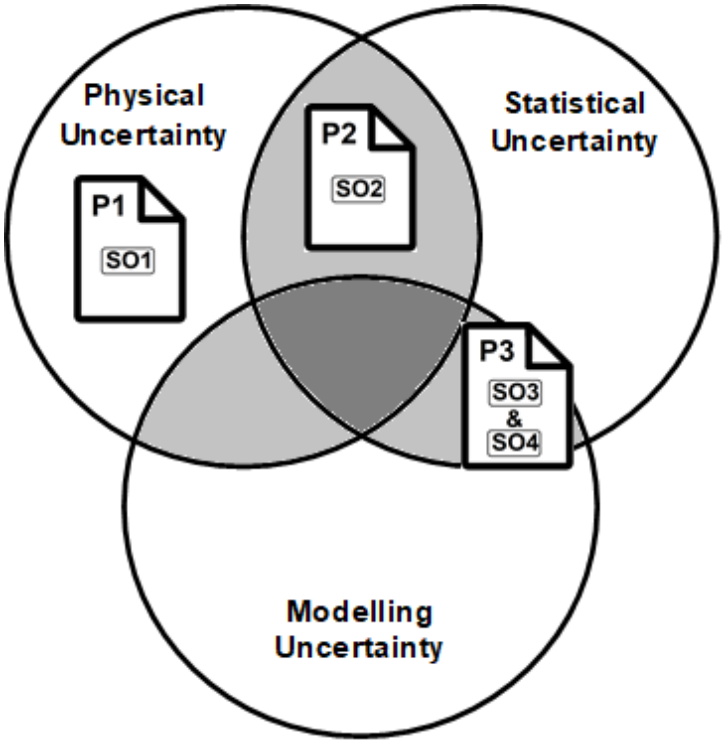

Figure 1.6: Overview of the relationship between the developed papers, their relation to research objectives, and the type of uncertainty they address.

It is necessary to highlight the importance that high-performance computing (HPC) has had for the development of the present research. One of the main challenges faced by simulation-based probabilistic approaches is the large number of simulations. This is crucial to achieving the stability of the statistical parameters obtained from the simulations. Also, there is an impact of the time required to perform each simulation, which can be very demanding depending on the structural system and the simulation length required. If both aspects are considered, it is possible to arrive at scenarios where the execution of all the necessary simulations is not feasible with an ordinary computer. Therefore, for the development of **P1**, it was necessary to use a computer with superior characteristics to those commonly found in a desktop computer. As a reference, it was obtained a performance rate of about 7 min-(sim)/min(real) with an 8-cores computer, this means that for each minute in real-time it was possible to run 7 minutes of simulated time. In this case, a total of 300 simulations of 10-min were run.

Similarly, for **P2** and **P3**, it was necessary to use the High-Performance Computing [(4)] of Queen's University Belfast. In this case, the performance ratio raised to a value of about 13 min-(sim)/min(real). For those papers, a total of 7500 10-min simulations, 11700 20-min simulations, 1200 30-min simulations and, 2400 1-hour simulations were run.

1.5 CONTRIBUTIONS OF THIS THESIS TO THE EXISTING STATE OF THE ART

The contributions of the present research are directly related to the aspects introduced in **section 1.2**. In the present subsection, this study will be referred to as **P0**. Also, some additional discussions directly focused on the scope of each specific objective stated in **section 1.3** can be found in each chapter. In the following lines, it will be explained how the work in this thesis has been done, and how the results obtained have covered some of the gaps previously described.

In an offshore wind turbine, wave loading has a high influence in the extreme dynamic responses. Moreover, when a probability-based approach is considered, the environmental parameters are related to each other through joint probability distributions. Thus, environmental parameters can only take certain specific combinations based on a specific return period. In **P0**, the authors mention that *"The parameters were considered independent of one another"*. In the same way, **P0** was applied to an onshore wind turbine and therefore waves were neglected. This aspect has been one of the first gaps addressed in the present work.

In the analyses performed in papers **P1**, **P2** and **P3** joint probability distributions that consider both wind (U_W) and wave parameters (H_S, T_P) have been taken into account. Although several environmental parameters govern the design of offshore wind turbines, the three previously mentioned are the ones which are mainly addressed in the relevant literature. In this case, conditionality among parameters means that only certain combinations of environmental conditions are suitable to be used in the simulations. The combinations of environmental parameters are directly related to the return period established in

[4] https://www.qub.ac.uk/directorates/InformationServices/Services/HighPerformanceComputing/

the probabilistic analysis. In the literature, the recommended and widely employed return period for offshore wind turbines is 50 years. Then, the combinations of environmental parameters corresponding to this return period were calculated by applying the environmental contour method. This method is used regularly in the development of this thesis, either in the traditional or in the modified version.

In particular, the results of **P1** confirmed the important contribution of waves to the system's outputs. In the same way, it was observed in **P2** that the fore-aft shear force at mudline (F_X) is mainly governed by the waves. Finally, in **P3** the discussion on the applicability of the simulation interval needed to ensure stochastic independence, and how this is affected by the presence of waves is presented. It was shown that there is no consensus yet on the applicability of the 10-minute interval, which is currently used. From the results of **P3**, it was seen that the presence of waves particularly affects long-term responses.

The second problem identified at **P0** was related to the fact that the ultimate loads were estimated by averaging the absolute maximum values. Also, they were only addressed to short term responses. A more accurate method to estimate ultimate loads is addressed by calculating the most probable value of a probability distribution fitted from extreme values extracted from multiple simulations. Attending to this issue, in papers **P2** and **P3**, the Global Maxima Method (GMM) was employed. Then, the data were fitted to a Gumbel distribution to find the most probable value of extreme responses at the mudline of the monopile. Thus, a more precise estimation of the response was obtained to perform better comparisons.

Since in **P0** only short term loads were evaluated, in this thesis also long-term loads were studied. This aspect was included in the analysis by using a proper extrapolation technique. The relevance of this point is related to the fact that at a long-term level the turbine control system has a great influence on the extreme long-term load calculation. The control system introduces nonlinearities in the system's behaviour and makes the calculation of long-term responses difficult. This problem is bypassed in this thesis by the inclusion of the Modified Environmental Contour Method (MECM) in chapter 3 and 4. With the support of this method, it was possible to verify the influence that the survival control strategy has on the long-term load's calculation. From the results obtained in **P2** and **P3**, it

was found that the critical environmental condition for F_X is near 24 m/s and for M_Y (fore-aft bending moment) is around 16mps, in the specific case of the NREL 5MW wind turbine. It was also found that the location of the critical environmental condition for F_X is particularly affected by wind shear whereas the location of this condition is unaffected for M_Y.

A third aspect addressed in the present thesis and that is derived from the limitations explained in section 1.2 is referred to the dynamic responses considered in **P0**. In that study the fore-aft bending moment ("Tower-base moment") was taken into consideration, however, the fore-aft shear force at the base was ignored within the analysis. Also, the results of **P0** showed that most of the ultimate dynamic responses were very sensitive to the wind shear value, except for the fore-aft tower base moment. Since **P0** does not consider wave loading, conditionality on environmental parameters, or methods based on extreme statistics, (see previous paragraphs), and considering that wind shear was very relevant for most dynamic responses, it was deemed necessary to examine the sensitivity of the wind shear in more detail taking into consideration all these aspects. In chapter 3 additional arguments that reinforce the relevance of studying wind shear are given based on the literature review.

The sensitivity analysis for wind shear has been extensively covered in chapter 3 (**P2**). All the aspects described lines above, which were not considered in **P0**, were included in the development of this thesis. That provided a better understanding of the influence of this parameter. In this case, the fore-aft shear force at mudline (which is governed by waves in the case of a bottom-fixed offshore wind turbine, see Chapter 3) was taken into account (not considered in **P0**), as well as the fore-aft bending moment at mudline. The results from **P2** supported that M_Y was not very sensitive to wind shear, but it was also found that F_X was not sensitive to it. It is important to mention that in **P0** the responses were addressed only in the short term. However, in this thesis, the analysis was made to obtain the estimation of the 50-yr long-term responses. This involved the execution of several simulations and the use of the MECM to bypass the discontinuity produced by the turbine control system.

A very important aspect that is often ignored during the modelling of a bottom-fixed offshore wind turbine is the soil-structure interaction. This aspect allows guaranteeing a high fidelity of the numerical model of the offshore wind turbine. Unfortunately, this feature is often neglected or addressed through oversimplified approaches. Within the literature, it is very common to find that the foundation is modelled as a completely rigid connection. In the case of **P0**, the wind turbine was modelled according to this approach. This situation could be acceptable for an onshore wind turbine, but in an offshore context, the effects of the foundation may be important due to the combined loading. This is particularly important if one considers that waves have an important contribution in the shear force in the monopile.

To evaluate the effects that a flexible soil model can induce on the extreme responses of an offshore wind turbine, the improved apparent fixity (IAF) soil model was used in **P3**. This is a relatively new model that has shown good results in replicating the soil-structure interaction, without excessively increasing the computational effort needed to perform the simulations. From the results of **P3,** it was observed that the inclusion of the soil flexibility induced a particular effect on the fore-aft bending moment. When a completely rigid foundation was considered, the critical wind speed identified by the MECM was 16.5 m/s. However, when the IAF model was employed in simulations, this critical speed was shifted to 18 m/s. Also, the value of the 50-yr long-term extreme response experienced a slight increase in its value.

In the development of this thesis, other gaps not directly related to limitations derived from **P0** were also addressed. In chapter 4, there was a literature review, and it was found that there are on-going discussions about the suitability of adopting a simulation length of 10-minutes for offshore wind energy applications. For onshore wind turbines, 10 minutes (as used in **P0**) has been the standard for many years, and it is widely employed in the wind energy field. It allows greatly reducing the computational efforts for the simulation in the design phase. However, since offshore wind turbines are affected by wave loading, it is not entirely clear whether 10-minutes can guarantee the stochastic independence of dynamic responses governed by combined load since there are many

phenomena associated with waves that occur at low frequencies. In chapter 4 (**P3**) the effects of simulation length were assessed. It was found that a 10-minute simulation length gives acceptable results for obtaining extrapolated extreme responses for the one hour level. However, it does not provide adequate results for the extrapolation of long-term extreme responses. This makes it necessary to use durations longer than 30 minutes in the simulations.

An additional contribution not related to any previous research and obtained as a result of the development of **P1** is related to the polynomial model shown in chapter 2. It was found that the propagation of uncertainty on the system outputs, measured through sensitivity indices, fit with adequate precision to a polynomial model dependent on the wave parameters (H_S and T_P). This is expected to be useful to estimate the uncertainty present in the dynamic responses for sea states that were not simulated.

As a concluding point, it is deemed necessary to mention some relevant aspects. Although a specific type of wind turbine and a particular location has been addressed in the development of this thesis, the methodology here employed can be replicated and applied to other similar scenarios. Also, the wind turbine numerical model used in this research is the standard model used by most studies, so the results obtained can be used for comparison purposes by other researchers.

1.6 JUSTIFICATION AND IMPORTANCE OF THIS RESEARCH

The present thesis is within the study field of the **Uncertainty Quantification (UQ)**. This is a relatively new field, and although there are several approaches, there is not yet a single, general theory that covers all aspects in the domain of uncertainty quantification [8]. Uncertainty Quantification can be defined as *"the process of quantifying uncertainties associated with model calculations of true, physical quantities of interest (Q_OIs), with the goals of accounting for all relevant sources of uncertainty and quantifying the contributions of specific sources to the overall uncertainty"* [9].

The importance of this field is associated with the fact that in engineering it is frequently necessary to rely on complex models. These models depend largely on physical parameters. Sometimes these parameters manifest a great influence on the calculation of one or several output parameters. This means that a small uncertainty in some inputs can propagate and produce a large effect on the output quantities. Thus, the quantification and control of this influence or also called "propagation of uncertainty" becomes crucial. As this enables to systematically address the study with respect to the level of reliability that must be achieved in the inputs to keep the uncertainty in the output within acceptable bounds. Uncertainties are present in every physical phenomenon, and if the control of these uncertainties is not possible, then there is no way to determine the confidence in the results of the model that replicates the phenomenon.

In the field of wind energy, the quantification of uncertainty is also relevant. It is closely related to the achievement of a high-level objective within the offshore wind industry, the lowering of the Levelized Cost of Energy (LCOE) [10]. This is one of the main issues that hinder the massive deployment of wind energy projects. The objective of lowering the LCOE can be achieved by minimizing uncertainties in the design process that could lead to excessive material consumption or reduced operational lifetime since large uncertainties imply the use of high safety factors. For this purpose, it is required to ensure high confidence in each stage of the structural design process. The importance of the uncertainty quantification has been recognized and studied in the literature. Jiang et al. [11] concluded that the quantification of uncertainties is a critical and necessary aspect to facilitate the reliability-based design of wind turbines. He based his conclusions on an extensive review of the literature between the 1990s and 2017 on the subject of structural reliability analysis of wind turbines.

On the same subject, in the summer of 2016 several representatives from industry and academia involved in the field of wind energy were invited to take part in a workshop where the main purpose was to identify gaps in the understanding of the design process, exploring the impact of uncertainties in wind engineering design processes on the reliability of wind energy facilities, and proposing solutions through the evaluation and reduction of uncertainties present in both, the

analysis tools and the established criteria. Damiani et al. [10] presented the results of this workshop. It was established that future new developments should focus on innovations to lower the LCOE through the reduction of uncertainties. They also agreed that "*Uncertainty quantification become essential to advancing computational capabilities while introducing innovations in the quest toward lower LCOE*". It was also stated that the quantification of major uncertainties and advanced understanding of the operational environment can lead to changes in current established design processes. In the same vein, Fogle et al. [12] claim that it is expected to improve the predictions of the loads/responses associated with established return periods by controlling the level of uncertainty in the probabilistic models.

As can be noted, the treatment of uncertainties is currently a problem of great relevance, and its direct relation with the LCOE has already been discussed within the scientific community. Therefore, it is necessary to invest time and resources in providing an enhanced understanding of the uncertainties in the design process of offshore wind turbines and so, provide an important contribution to the achievement of LCOE reduction. For this purpose, it is necessary to use probabilistic-based approaches that rely on stochastic simulations. Among these techniques and approaches, the use of joint probability distributions, the stochastic treatment of environmental parameters, the environmental contour method, the global maxima method, the sensitivity analysis, among others can be mentioned.

Additionally, there is also a local component to justify the efforts invested in the present investigation. In recent years, interest in wind energy exploitation has grown in Peru. This has started due to the renewable energy auctions for the construction of onshore wind farms promoted by the Peruvian government [13]. Currently, 375.46 MW of wind power have been commissioned in Peru according to information from OSINERGMIN[5] [14]. There are currently five wind farms in operation, three in Ica [15]–[17] ("MARCONA", "TRES HERMANAS", "WAYRA I"), one in La Libertad [18] ("CUPISNIQUE") and one in Piura [19] ("TALARA"). Similarly, it is expected that in the next few years an additional capacity of 36.8 MW will be added with the "DUNA" [20] and "HUAMBOS" [21] projects.

[5] Peruvian Superintendence for Investment in Energy and Mining.

The Peruvian government aims to cover up to 20% of the country's energy needs with renewable resources by 2040 [22]. So it is feasible to expect that once the wind energy industry will be more established in Peru, offshore wind energy projects will attract more interest from investors as offshore areas have stronger winds, less turbulence and less visual impact. In this context, knowledge of environmental conditions and probability-based structural design approaches will be highly required. Therefore, it is important to initiate the study of these topics to be prepared for the near future and to offer adequate support to the decisions that will be taken to ensure the country's energy security.

1.7 SCOPE AND LIMITATIONS

This research has been focused on the analysis of the uncertainties present in specific input parameters in the design of offshore wind turbines. Given the broad extent of the field of study, the scope of this research has had to be limited to specific aspects. **Fig. 1.7** shows a general classification of the subjects associated with the energy field. In the lower part, a subdomain, where the uncertainty quantification can be applied, is highlighted.

Offshore wind turbines are subjected to various conditions during their lifetime. Among these conditions can be mentioned: operational, parked, idling, start-up, in transport, in installation, and others. Each of these modes induces a different load configuration and therefore each structural analysis presents unique characteristics. Considering that all these conditions would have highly increased the computational effort required in the present work. It was deemed necessary that only the operational condition was addressed in this thesis.

Two open-source numerical programs, both developed by the National Renewable Energy Laboratory (NREL), have been mainly used to simulate the operating conditions of the wind turbine. TurbSim was used for the generation of the stochastic full-field turbulent wind. This program is based on statistical models instead of physics-based models and it is practically the standard in the field of study in which this thesis is included. Later, for the simulation of the dynamic behaviour of the wind turbine, the software FAST was considered.

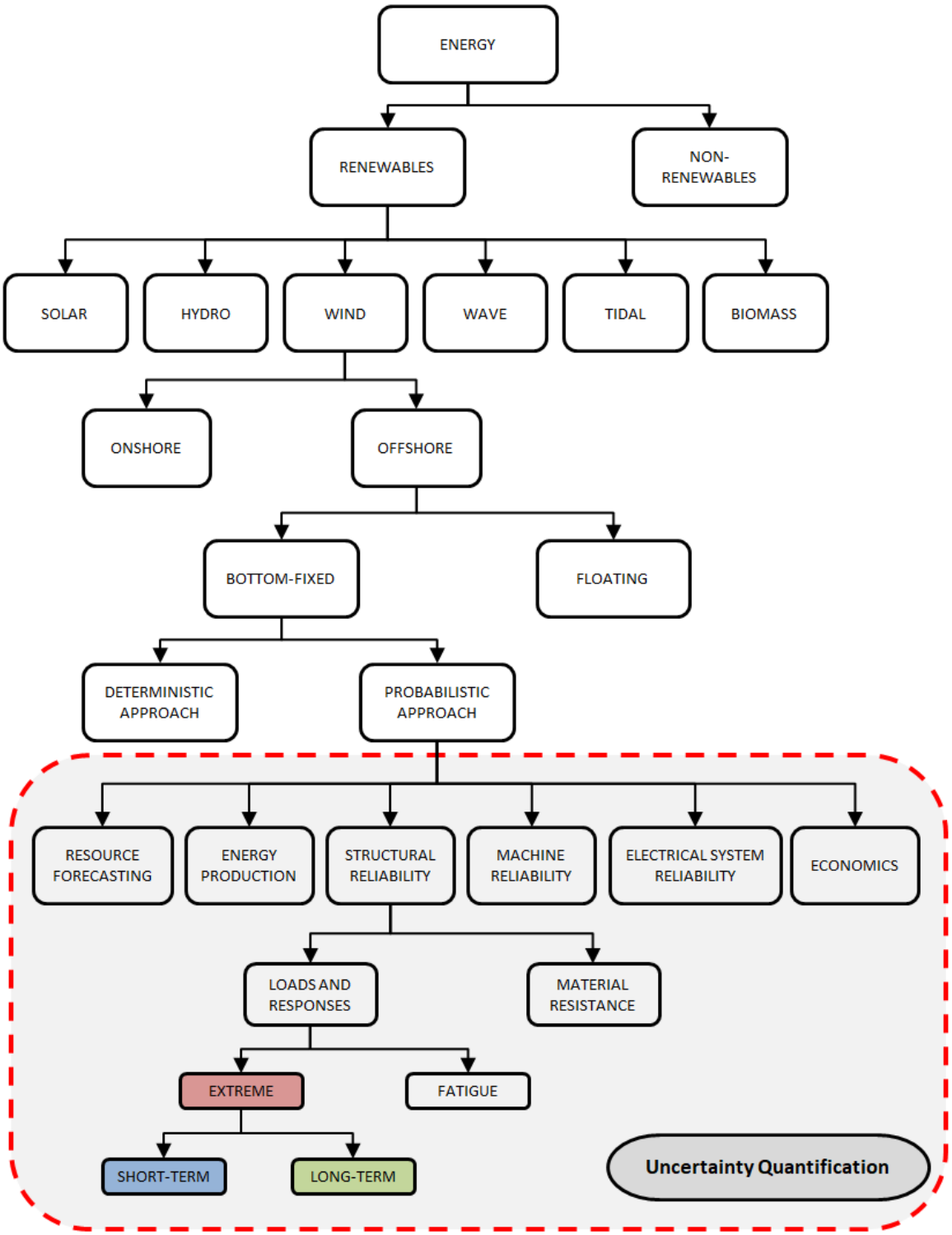

Figure 1.7: General classification of the field in which the scope of the present investigation is situated.

When a probability-based structural design is addressed, several criteria and load conditions have to be taken into consideration. These conditions include ultimate or extreme loads and fatigue loads. In this research only ultimate loads have been addressed as the fatigue phenomenon involves an additional scope that would not have allowed obtaining results within an adequate deadline.

Several types of dynamic responses can be analysed in an offshore wind turbine. These include forces, moments, deflections, velocities, accelerations, among others. They can also be associated with specific parts of the wind turbine e.g. the blade-root, the base of the nacelle, the transition piece, the mudline, etc. In the present research, the analysis has been focused on the fore-aft shear force and bending moment at the mudline as they are the ones that best represent the combined action of wind and wave. Main details of the OWT, as well as the reference coordinate system, can be seen in **Fig. 1.8**.

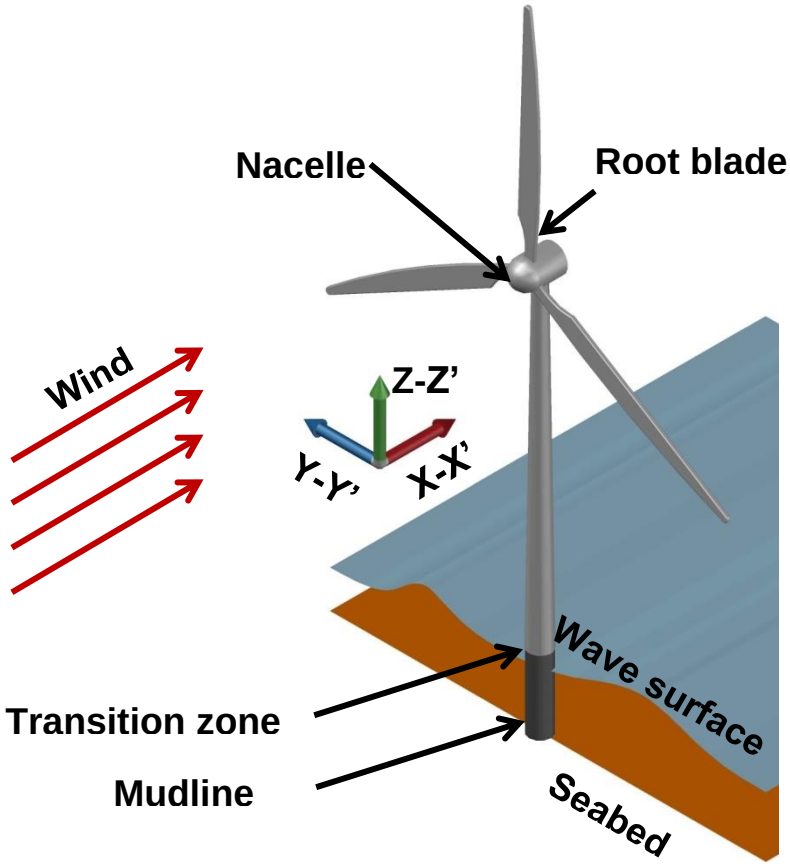

Figure 1.8: General scheme of an offshore monopile wind turbine.

CHAPTER II. EFFECTS OF UNCERTAINTY IN WAVE PARAMETERS ON SHORT-TERM STOCHASTIC RESPONSES OF A MONOPILE WIND TURBINE

2.1 INTRODUCTION

For stochastic processes, the propagation of uncertainty is an important matter when getting high confidence in the outputs predicted by models is required. The stochastic approach of dynamic analysis of structures is not indifferent to this issue. One popular tool for quantifying the impact of uncertainties is sensitivity analysis. This is a useful tool which seeks to explain how the uncertainty in the output of a model can be apportioned to sources of uncertainty in the input parameters of the model. The main purpose of the analysis is to comprehend the model and understand how uncertainty is propagated through it. Under this analysis, it is possible to address some important aspects e.g. which factors contribute most/less/nothing to the output uncertainty? How the output variance can be reduced to a specific desired level? [23].

There are two main approaches to perform a sensitivity analysis: the **global approach** and the **local approach**, whereas the first is focused on analysing the sensitivity in the entire domain of the input variable, the second one focuses on the sensitivity around a specific optimal point. The last approach requires that a good “baseline” or “nominal point” is set with high accuracy. Both approaches involve many different methods, each one useful for a specific context e.g. OAT, Sobol method, Elementary Effects, etc [24]. Investigations in the wind energy field related to sensitivity analysis have been done by Rinker et al. [25], Karimirad et al. [26], Horn et al. [27] and Robertson et al. [28], just to mention the most recent. Each work focused on different aspects of wind turbines to find out the influence of input parameters on the outputs of interest.

2.2 THE ENVIRONMENTAL CONTOUR METHOD

This method is based on the Inverse First Reliability Method approach (IFORM). Under this procedure, a sphere in a non-physical standardized normal space (U-space) can be generated for a given annual exceedance probability **q** or desired return period **N**. The radius of this sphere (β) can be calculated with Eq. (2.1), where md is the expected number of d-hour sea states per year, and $\mathbf{\Phi}^{-1}$ denotes the operator of the inverse standard normal distribution. Later, three non-physical variables (U) can be determined with Eq. (2.2).

$$\beta = \Phi^{-1}\left(1 - \frac{1}{N * m_d}\right) = \Phi^{-1}\left(1 - \frac{q}{m_d}\right) \tag{2.1}$$

$$\beta^2 = U_{U_W}^2 + U_{H_S}^2 + U_{T_P}^2 \tag{2.2}$$

These non-physical variables are linked to the physical parameters through the Rosenblatt Transformation, Eqs. (2.3)-(2.5), **F** denotes the cumulative distribution function of the respective environmental parameters. With all the combinations of environmental parameters which satisfies Eqs. (2.2)-(2.5), it is possible to generate a contour surface (ECS) which represents all the combinations of environmental conditions corresponding to the desired annual exceedance probability [29].

$$\Phi\left(U_{U_W}\right) = F(U_W) \tag{2.3}$$

$$\Phi\left(U_{H_S}\right) = F(H_S|U_W) \tag{2.4}$$

$$\Phi\left(U_{T_P}\right) = F(T_P|U_W, H_S) \tag{2.5}$$

When a long-term extreme prediction is required, the ECM considers short-term simulations and the corresponding short-term extreme distribution to find the environmental condition with the largest value among all short-term extremes. The ECM initially considers on its analysis that the value of the short-term extreme distribution is the median (p-fractile of 50%) but, this is not totally accurate. To bypass this inaccuracy, it is needed to use an empirical higher fractile to correct the predicted long-term value e.g. 90% is a usual p-fractile value.

Recent studies have shown that a modified version of the traditional ECM is required for offshore wind turbines (OWT) as the responses are not monotonically

related to the main environmental parameters e.g. for wind speeds higher than cut-out wind speed, OWT remains parked to reduce loads [30], [31]. In this case, it is necessary to find an equivalent return period (N) to bypass the occurrence of the change in the operational mode of the OWT. An iterative process, where inner contours are tested, is required to find this equivalent return period. After this process, the largest value of all the short-term extremes for all the environmental conditions on all the inner contours is then considered for the long-term response prediction [31].

The present chapter is not mainly focused on the sensitivity in the long-term extreme predicted responses, but rather on the impact in the short-term responses when uncertainties in the input parameters are introduced. Therefore, at this stage, the traditional ECM is considered suitable for the analysis. In further research, the use of the Modified ECM will be mandatory if the operational conditions need to be reflected in the sensitivity analysis. Especially, for the cases where long-term extreme responses are the main focus.

2.3 SENSITIVITY ANALYSIS

The methodology used in this work is known as **OAT (One-at-a-time)** method which is a local approach. The term 'local' refers to the fact that all the derived cases are taken with respect to a single point, also known as the baseline. The characteristic of the baseline point is that it is a safe starting point where the model properties are well known. Then, specific percentage variations (δ, ε) for the sea states calculated by the ECM are considered.

For this analysis, the 5 MW NREL Wind Turbine supported by a monopile will be used [32]. This configuration has been widely studied and also has been validated with results from the OC3 project to verify the simulation capabilities of FAST [33]. The main dimensions of the wind turbine are presented in **Fig. 2.1**, as well as, the main characteristics are summarized in **Table 2.1**.

The cases considered in this work can be observed in **Fig. 2.2.** The baseline (star) is taken directly from the environmental contour line (base case), and the sensitivity to variation of wave height (triangles), variation of spectral peak period (circles), and the case when it is applied the same variation for H_S and T_P

(squares) are calculated according to Eqs. (2.6) and (2.7). The values H_S* and T_P* are the wave height and peak period considered for the derived cases.

$$H_S^* = H_S\,(1 + \delta\%) \tag{2.6}$$

$$T_P^* = T_P\,(1 + \varepsilon\%) \tag{2.7}$$

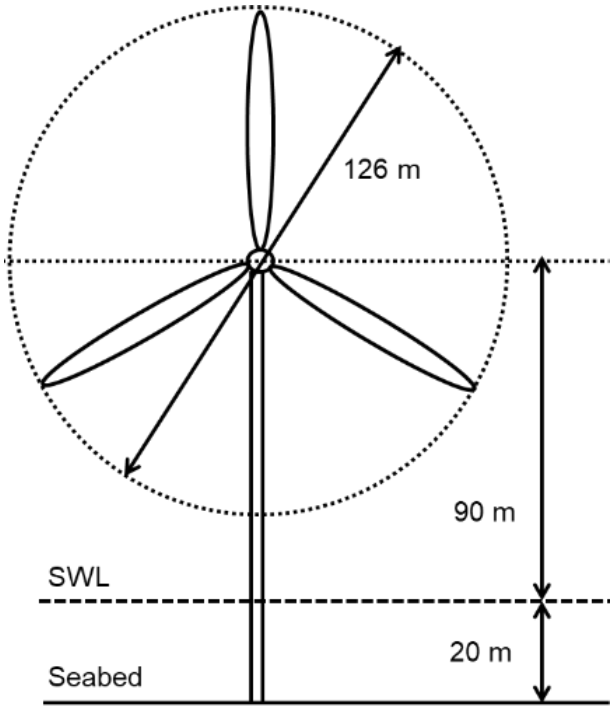

Figure 2.1: Main dimensions of the NREL 5 MW Wind Turbine.

Table 2.1: Main characteristics of the NREL 5MW wind turbine [32].

Rating	5 MW
Rotor Orientation, Configuration	Upwind, 3 Blades
Control	Variable Speed, Collective Pitch
Rotor, Hub Diameter [m]	126, 3
Hub Height [m]	90
Cut-In, Rated, Cut-Out Wind Speed [m/s]	3 / 11.4 / 25
Rotor Mass [kg]	110 000
Nacelle Mass [kg]	240 000
Tower Mass [kg]	347 460

With all the combinations of the inputs parameters (U_W, H_S, T_P), several coupled simulations are run in FAST. Then, the standard deviations (STD) are calculated from the resulting simulated dynamic responses.

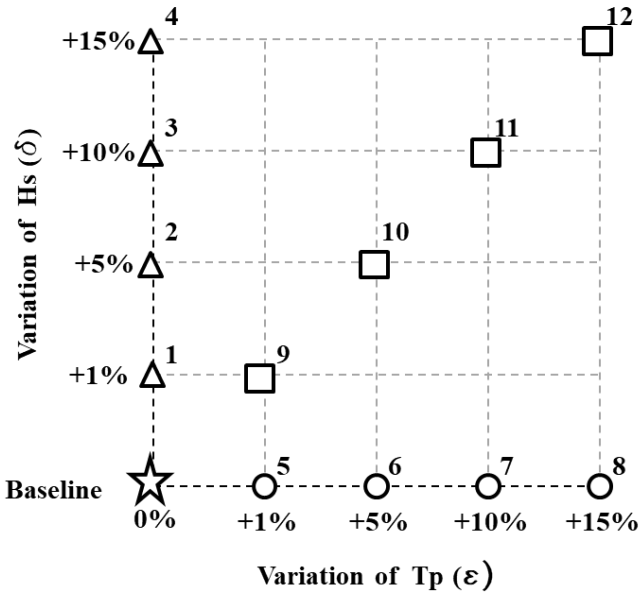

Figure 2.2: Matrix of percentage variation applied to the selected sea states in each contour line.

Finally, the values are used to find a sensitivity index (S), Eq. (2.8). This indicator helps us to better reflect and quantify the sensitivity (uncertainty propagation) in the short-term response (simulated response) when uncertainties in the sea state parameters are introduced. In future studies, the impact of these uncertainties in a predicted long-term response, and a ULS analysis could be assessed. However, this analysis is out of the scope of this work.

$$S(Case) = \left(\frac{\sigma_{X_{derived}} - \sigma_{X_{base}}}{\sigma_{X_{base}}}\right) x100\% \qquad (2.8)$$

In Eq. (2.8), $\sigma_{X_{derived}}$ and $\sigma_{X_{base}}$ are the standard deviation of the resulting time series of the response X, considering the environmental parameters from the baseline case and derived case, respectively. **S(Case)** represents the sensitivity of the response X to the variations in the environmental parameters for a specific case. All the baseline cases correspond to one of the ten points selected in the environmental contour line (ECL).

The nomenclature used in the numerical analysis is:

- **S(H_S):** Sensitivity index for the case when the variation is applied only to the wave height (triangles).
- **S(T_P):** Sensitivity index for the case when the variation is applied only to the peak period (circles).
- **S(H_ST_P):** Sensitivity index for the case when the same variation is applied to the wave height and peak period (squares).

2.4 NUMERICAL ANALYSIS

The site selected for the analysis is the one presented by Li et al. [34] labelled as “Site 15”. This site is located in the North Sea Center, see **Fig. 2.3**. The models considered for representing the environmental stochastic processes are summarized in **Table 2.2**. The respective parameters for the probability distributions can be found in the previously mentioned study. As a reference, the 50-year return extreme parameters for this location are U_{10}=27.20 m/s, H_S=8.66 m and T_P=6.93 s.

Figure 2.3: Location of “Site 15” [34].

In this analysis, two operational mean wind speeds at hub height are considered, the rated and the cut-out wind speed. To use the marginal distribution of the mean wind speed, it is necessary to transform these wind speeds to a height of 10 m above the mean sea level. This task can be done by considering the wind power-law, Eq. (2.9). The wind shear power exponent (α) is taken as 0.14

according to the IEC-61400 [35]. Therefore, the mean wind speeds to be used in the marginal and conditional distributions for the environmental contour method (ECM) are presented in **Table 2.3**.

$$U_{90} = U_{10}\left(\frac{Z_{90}}{Z_{10}}\right)^{\alpha} \tag{2.9}$$

For each operational wind speed, an ECL is generated. Ten sea states are selected in each ECL (Base Case), see **Fig. 2.4** and **2.5**. These points have been selected according to the following criteria: i) trying to have the points equally distributed along the ECL, and ii) choosing important points e.g. point with the highest/lowest H_S, the highest/lowest T_P. The corresponding sea states selected from the ECLs are summarized in **Table 2.4**. This data is taken as baseline input data for the FAST model. The wind field is generated in TurbSim [36] considering the mean wind speed at the hub, and the wind profile power-law. Main details of the configurations considered for the simulation of wind and wave conditions are presented in **Tables 2.5 - 2.7**. The scripts used in the present analysis are shown in Appendix I and II.

Table 2.2: Probability models for joint environmental distributions.

Parameter	Model
Mean wind speed at 10 meters height (u_W)	Marginal - Weibull 2 parameters
Significant wave height (H_S)	Conditional – Weibull 2 parameters
Wave spectral peak period (T_P)	Conditional – Log-normal

Table 2.3: Mean wind speeds considered in the analysis.

Uw	U_{90}	U_{10}
Rated (m/s)	11.4	8.38
Cut-out (m/s)	25	17.64

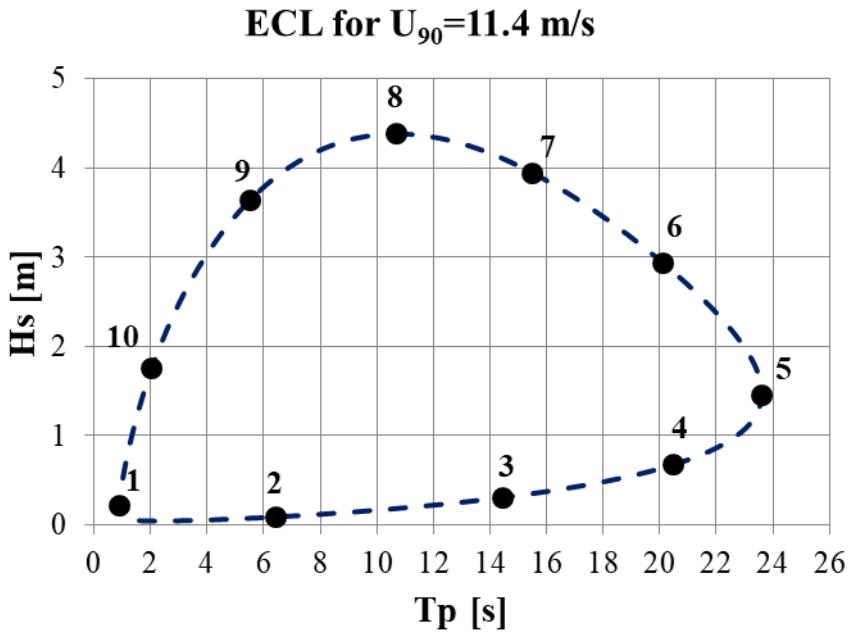

Figure 2.4: Contour line for a 50yr return period, and selected sea states (circles) for U_W=11.4 m/s (dashed).

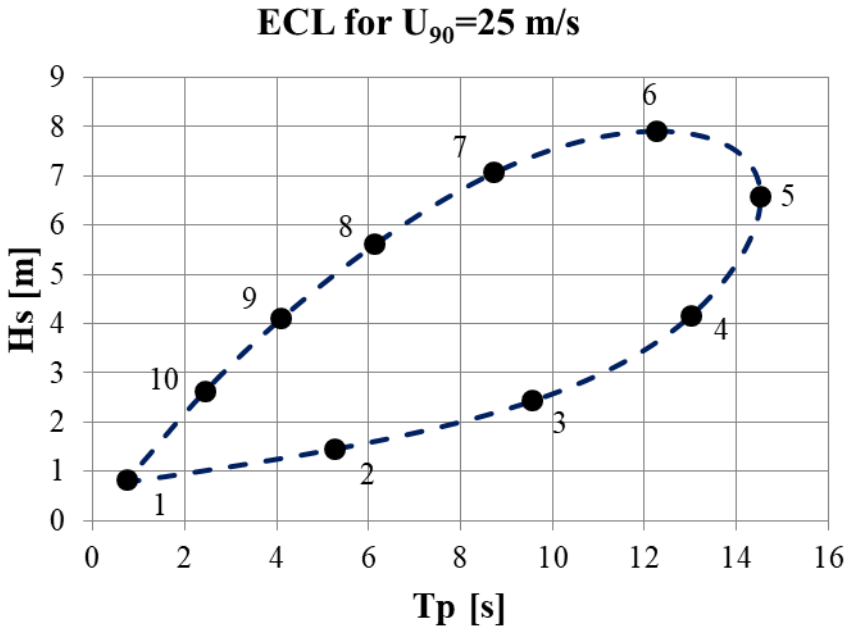

Figure 2.5: Contour line for a 50yr return period, and selected sea states (circles) for U_W=25 m/s (dashed).

Table 2.4: Sea states considered for analysis.

Sea State	U_W=11.4 m/s		U_W=25 m/s	
	H_S [m]	T_P [s]	H_S [m]	T_P [s]
1	0.212	0.906	0.821	0.738
2	0.086	6.434	1.453	5.273
3	0.305	14.462	2.432	9.575
4	0.672	20.482	4.167	13.018
5	1.452	23.602	6.571	14.527
6	2.935	20.103	7.908	12.272
7	3.941	15.512	7.065	8.741
8	4.380	10.705	5.606	6.136
9	3.636	5.504	4.093	4.089
10	1.751	2.042	2.630	2.447

Table 2.5: General configuration considered for the simulation of wind conditions.

Parameter	Value
Turbulence Model	Kaimal
IEC turbulence characteristic	B
IEC turbulence type	NTM
Wind profile type	Power Law
Height of the reference wind speed	90 m
Mean (total) wind speed at the reference height [m/s]	11.4 / 25
Power law exponent	0.14
Coherence model	IEC 61400-1 3° ed.
Simulated Time [s]	1200
Time Step [s]	0.05

Table 2.6: General configuration considered for the simulation of sea conditions.

Parameter	Value
Incident wave kinematics model	JONSWAP
Analysis time for incident wave calculations [s]	3630
Heading direction	0°
Water depth [m]	20

Table 2.7: Data of monopile model.

Parameter	Value
Diameter of the Pile [m]	6
Thickness of the Pile [m]	0.06
Young's Modulus [N/m^2]	2.1E+11
Shear Modulus [N/m^2]	8.08E+10
Density [kg/m^3]	8050
Drag Coefficient (C_D)	0.9
Added Mass Coefficient (C_A)	0.75
Froude-Krilov/Pressure Coefficient (C_P)	1

Regarding **Table 2.7**, the Morison Coefficients (C_D, C_A, and C_P) are very important to determine with a proper accuracy the wave loading. According to [37] the usual parameter ranges for fixed structures are $1.5 \leq C_P + C_A \leq 2$, and $0.6 \leq C_D \leq 1.2$. The pressure coefficient (C_P), also known as the Froude-Krilov coefficient, can be usually considered 1 for a slender circular cylinder. It can be found in the literature that the Morison parameters depend on Reynolds number, Keulegan-Carpenter number and the relative roughness but, for this analysis, the mean values could serve as a good start. Therefore, the values taken for this work will be the mean of the range (C_D=0.9, C_A=0.75, C_P=1).

In **Figs. 2.6** and **2.7**, the influence of these parameters in the standard deviation of two main structural responses can be observed. These figures show that the C_D affects much lower the STD of the responses analysed. It varies over a range of ±0.4% for the shear force and ±0.1% for the bending moment (**Fig. 2.6**). On the other hand, the parameter C_A has a major effect in the dynamic responses and makes the STD change over a range of ±15% for the shear force and ±3% for the bending moment (**Fig. 2.7**).

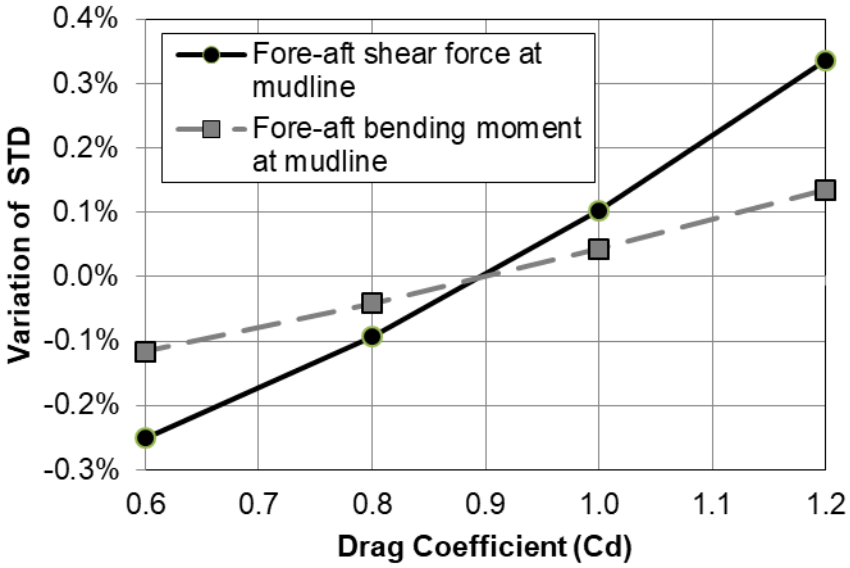

Figure 2.6: Influence of C_D in the standard deviation of dynamic responses.

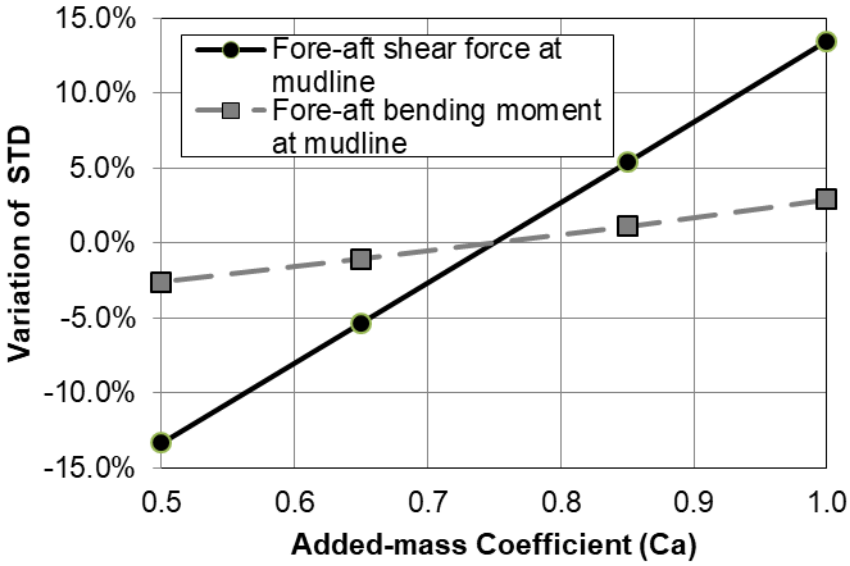

Figure 2.7: Influence of C_A in the standard deviation of dynamic responses.

2.5 RESULTS

Before process and analyse the results obtained from coupled simulations in FAST, it is necessary to consider the context and nature of the responses to identify the most representatives for this work. The first aspect to consider is that any tridimensional structural system has six degrees of freedom. However, in this study, the corresponding dynamic responses related to the vertical axis (z-axis) are ignored because the monopile model is considered fixed at the seabed (no displacement) and the rotational effect in that axis is considered almost constant

for all the cases. The second aspect is related to the side-to-side direction (y-axis). As we are considering a heading angle of 0° for wind and wave, the dynamic responses in y-axis will be mostly a result of the gust component. The value of that perturbation is smaller compared with the full wind field in the fore-aft direction (x-axis). Therefore, analysing the responses associated with that direction will not give useful information in this case. Finally, there are many critical points in the monopile wind turbine that are usually regarded by designers and researchers (blade root, top of the tower, transition piece, etc). However, for this work, it is necessary to identify the point which better reflects the combined action of wind and wave. The point of interest in this work is where the seabed joints with the monopile, which is also known as mudline (ML).

In summary, attending the reasons previously exposed, only the results for the fore-aft shear force (F_X) and fore-aft bending moment (M_Y) at mudline are presented in the following sections. **Fig.2.8** shows the time series of response M_Y for rated wind speed and sea state 8, as an example. In all cases, the first 60 seconds of simulation, the transient part, are ignored to have more realistic sensitivity indexes. It is considered that the transient part fades away after 60 seconds because after that time no disproportionate peaks are observed in the time series. As a reference, the relation between the maximum hydrodynamic load and the maximum aerodynamic load for the sea states with the largest significant wave height is 1.97 (U_W=11.4 m/s, H_S=4.380 m, T_P=10.705 s), and 7.04 (U_W=25 m/s, H_S=7.908m, T_P=12.272 s).

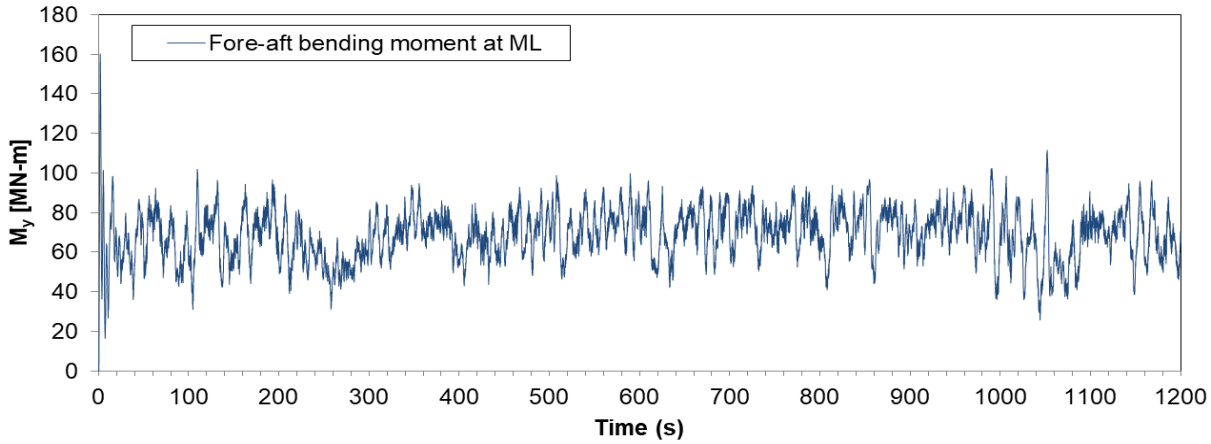

Figure 2.8: Time series of M_Y for U_W=11.4 m/s and sea state 8 (Mean=68.78 MN-m, STD= 12.72 MN-m)

The effect of the change in the sea states parameters can be more evident in a spectrum plot. **Figs. 2.9** and **2.10** show the spectrum of F_X for U_W=25 m/s and sea state 6 as examples. These spectrums have been calculated with WAFO [38]. **Fig. 2.9** shows the spectrum for the baseline and derived cases where the T_P has not suffered any variation. In this case, an upward displacement in the peak value can be noticed as long as the H_S increases, and the peak frequency remains the same for all the cases. On the other hand, **Fig. 2.10** shows the spectrum for the cases in which the H_S does not suffer any change with respect to its baseline case. As expected, a decrement in the peak frequency can be observed as long as the T_P increases.

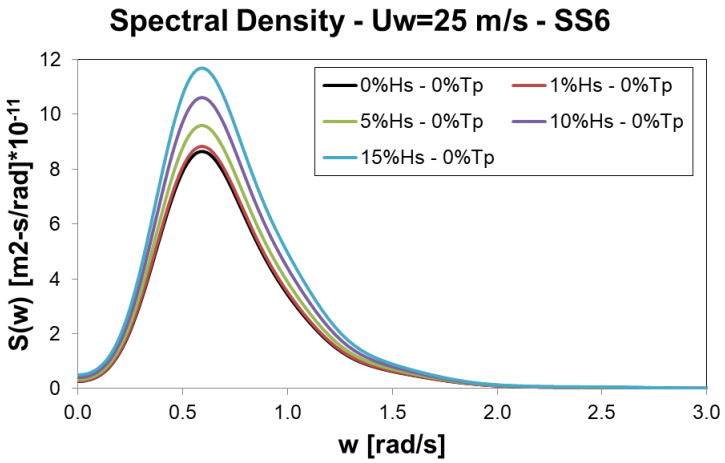

Figure 2.9: Spectrum of F_X for U_W=25 m/s, H_S=7.91 m, T_P=12.27 s, and ε=0%.

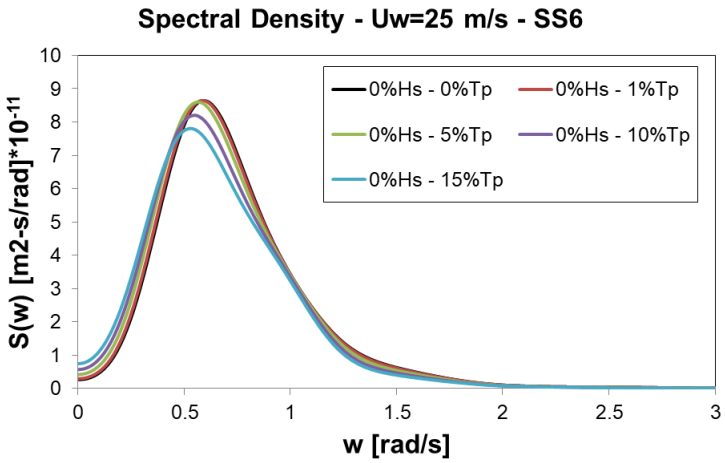

Figure 2.10: Spectrum of F_X for U_W=25 m/s, H_S=7.91 m, T_P=12.27 s, and δ=0%.

Some exemplary cases to show the relationship between the sensitivity indexes and the percentage variations in a specific environmental condition are given in **Figs. 2.11-2.14**. It is noticed a very clear linear relationship between $S(H_S)$ and its percentage variation (triangles) whereas the relation between $S(T_P)$ and $S(H_ST_P)$ to their respective percentage variations, could be well represented by a nonlinear function of second degree (circles and squares, respectively). Therefore, the sensitivity indexes can be modelled as Eqs. (2.10)-(2.12).

$$S(Hs) = A * (\delta) \tag{2.10}$$

$$S(Tp) = B_1 * (\varepsilon)^2 + B_2 * (\varepsilon) \tag{2.11}$$

$$S(HsTp) = C_1 * (\delta)^2 + C_2 * (\delta) \tag{2.12}$$

Where δ and ε are the variations expressed in percentages. $S(H_S)$, $S(T_P)$ and $S(H_ST_P)$ are the sensitivity indexes, and the coefficients A, B_1, B_2, C_1, C_2 can be found with a regression analysis using the least-squares method. The goodness of the fitting values can be measured by the coefficient of determination (r^2).

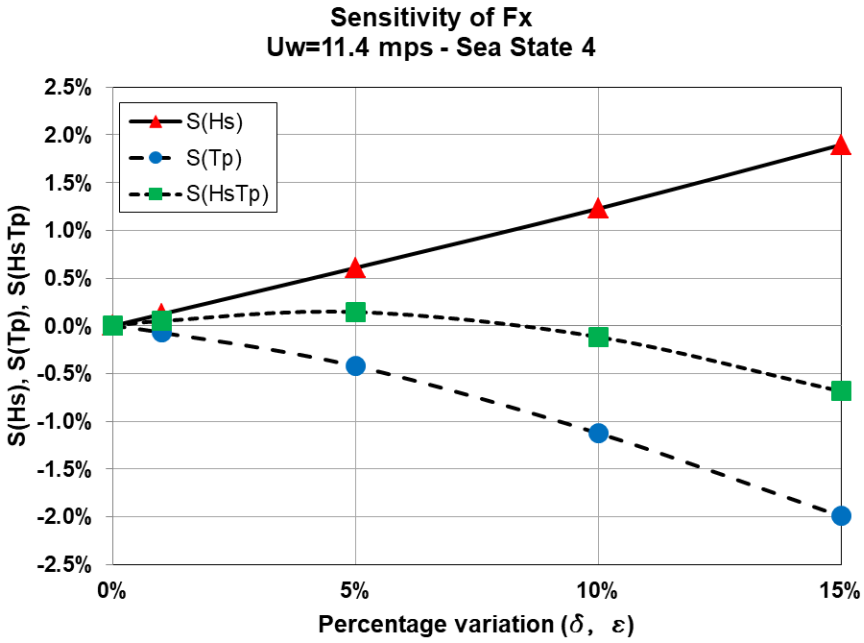

Figure 2.11: Sensitivity plot of F_X for U_W=11.4 m/s and sea state 4.

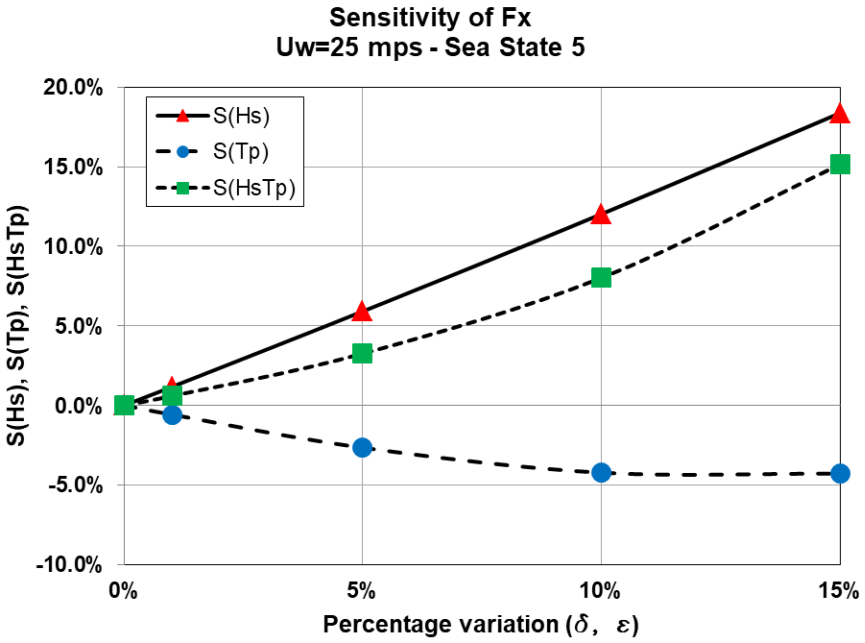

Figure 2.12: Sensitivity plot of F_X for U_W=25 m/s and sea state 5.

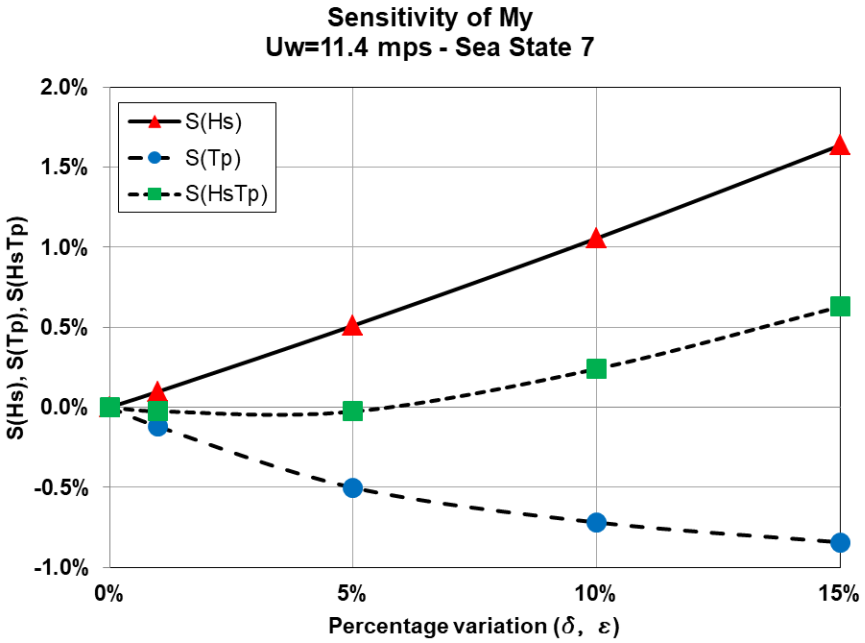

Figure 2.13: Sensitivity plot of M_Y for U_W=11.4 m/s and sea state 7.

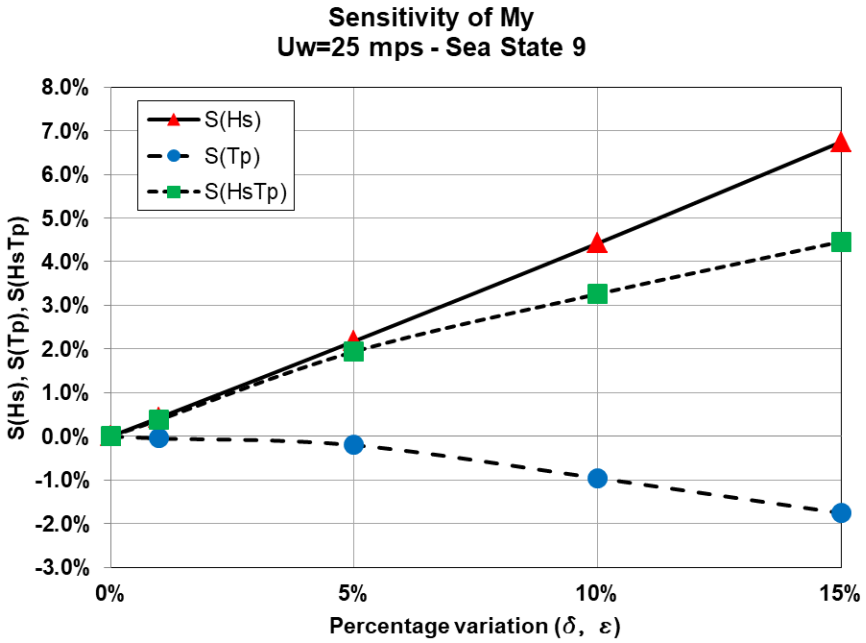

Figure 2.14: Sensitivity plot of M_Y for U_W=25 m/s and sea state 9.

Tables 2.8-2.11 summarize the values of r^2 coefficients for each environmental condition and each sensitivity index. The coefficients are coloured according to the goodness of fitting, green for the best relationships and red for the worst cases. **Table 2.8** and **2.9** are referred to the fore-aft shear force at mudline (F_X) whereas **Table 2.10** and **2.11** are for the fore-aft bending moment at mudline (M_Y). In both cases, the coefficients are grouped by the mean wind speed considered in the simulation. In general, the r^2 coefficients show that the sensitivity coefficients fit well to the linear and quadratic models. Only a few cases have an r^2 lesser than 98% with a minimum of 91.17%.

Table 2.8: Coefficient of determination of sensitivity indexes for F_X.

EC		1	2	3	4	5
U_{RATED}	$S(H_S)$	99.97%	99.88%	99.97%	99.98%	99.98%
	$S(T_P)$	100.00%	99.33%	99.75%	99.99%	99.88%
	$S(H_ST_P)$	99.80%	99.76%	96.79%	99.90%	98.16%
$U_{CUT-OUT}$	$S(H_S)$	99.99%	100.00%	100.00%	100.00%	99.99%
	$S(T_P)$	100.00%	99.83%	99.87%	99.99%	99.97%
	$S(H_ST_P)$	100.00%	100.00%	96.84%	99.98%	99.98%

Table 2.9: Coefficient of determination of sensitivity indexes for F_X.

EC		6	7	8	9	10
U_{RATED}	$S(H_S)$	99.99%	100.00%	100.00%	100.00%	100.00%
	$S(T_P)$	100.00%	99.91%	99.99%	100.00%	99.47%
	$S(H_ST_P)$	99.92%	99.98%	99.98%	100.00%	99.96%
$U_{CUT-OUT}$	$S(H_S)$	99.99%	100.00%	100.00%	100.00%	100.00%
	$S(T_P)$	97.13%	96.90%	98.04%	99.96%	99.92%
	$S(H_ST_P)$	99.97%	99.94%	100.00%	100.00%	99.95%

Table 2.10: Coefficient of determination of sensitivity indexes for M_Y.

EC		1	2	3	4	5
U_{RATED}	$S(H_S)$	99.98%	99.65%	99.70%	97.49%	98.67%
	$S(T_P)$	99.99%	99.78%	99.02%	99.86%	99.98%
	$S(H_ST_P)$	91.17%	99.85%	99.04%	99.85%	99.97%
$U_{CUT-OUT}$	$S(H_S)$	99.97%	99.98%	99.98%	99.97%	99.94%
	$S(T_P)$	99.98%	100.00%	99.96%	99.99%	99.94%
	$S(H_ST_P)$	99.70%	100.00%	99.95%	99.93%	99.88%

Table 2.11: Coefficient of determination of sensitivity indexes for the M_Y.

EC		6	7	8	9	10
U_{RATED}	$S(H_S)$	99.92%	99.96%	99.98%	99.99%	99.97%
	$S(T_P)$	100.00%	99.86%	100.00%	100.00%	99.95%
	$S(H_ST_P)$	100.00%	99.65%	99.75%	100.00%	99.92%
$U_{CUT-OUT}$	$S(H_S)$	99.97%	99.99%	99.99%	99.99%	99.97%
	$S(T_P)$	99.85%	99.75%	99.94%	99.67%	99.99%
	$S(H_ST_P)$	99.97%	99.92%	99.99%	99.96%	99.54%

To develop a model which could predict any sensitivity coefficient in the corresponding ECL, it is necessary to use a polynomial regression model which could be able to represent all the sensitivity coefficients as a function of the wave height and peak period for any sea state. In our case, for polynomial interpolation, it is necessary to define two vectors which reflect the degree of the polynomial model, Eqs. (2.13) and (2.14). The fitting polynomial is represented by a matrix of coefficients (P), Eq. (2.15). Through a matrix multiplication, Eq. (2.16), any specific

sensitivity coefficient (SCF) can be obtained. It is also possible to use the expanded formula for this polynomial, Eq. (2.17).

$$\overrightarrow{H_S} = [1 \quad H_S \quad H_S^2 \quad H_S^3] \tag{2.13}$$

$$\overrightarrow{T_P} = [1 \quad T_P \quad T_P^2 \quad T_P^3] \tag{2.14}$$

$$P_k = \begin{bmatrix} p_{00} & p_{01} & p_{02} & p_{03} \\ p_{10} & p_{11} & p_{12} & 0 \\ p_{20} & p_{21} & 0 & 0 \\ p_{30} & 0 & 0 & 0 \end{bmatrix}_k \tag{2.15}$$

$$\{SCF\}_k = \overrightarrow{H_S} \cdot P_k \cdot \overrightarrow{T_P}^T \tag{2.16}$$

$$\{SCF\}_k = \sum_{i=0}^{n} \sum_{j=0}^{n} \{p_{ij}\}_k \cdot Hs^i \cdot Tp^j \tag{2.17}$$

A third-degree polynomial model has been considered necessary because the relation between H_S and T_P is a non-injective function and shows a nonlinear behaviour (See **Fig. 2.4** and **2.5**). However, we will see in the next paragraphs that in some cases there could be some terms that can be neglected as their contribution to the sensitivity index calculation is very low. The fitted polynomial coefficients (PCF), Eq. (2.15), are summarized in **Tables 2.12** and **2.13** (Fore-Aft Shear Force), and **2.14** and **2.15** (Fore-Aft Bending Moment).

As two operational wind speeds, two dynamic responses, and five sensitivity coefficients have been considered then, there are 20 SCF to predict. Each specific coefficient can be identified by the index 'k' where $k \in \{1,2,3,\dots,20\}$. In both cases, they are referred to their specific operational wind speed and are presented with their respective r^2 parameter to show the goodness of the fit. In general, the polynomial models show good fitting, only the SCF C_2 for F_X and M_Y, and C_1 for M_Y have a low r^2 value but, they could be still considered to be acceptable as they are over 88%.

Table 2.12: Fitted polynomial coefficients for F_X, U_W=11.4 m/s.

$\{p_{ij}\}$	U_W=11.4 m/s				
	A {k=1}	**B_1 {k=2}**	**B_2 {k=3}**	**C_1 {k=4}**	**C_2 {k=5}**
p_{00}	-0.136	1.511	1.21E-03	2.152	-0.182
p_{10}	0.963	5.287	-1.548	4.592	-0.679
p_{01}	3.45E-02	-0.791	5.39E-02	-1.027	0.110
p_{20}	-0.562	8.770	1.85E-02	12.220	-0.770
p_{11}	0.286	-12.820	1.092	-15.900	1.670
p_{02}	-7.48E-03	0.230	-1.87E-02	0.290	-3.18E-02
p_{30}	3.66E-02	2.44E-02	-0.146	-0.217	-0.104
p_{21}	-2.20E-02	1.063	-7.99E-02	1.336	-0.127
p_{12}	-7.88E-03	0.353	-3.24E-02	0.435	-4.83E-02
p_{03}	8.93E-05	-2.67E-03	3.02E-04	-3.31E-03	4.58E-04
r^2	**100.00%**	**99.71%**	**99.96%**	**99.78%**	**100.00%**

Table 2.13: Fitted polynomial coefficients for F_X, U_W=25 m/s.

$\{p_{ij}\}$	U_W=25 m/s				
	A {k=6}	**B_1 {k=7}**	**B_2 {k=8}**	**C_1 {k=9}**	**C_2 {k=10}**
p_{00}	0.572	-4.599	0.896	-3.337	1.508
p_{10}	0.898	70.190	-14.720	67.880	-14.880
p_{01}	-0.665	-71.580	14.380	-71.140	14.780
p_{20}	-0.391	-53.740	10.450	-53.570	10.850
p_{11}	0.316	58.800	-10.910	59.690	-11.450
p_{02}	6.28E-02	2.748	-0.725	2.471	-0.708
p_{30}	2.85E-02	1.396	-0.385	1.146	-0.379
p_{21}	-4.38E-02	-2.874	0.693	-2.585	0.694
p_{12}	2.03E-02	0.606	-0.200	0.440	-0.191
p_{03}	-1.00E-02	-0.887	0.190	-0.857	0.193
r^2	**99.98%**	**99.75%**	**96.08%**	**100.00%**	**88.41%**

Table 2.14: Fitted polynomial coefficients for M_Y, U_W=11.4 m/s.

$\{p_{ij}\}$	U_W=11.4 m/s				
	A {k=11}	**B_1 {k=12}**	**B_2 {k=13}**	**C_1 {k=14}**	**C_2 {k=15}**
p_{00}	-1.25E-03	4.47E-02	3.74E-02	0.132	4.04E-02
p_{10}	1.76E-02	0.299	-0.126	0.209	-0.130
p_{01}	4.76E-04	-2.46E-02	-9.67E-03	-5.39E-02	-1.01E-02
p_{20}	3.71E-02	0.324	0.156	0.757	0.201
p_{11}	9.15E-03	-0.528	-8.90E-02	-0.930	-7.60E-02
p_{02}	-2.01E-04	8.14E-03	1.93E-03	1.55E-02	1.79E-03
p_{30}	-5.57E-03	2.12E-03	-2.06E-02	-3.30E-02	-2.77E-02
p_{21}	-1.79E-03	4.91E-02	9.63E-03	8.87E-02	7.41E-03
p_{12}	-3.12E-04	1.38E-02	2.15E-03	2.39E-02	1.75E-03
p_{03}	3.20E-06	-4.31E-05	-1.19E-05	-8.91E-05	-1.13E-05
r^2	**100.00%**	**99.99%**	**100.00%**	**99.98%**	**99.99%**

Table 2.15: Fitted polynomial coefficients for M_Y, U_W=25 m/s.

$\{p_{ij}\}$	U_W=25 m/s				
	A {k=16}	**B_1 {k=17}**	**B_2 {k=18}**	**C_1 {k=19}**	**C_2 {k=20}**
p_{00}	0.315	-1.897	0.323	-1.755	0.661
p_{10}	-1.425	35.800	-6.274	37.350	-8.318
p_{01}	1.315	-36.980	6.301	-39.150	8.256
p_{20}	1.080	-27.150	4.606	-28.730	6.148
p_{11}	-1.087	29.500	-4.919	31.500	-6.510
p_{02}	-5.50E-02	1.612	-0.291	1.658	-0.374
p_{30}	-4.70E-02	0.792	-0.152	0.759	-0.211
p_{21}	7.30E-02	-1.573	0.285	-1.576	0.384
p_{12}	-2.04E-02	0.376	-7.47E-02	0.350	-0.101
p_{03}	1.79E-02	-0.469	8.11E-02	-0.490	0.107
r^2	**99.93%**	**97.85%**	**99.84%**	**91.01%**	**90.64%**

These PCF allow us to compare the sensitivity coefficient models. The first thing that can be observed is that the absolute values of most of the PCF for the rated wind speed are relatively lesser than the respective values corresponding to the cut-out wind speed. From **Tables 2.12**-**2.15**, it is noticed that many PCF have absolute values near to zero around an order of 10^{-2} or even much lesser. The PCF at the bottom of the table (p_{30}, p_{21}, p_{12}, p_{03}) are more significant because they are coefficients for third-degree terms (Hs^3Tp^0, Hs^2Tp^1, Hs^1Tp^2, etc.). Therefore, when the multiplication is done, the whole product acquires more importance for determining the corresponding sensitivity index. In contrast, low PCF values in the top of the table (p_{00}, p_{10}, p_{01}, p_{20}, etc.) mean that their contribution to the sensitivity index could be neglected, especially for the independent (p_{00}) and linear terms (p_{10} and p_{01}).

From the previously exposed paragraph, for cut-out wind speed all the terms are relevant for the sensitivity indexes as all the PCF are relatively high. On the other hand, there are some low degree terms for the rated wind speed case that are very small and they can be probably set to zero in a new regression analysis considering lesser terms. For example, in **Table 2.14**, X=My, U_W=11.4 m/s, k=11, the coefficient p_{01} is 4.76E-04 (≈0). As a consequence, if the coefficients p_{00} (Hs^0Tp^0 term) and p_{01} (Hs^0Tp^1 term) for F_X and M_Y at rated wind speeds are analysed, it could be observed that in many cases they have very low values. In those cases, the terms have a low contribution to the SCF, and it means that a variation in the wave height will impact more in the calculation of the sensitivity coefficients than the peak period.

CHAPTER III. INFLUENCE OF WIND SHEAR UNCERTAINTY IN LONG-TERM EXTREME RESPONSES OF AN OFFSHORE MONOPILE WIND TURBINE

3.1 INTRODUCTION

According to the International Energy Agency (IEA), the wind energy sector is expected to become a $1 trillion business in the next two decades. Among the main reasons why the wind energy, especially offshore, is becoming a popular source of energy are: a) the need for affordable low-carbon technologies, b) the quick growth of the offshore market (near 30% per year between 2010 and 2018), c) the vast untapped potential of offshore wind, d) the technology improvements which allows wind power plants to reach capacity factors up to 50%, and e) the lower resource variability [6].

Regarding the economical aspect of offshore wind turbines (OWT), foundations account for nearly a quarter of total project costs. The intrinsic aspects of each offshore project will depend on finding an optimal option regarding variables as the distance from shore, water depth, ease of access, and quality of wind resource. Two types of foundations are used in the offshore environment: fixed and floating. Fixed foundations have been preferred by most projects installed in shallow waters (less than 50 m), especially the relatively low-cost monopile foundations, more details about fixed foundations can be found in [39]. Floating foundations for deeper waters is considered the next frontier for offshore wind to access a vast and stable resource, which is currently only affordable for projects with specific and well-known characteristics. On the other side, the wind turbine itself accounts for 30-40% of the total cost of the offshore project. Seeking to reduce the unitary cost of the component, manufacturers are developing larger turbines and thus, projects could be benefited from economies of scale. However, larger turbines require larger foundations, and larger foundations require precise knowledge and understanding of the conditions it is subjected to [6].

Wind turbines are complex machines that are subjected to many environmental parameters, and also the control system of the turbine adds nonlinearities to the behaviour of the system [40]. Due to this, the wind turbine experiences loads and produces responses that govern the design of the entire system. Generally, there are two approaches for structural design, the deterministic and the probabilistic/stochastic. The deterministic approach is easier to apply; but, it usually leads to an over or under-designed system. The probabilistic approach is recommended to get a reliability-based design [11], [41]. For more details about reliability-based methods, the reader is referred to [42]. The probabilistic approach is also considered in IEC 61400 [43] and other industry guidelines for load analysis of wind turbines.

In the current state of the art of structural reliability it is usual to take some environmental conditions as stochastic i. e. wind speed, wave height, wave period, among others. However, some other parameters are considered as deterministic e. g. wind shear, turbulence intensity, etc. The values of these parameters are in most cases taken from recommended values in standards or simply assumed. This consideration could produce some uncertainties in the calculation of wind turbine responses as every site is expected to have specific characteristics. However, not many studies addressing the assessment of the impact that these uncertainties can have in the OWT responses have been found in the literature. Ernst et al. [44] performed a study for the site “FINO 1”. The focus of their research was related to the effects of WSC and turbulence intensity (TI). They performed a comparison of fatigue and extreme loads calculated with the specific parameter of the site against loads calculated with values recommended in IEC standard 61400-3 [35]. They focused their attention on the flapwise and edgewise bending moment at the blade root. It was found that fatigue and extreme loads (at blade root) are more affected by the TI than by the WSC. It was also concluded by the author that the IEC value is very conservative for the design of the rotor blades. They also found that WSC has a very strong dependence on wind speed. Kim et al. [45] studied the effect of different substructures (monopile and jacket) in the ultimate and fatigue loads, for this case the WSC was taken as 0.14 and the turbulence intensity around 15%. The results were focused only on the

superstructure (wind turbine) and no attention was given to the mudline point. Slot et al. [46] performed a study considering 99 international sites to evaluate the influence of WSC in fatigue loads of an onshore wind turbine. In this case, the error found for fatigue damage assessment was between 13% of under-prediction to 16% of over-prediction.

Lastly, Robertson et al. [7] focused their research on a sensitivity analysis of an onshore wind turbine. The main objective of this research was to find the most influential input parameters for turbine power, fatigue and ultimate loads during the operational regime. They used the elementary effects method for the assessment of parameters sensitivity; even if this method was useful mostly for ranking parameters instead of providing accurate sensitivity indicators by using more computationally intensive sensitivity analysis. The authors pointed out that their analysis was useful to provide a list of the most important parameters to examine in more detail in future work. The results of this analysis showed that WSC was most influential for ultimate loads in most points of the wind turbine, except for the tower-base bending moment and Blade-root pitch moment. In the case of fatigue loads, WSC was among the top three of the most influential parameters. It is important to highlight that this study was performed in an onshore wind turbine and then, wave loads were not considered. Also, it did not consider a specific site and thus, no dependence or conditionality among environmental variables was considered e. g. joint probability distributions. Finally, the most recent work found in the literature which deals with the influence of uncertainty of deterministic parameters of environmental conditions for OWT was made by Chen et al. [47]. They studied the influence of variable TI on extreme loads of a monopile OWT. For this purpose, they used the MECM to find the most important wind speed and the corresponding extrapolated long-term extreme. Results for the fore-aft shear force at mudline were assessed.

Not much attention has been given to the effects of deterministic values of environmental conditions to design loads of support structure of OWT as it can be noticed. This work seeks to provide some insights about the influence of different values of WSC in the extrapolated long-term responses (ultimate response) of a bottom fixed OWT. This parameter has been identified as relevant as it has a

direct relationship with the mean wind speed at hub height, an important input parameter for OWT design. Through a joint probability distribution the WSC can influence the main wave parameters i. e. wave height and peak spectral period. Therefore, the study of this type of relationship during a normal OWT operation acquires great importance.

3.2 WIND SHEAR

The offshore environment has its proper particularities compared to land sites. The main difference is the low surface roughness which causes stronger winds with good vertical uniformity, small wind speed changes, and lower turbulence intensity. Due to a lack of information in most offshore sites, IEC recommends a power-law wind shear exponent (WSC) of 0.14 for operational conditions of offshore wind turbines with a lower value of 0.11 for extreme conditions. But, those values are mainly referential as WSC is depending on the intrinsic atmospheric conditions of the site, and it is heavily influenced by other aspects as the distance from the turbine to the coast, ocean waves, surface temperatures, climate change, etc. Values between 0.06 and 0.16 have been found for the North Sea [48] and western Atlantic [49]. Representative values of WSC for the offshore environment are given in [2], see **Table 3.1**.

Table 3.1: Representative WSC values for the offshore environment [2].

WSC	Condition
0.05	Extreme storm conditions, such as Nor'easters
0.08	Low end of mean annual offshore wind conditions
0.11	IEC-specified shear for extreme conditions for offshore wind turbines
0.14	IEC-specified operational conditions for offshore wind turbines
0.17	Mean annual near-shore wind conditions (high offshore value)

In the specific case of bottom fixed OWTs which are mainly located in shallow waters near to coastlines and islands, the WSC can be highly influenced by the transition zone within the marine atmospheric boundary layer (MABL, also known as an internal boundary layer) which starts at the land-water interface and

propagates seaward for several kilometres until it becomes stable. Another parameter that influences the stability of the atmospheric layer near to shore is the temperature gradient between the atmosphere and the sea surface which could create low-level jets (zones of high wind speeds in the upper layers of the MABL). This situation is particularly special when there is cold air blowing over warm water (a usual condition in fall and winter in the northern hemisphere). Unstable conditions of the lower MABL are associated with this situation and it could cause vertical mixing and relatively low WSC values. A broader analysis of all these phenomena related to wind behaviour in an offshore environment can be found in [2]. Unfortunately, the lack of quality wind speed measurements at or near the hub height of OWT is common. It does not contribute to reducing the uncertainty in the estimation of WSC because it cannot be accurately found. Most offshore wind data comes from buoys or satellite estimations for heights between 5 to 10 m. Then, extrapolation methods become necessary to know wind speeds at higher heights, and then the uncertainty in WSC is propagated through all the stages of the OWT design.

Some efforts to determine the WSC in specific offshore sites have been found in the literature. Camp et al. [50] performed a monitoring campaign to measure the environmental conditions experienced by one of the turbines in the Blyth (UK) offshore wind farm. They found values of WSC between 0.05 (from sea to land direction) and 0.29 (from land to sea direction). Peña et al. [51] analysed different offshore sites in the North and Baltic seas under the project NORSEWInD. In this case, the values of WSC were in the range of 0.05 to 0.12, they also verified the relation that exists between the WSC and the wind speed. In the research performed by Viselli et al. [52], the Gulf of Maine was studied. They found WSC values between 0.13 and 0.16 (with an outlier of 0.19). The site FINO 1 is a matter of analysis for Krogsæter et al. [53], the main conclusion of this work is that a WSC value of 0.1 could be appropriate for OWT design. In the research of Corrigan et al. [54], a WSC value of 0.1038 was found for the Cleveland water intake crib zone in Lake Erie. Shu et al. [55] focused their research on an offshore site in Hong Kong (South China Sea). They found values from 0.036 to 0.1161 for WSC. For site FINO 3, a value of 0.2 for neutral conditions and values between

0.4 and 0.08 for unstable conditions were found by Gualtieri [56]. The dependence between WSC and surface temperature is highlighted by Albani et al. [57]. In this research, the WSC for near-coastal sites is studied, and values between 0.47 (for coastal sites with many buildings and trees) to 0.20 (for flat coastal sites) were found. Later, it is shown that these values tend to decrease with higher surface temperature, according to the author. Moreover, Gonzales et al. [58] focused his research on Anholt wind farm. In this study, a WSC range between 0.06 and 0.14 was identified. In the present work WSC values of 0.06, 0.08, 0.10, 0.12 and 0.14 will be used to explore their influence in 50yr long-term extreme responses.

3.2.1. Wind power-law

A practical way to correlate wind speeds at two different heights (less than 150 m) is the power-law (also known as the Hellman exponential law) [59], see Eq. (3.1). In **Fig. 3.1**, different wind profiles corresponding to different WSC are observed. Only heights between 153 m and 27 m are showed because it corresponds to the length of the entire rotor of the NREL 5MW wind turbine (Rotor diameter=126 m, Hub height=90m). The percentages of variation are referred to the mean wind speed at hub height. For a WSC of 0.06, the range of variation of wind speed for upper and lower blade tip is between +3.2% to -7.0% whereas, for a WSC of 0.14 this range varies from +7.7% to -15.5%.

$$\frac{U_H}{U_{ref}} = \left(\frac{H}{H_{ref}}\right)^{WSC} \tag{3.1}$$

Where:

U_H, H= Mean wind speed and height referred to the still water level (SWL).

U_{ref}, H_{ref} = Mean wind speed, and height of reference.

WSC= Wind shear coefficient.

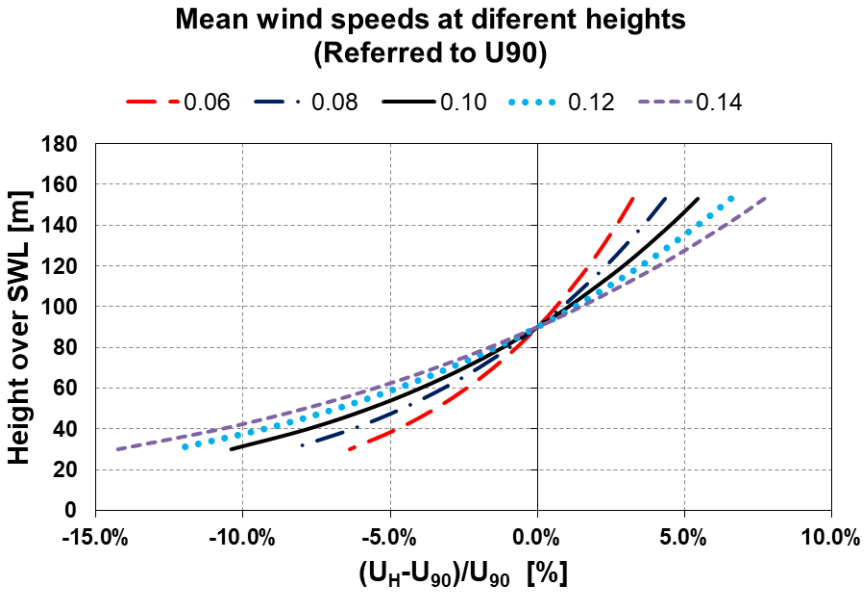

Figure 3.1: Wind profiles for different values of wind shear coefficients (WSC) over the length of the rotor.

3.3 MODIFIED ENVIRONMENTAL CONTOUR METHOD

Haver et al. [29] proposed the Environmental Contour Method (ECM) as a practical approach for estimating long term extremes by a short term analysis. This analysis was based on the IFORM (First Order Reliability Method) to find the most important environmental conditions associated with a specific reliability target level. Also, this method used joint probability distributions, and through the Rosenblatt transformation, the physical parameters could be transformed into a non-physical space and vice versa.

The method is very practical. First, a sphere in a non-physical standardized normal space (U-space) can be generated for a given annual exceedance probability q or desired return period N, the radius of this sphere is calculated using Eq. (3.2), $\mathbf{\Phi}^{-1}$ denotes the operator of the inverse cumulative distribution function (cdf) of the standard normal distribution, and **md** is the expected number of d-hour sea states per year. Using Eq. (3.3), the three non-physical variables associated with wind speed (U_W), wave height (H_S) and peak period (T_P) can be obtained. Then, the physical parameters can be calculated by using inverse transformations, Eqs. (3.4)-(3.6). In these equations, **F** denotes the cumulative distribution function of the respective environmental parameters. With all the combinations of these environmental parameters, it is possible to generate a

contour surface (ECS) or contour lines (ECL) which represent all the combinations of environmental conditions corresponding to the desired annual exceedance probability.

$$\beta = \Phi^{-1}\left(1 - \frac{1}{N * m_d}\right) = \Phi^{-1}\left(1 - \frac{q}{m_d}\right) \tag{3.2}$$

$$\beta^2 = U_u^2 + U_{Hs}^2 + U_{Tp}^2 \tag{3.3}$$

$$\Phi(U_u) = F(u) \tag{3.4}$$

$$\Phi(U_{Hs}) = F(Hs|u) \tag{3.5}$$

$$\Phi\left(U_{Tp}\right) = F(Tp|u, Hs) \tag{3.6}$$

Although this method is useful for most marine structures, some problems have been detected when dealing with devices with survival strategies e. g. offshore wind turbines, wave energy converters, etc. Due to the control system of these devices, the assumption of monotonic behaviour of loads required by the ECM is violated, and then the method does not perform very well for long-term extreme estimation. To bypass this restriction, Li et al. [31] proposed the Modified Environmental Contour Method (MECM). This method, which is mainly based in Eqs. (3.7) and (3.8), is used to bypass the discontinuity produced by the cut-out wind speed when the OWT passes from operational to parked condition. In Eq. (3.8), u_N, h_N, t_N represent the environmental condition leading to the largest extreme response on the N-yr contour

$$F_{X_{1-hr,50-yr}}(\xi) = \left[F_{X_{1-hr,N-yr}}\right]^{50/N} \tag{3.7}$$

$$\left[F_{X_{1-hr,N-yr}}\right]^{50/N} \coloneqq \left[F^{ST}_{X_{1-hr|U_W,H_S,T_P}}(\xi|u_N, h_N, t_N)\right]^{50/N} \tag{3.8}$$

The procedure of this method is as follows: a) Select multiple wind speeds between rated and cut-out wind speeds, b) Calculate their corresponding return periods, Eqs. (3.9)-(3.10), c) Find the most probable sea states associated with each wind speed, Eq. (3.11), d) Get the largest value of the most probable 50yr response by using a load extrapolation method (see next section), e) Determine the important wind speed (**U_W***) and their correspondent return period (**N***) associated to the largest most probable 50-yr response, f) Test additional environmental conditions in the ECL generated for return period **N***. The largest value among all the results is the long-term extreme response. In Eq. (3.3)-(3.6)

and (3.10), **u** represents the wind speed at 10 m (or the height at which the wind speed probability distribution was calculated). It would be the equivalent to $\mathbf{U_{ref}}$ in Eq. (3.1).

$$F_{U_W}(u) = \Phi(\beta) = 1 - \frac{1}{N \cdot md} \tag{3.9}$$

$$N = \frac{1}{\left(1 - F_{U_W}(u)\right) \cdot md} \tag{3.10}$$

$$F(H_S|U_W) = 50\% \;\; ; \;\; F(T_P|U_W, H_S) = 50\% \tag{3.11}$$

3.4 LOAD EXTRAPOLATION

Wind turbines have been growing in size and power since the last decade and so, their weights and the loads they will expect during their service life. The offshore environment is characterized by stochastic weather conditions and then, an OWT is expected to experience various loading conditions during operation. The assessment of extreme events in which loads exceed the desired reliability level is of vital importance in the design phase to ensure the safety of the structure, and avoid catastrophic undesired events. This assessment could be done by measurement campaigns or by performing coupled simulations. In any case, to cover various loading responses, a proper extrapolation procedure will be necessary to estimate loads during the entire service life [60].

Most of the relevant standards for offshore design [35], [61] recommend the use of statistical extrapolation with a recurrence of 50 years to determine the extreme loads in an operating state. More details about extrapolation methods can be found in [62]–[64]. In the present work, the Global Maxima Method (GMM) is used for load extrapolation. The extremes values of aero-hydro-servo-elastic simulations will be fitted to a Gumbel distribution, Eq. (3.12). **X** is the response analysed, $\boldsymbol{\mu_G}$ and $\boldsymbol{\beta_G}$ are the location and shape parameters (Gumbel parameters), respectively. For this type of distribution, the most probable value (also known as the mode) is shown in Eq. (3.13).

$$F(X) = exp\left(-exp\left(-\frac{(X - \mu_G)}{\beta_G}\right)\right) \tag{3.12}$$

$$Mo_X = \mu_G \tag{3.13}$$

For MECM, a load extrapolation from 1-hr extremes to 50yr is required. After extrapolation, the most probable value of the Gumbel distribution is given by Eq. (3.14). In this equation, **N** is the return period of the environmental condition (EC) considered. The parameter 'r' will depend on the length of simulation from which we have extracted the extremes for fitting purposes. The value of r is 1, 3 or 6 if the extremes for Gumbel fitting come from 1hr, 20-min or 10-min simulations, respectively.

$$Mo_X = \mu_G + \beta_G \cdot ln\left(r \cdot \frac{50}{N}\right) \tag{3.14}$$

In the original definition of the MECM, the authors used 10-min simulations. This simulation length attends the criteria of the spectral gap of wind variation in the wind spectrum, and then, wind can be considered a stationary process during this period. On the other side, a simulation length of 6 hours is a common practice for floating structures to account for the spectral gap of waves at low frequency and low natural frequencies of floating structures [65]. Some studies addressing how the simulation length affects the load extreme prediction have been found in the literature [65]–[68]. The discussion of which simulation length is appropriate falls out of the scope of this research, and it will be addressed in further research.

Although a monopile OWT cannot be considered a floating structure to justify the use of long simulations, it will be influenced by wave loading, and then the load extrapolation will be made from 20-min simulations in this work. Finally, the main problem in reliability analysis is associated with dealing with the estimation of small probabilities to capture rare events. To reach a good level of accuracy, a sufficient number of simulations are necessary but, in contrast, there is a computational cost, in terms of time, which is usually prohibitive. It has been suggested that 90 stochastic simulations should be enough to reach a good level of accuracy in the load extrapolation and thus, capture the stochasticity of the combined wind and wave loading [31], [69]. For this research, 100 simulations of 20-min with different random seeds are performed for each EC analysed.

3.5 NUMERICAL MODEL

The model used in this work is the NREL 5MW wind turbine supported by a monopile foundation. This is a model widely employed in the literature. All the details of this model can be found in [32]. The main dimensions of the wind turbine are shown in **Fig. 3.2**.

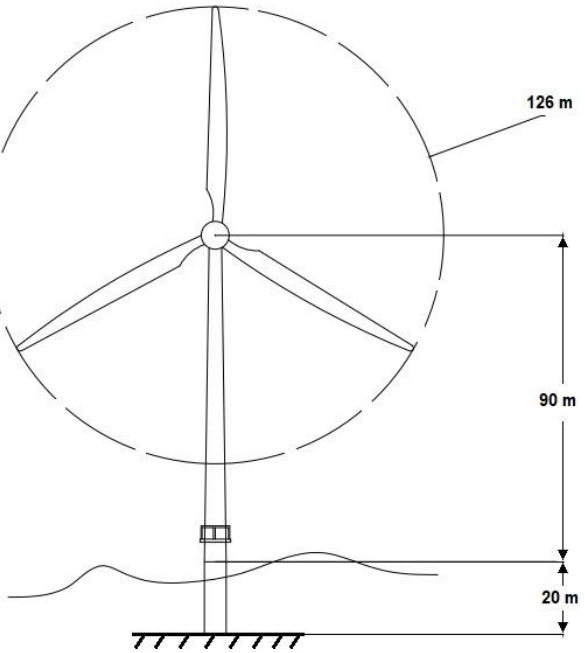

Figure 3.2: Main dimensions of the NREL 5 MW Wind Turbine

Two stochastic simulators are used. First, the inflow wind profiles for each wind speed and specific WSC are generated in TurbSim [36]. The main details of the wind simulation are summarised in **Table 3.2**. The wind fields generated in TurbSim are used to feed FAST [70] and simulate the structural and mechanical responses. For this work, it was only necessary to modify the input files for HydroDyn [71]. For each EC, wave height (H_S), peak period (T_P), and cut-off frequencies of the wave spectrum were the only input values treated as variables. The main details of the inputs considered for the simulation of wave conditions are presented in **Table 3.3**.

An important part of the simulations is to properly set the Morison Coefficients (Drag, added mass and pressure). For this work, the coefficients have been taken as C_D=0.9, C_A=0.75, C_P=1, for a detailed explanation about the selection of these values the reader is referred to [72]. Other input parameters have been left as they were defined in the NREL 5MW baseline.

Table 3.2: Details of configuration for wind simulation in TurbSim.

Parameter	Value
Turbulence model	Kaimal
IEC turbulence characteristic	B (I_{REF}=0.14)
IEC turbulence type	NTM
Wind profile type	Power Law
Hub height	90 m
Coherence model	IEC 61400-1, 3° ed.
Simulated Time [s]	1260
Time Step [s]	0.05

Table 3.3: Details of configuration for wave simulation in FAST-HydroDyn.

Parameter	Value
Incident wave kinematics model	JONSWAP
Peak-shape parameter	3.3
Analysis time for incident wave calculations [s]	3630
heading direction	0°
Water depth [m]	20

The site considered for this study is the one labelled as “Site 15” presented by Li et al. [34]. The models for the joint probability distribution are summarized in **Table 3.4**, and the corresponding parameters of each model can be found in the previously mentioned study. Finally, all these models and workflows are implemented in a Python script to generate the output files from FAST. The post-processing for Gumbel fitting is made with WAFO [38].

Table 3.4: Models for the joint probability distribution in “Site 15”.

Parameter	Model
Mean wind speed at 10 meters height (u)	Marginal - Weibull 2 parameters
Significant wave height (H_S)	Conditional – Weibull 2 parameters
Wave spectral peak period (T_P)	Conditional – Log-normal

3.6 RESULTS

The first part of the MECM involves several simulations in the operational range of wind speeds to find the important conditions for load extrapolation (U_W*, N*). The first round of simulations is performed only for WSC=0.10 to get a first estimate of the location of the important speed. This step is not done for all the WSC as it is computationally expensive. Only results for the fore-aft shear force (F_X) and bending moment (M_Y) at mudline are presented as they are the responses that better reflects the combined action of wind and wave. The trends of the most probable extrapolated 50yr responses are presented in **Fig. 3.3** and **3.4**. It was deemed important to also show the trend of the extreme responses when the only wind (red circles) or only wave (blue squares) loads are acting over the monopile OWT. The long term response of F_X is mainly governed for wave loading, and the long term response of M_Y is governed by the wind as it can be observed.

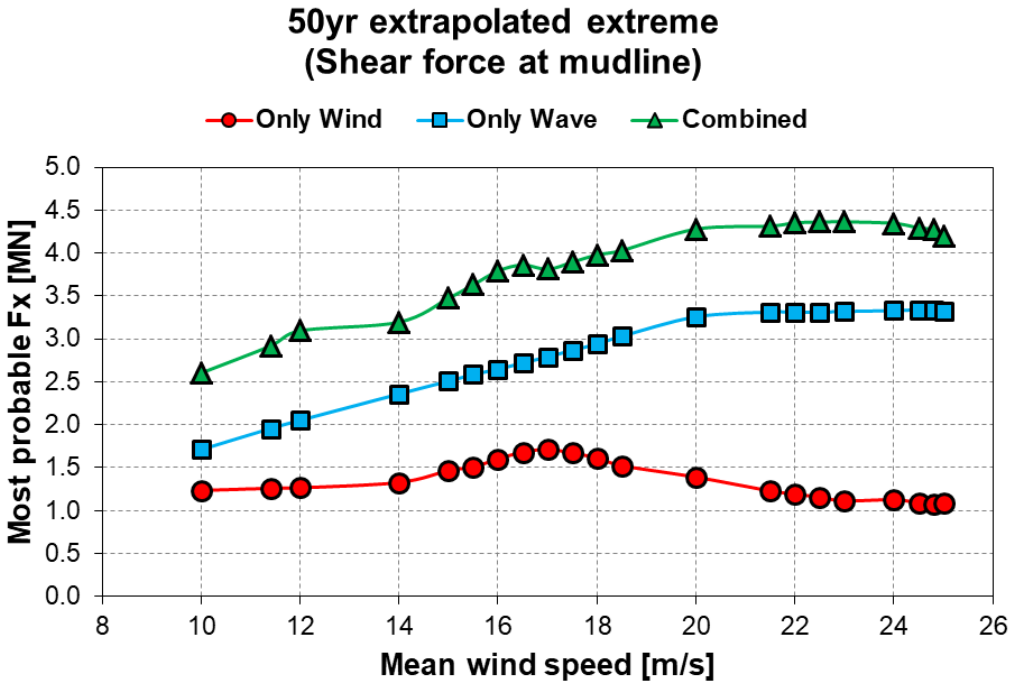

Figure 3.3: Most probable 50yr fore-aft shear force at mudline (WSC=0.10).

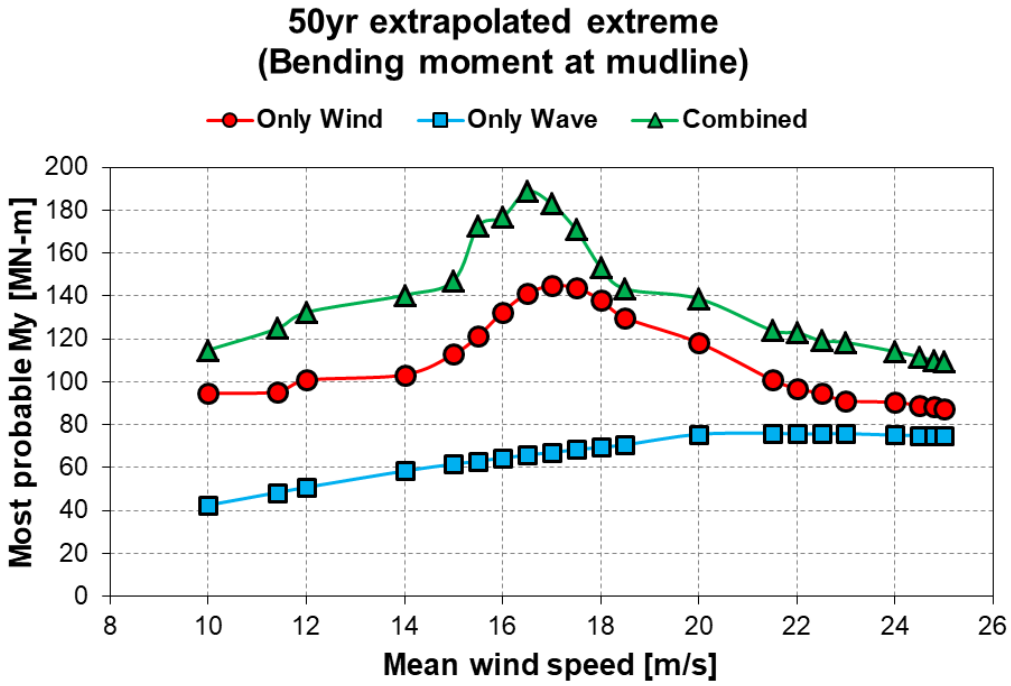

Figure 3.4: Most probable 50yr fore-aft bending moment at mudline (WSC=0.10).

The influence of wind and wave is much clearer if the 1hr extreme and the 50yr long term extreme are expressed in terms of their mean and standard deviation. For this purpose, a parameter 'k' is defined in Eq. (3.15). It measures how many standard deviations a parameter of interest (PoI) is away from the mean value. The standard deviation (σ) and mean (μ) are taken as the average of standard deviations and means from every 100 simulations in each EC, respectively.

$$k = \frac{(PoI - \mu)}{\sigma} \tag{3.15}$$

The k-value for 1-hr extremes of F_X and M_Y are presented in **Figs. 3.5** and **3.6**, whereas the k-values for the 50-yr long-term extremes are shown in **Figs. 3.7** and **3.8**, respectively. The governing parameter (wind or wave) of each response is noticed in these figures. Similar behaviour has been observed in other types of OWT (spar-type) [73]. As a consequence, the important wind speed (U_W*) for F_X has been identified to be around 23 m/s (see **Fig. 3.3**), whereas the U_W* for M_Y is expected to be in the vicinity of 16 m/s (see **Fig. 3.4**). Regarding fore-aft bending moment, the same wind speed has been identified in the literature [74], [75] as the important one for this type of response in a monopile OWT.

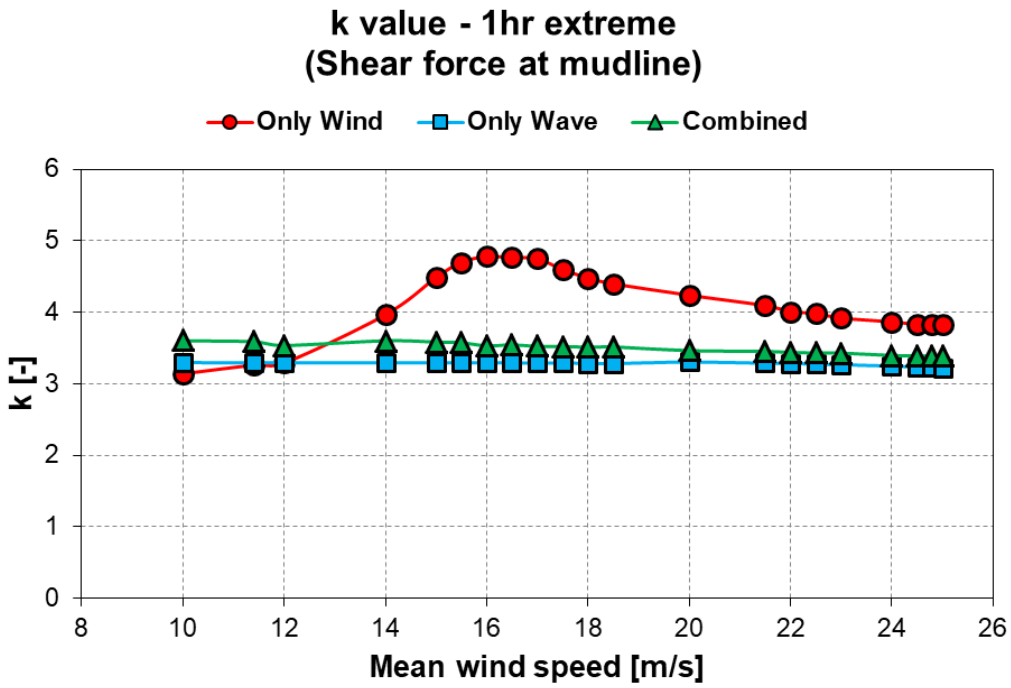

Figure 3.5: k-value for most probable 1hr extreme of F_X (WSC=0.10).

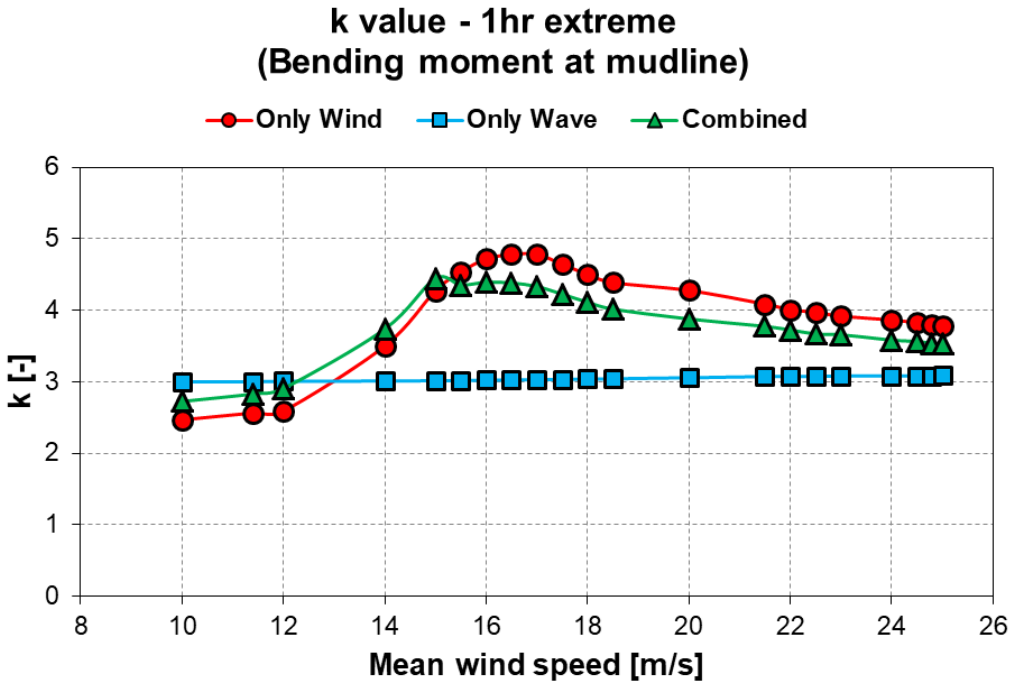

Figure 3.6: k-value for most probable 1hr extreme of M_Y (WSC=0.10).

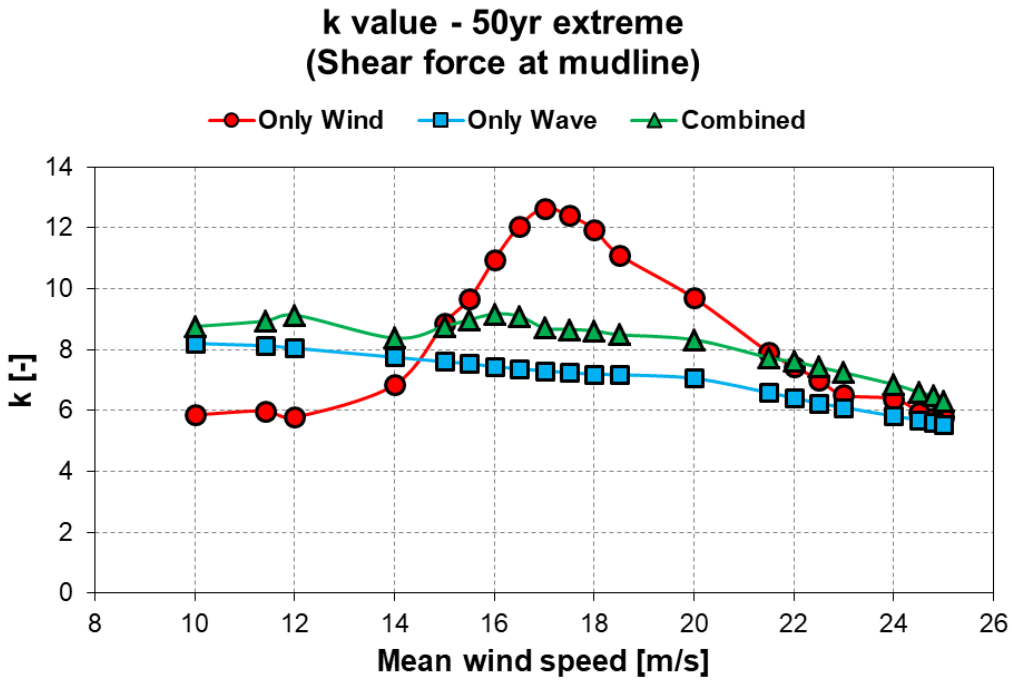

Figure 3.7: k-value for most probable 50yr extreme of F_X (WSC=0.10).

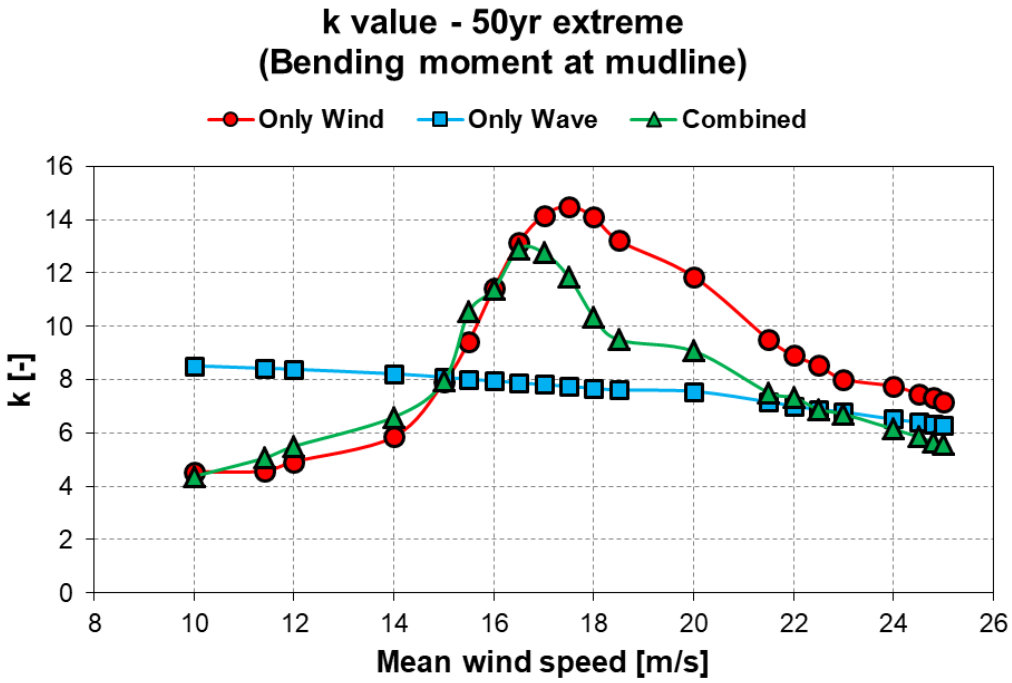

Figure 3.8: k-value for most probable 50yr extreme of M_Y (WSC=0.10).

With the first estimate of U_W* for F_X and M_Y, additional cases near to 16 m/s and 23 m/s are simulated to find the specific U_W* for each case. In this stage, cases for all the values of WSC are considered. **Tables 3.5** and **3.6** summarizes the environmental conditions identified as the most important by the MECM procedure. As it can be noticed, the largest value is always associated with a wind speed of 16.5 m/s for M_Y. In contrast, the wind speed associated with the largest extreme is changing for F_X. It starts at 20 m/s for the lowest WSC, then it moves to 23.5 m/s, and finally, the largest extreme is found at 24 m/s (WSC=0.14). The mean (μ), standard deviation (σ), Gumbel parameters and the 50yr extreme response for each EC are also shown. Once the U_W* and N* for each response are known, the final step of the MECM involves the simulation of additional environmental conditions located in the ECS with a return period N*. The procedure for this phase is the same as the traditional ECM, many ECs in the ECS need to be tested to find the combination which gives the largest extrapolated response. This combination is usually located near to the point with the highest wind speed or the highest wave height.

Table 3.5: Environmental conditions identified as the most important during the first phase of the MECM procedure, the corresponding statistical parameters (mean, standard deviation, Gumbel parameters) and the 50yr extrapolated extremes are given for each EC. Values for F_X is given in MN.

	WSC [-]	N [yr]	U_W [m/s]	H_S [m]	T_P [s]	μ	σ	μ_G	β_G	50-yr Extreme
F_X	0.06	1.29E-02	20.0	4.458	8.048	0.408	0.514	2.171	0.237	4.387
	0.08	8.18E-03	20.0	4.207	7.924	0.406	0.489	2.092	0.234	4.386
	0.10	3.07E-02	23.5	4.915	8.280	0.394	0.562	2.320	0.242	4.375
	0.12	1.79E-02	23.5	4.636	8.137	0.390	0.535	2.236	0.241	4.409
	0.14	1.38E-02	24.0	4.497	8.067	0.387	0.522	2.184	0.239	4.401

Table 3.6: Environmental conditions identified as the most important during the first phase of the MECM procedure, the corresponding statistical parameters (mean, standard deviation, Gumbel parameters) and the 50yr extrapolated extremes are given for each EC. Values for M_Y is given in MN-m.

	WSC [-]	N [yr]	U_W [m/s]	H_S [m]	T_P [s]	μ	σ	μ_G	β_G	50-yr Extreme
M_Y	0.06	2.38E-03	16.5	3.470	7.576	47.108	11.125	95.261	8.066	184.402
	0.08	1.78E-03	16.5	3.281	7.493	47.245	11.039	95.345	8.072	186.912
	0.10	1.36E-03	16.5	3.103	7.417	47.369	10.957	95.408	8.038	188.708
	0.12	1.07E-03	16.5	2.937	7.348	47.482	10.881	95.457	7.964	189.794
	0.14	8.66E-04	16.5	2.781	7.287	47.583	10.811	95.517	7.895	190.748

In this work, the ECs are searched in the ECLs located in the plane U_W-H_S, and the T_P is taken as the median value for a given U_W and H_S. Considering the return periods of **Table 3.5** and **3.6**, ECLs are generated (See **Fig. 3.9** and **3.10**) for each WSC, and five ECs between the points with the highest U_W and the highest H_S are tested. After simulation of these additional ECs, many of the environmental combinations presented in **Tables 3.5** and **3.6** remained as the ones with the largest 50yr extreme response, except for two conditions. The two first ECs of M_Y changed from the values presented in **Table 3.6** to the values showed in **Table 3.7**.

Finally, the sensitivity of 50yr long-term extremes is calculated from values in **Tables 3.5** and **3.6**. The sensitivity values for F_X and M_Y are shown in **Figs. 3.11** and **3.12**, respectively. Not only the sensitivity of extreme loads is presented but, also the sensitivity of the rest of the relevant parameters i. e. mean, standard deviation, and Gumbel parameters. These sensitivity coefficients are referred to the WSC of 0.14 as this value is considered the guideline to follow in industry, see Eq. (3.16).

$$S = \left(\frac{Value_{WSC} - Value_{WSC=0.14}}{Value_{WSC=0.14}}\right) x100\% \tag{3.16}$$

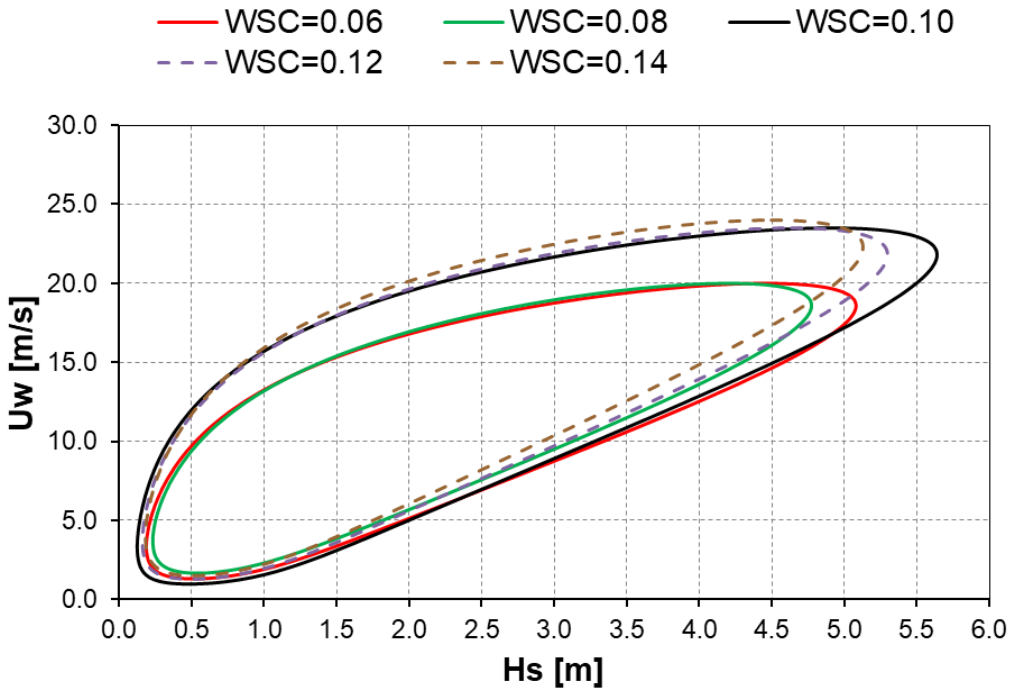

Figure 3.9: Environmental contour lines for F_X with return periods identified as most important for each value of WSC.

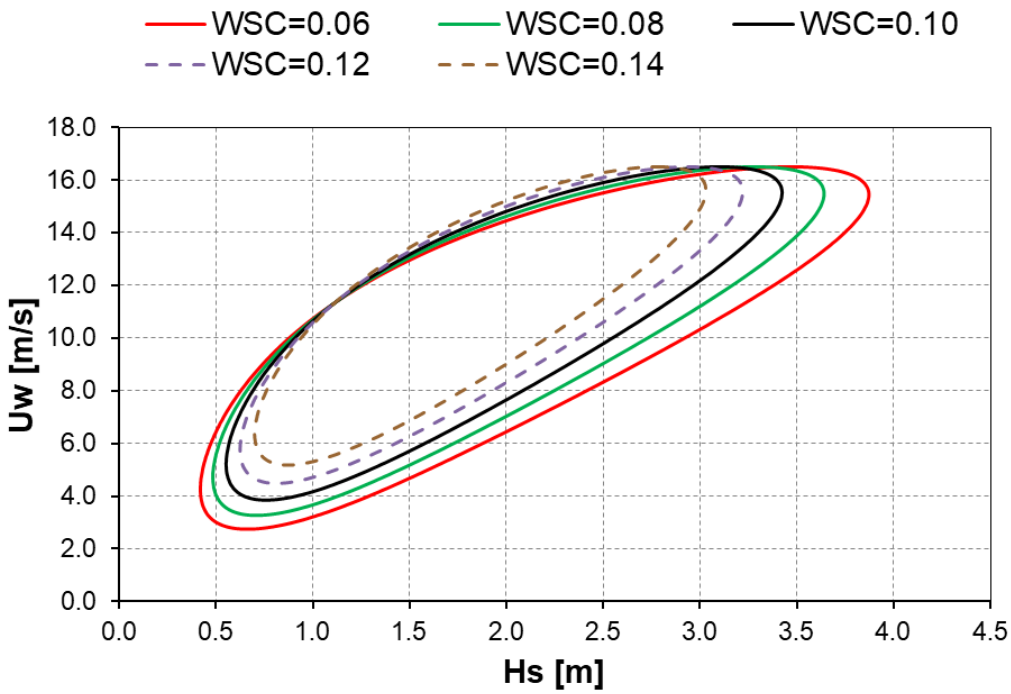

Figure 3.10: Environmental contour lines for M_Y with return periods identified as most important for each value of WSC.

Table 3.7: Additional environmental conditions identified as the most important during the last phase of the MECM procedure for M_Y, the corresponding statistical parameters (mean, standard deviation, Gumbel parameters) and the 50yr extrapolated extremes are given. Values M_Y are given in MN-m.

	WSC [-]	Uw [m/s]	Hs [m]	Tp [s]	μ	σ	μ_G	β_G	50-yr Extreme
M_Y	0.06	16.455	3.614	7.799	47.215	11.206	95.714	8.097	185.203
	0.08	16.457	3.408	7.692	47.347	11.111	95.761	8.037	186.929

Regarding the fore-aft shear force (F_X), in **Fig. 3.11** it can be observed that the value of the mean tends to grow when the WSC goes to a lower value. In contrast, the rest of the parameters show an oscillating trend around WSC=0.10 which could be related to the fact that the U_W* were found at different values for different WSC. The sensitivity of F_X to the WSC is almost around 0%, this can be explained by the wave governed trend of F_X and then, effects of changes in the force along the rotor influence very little to the mudline.

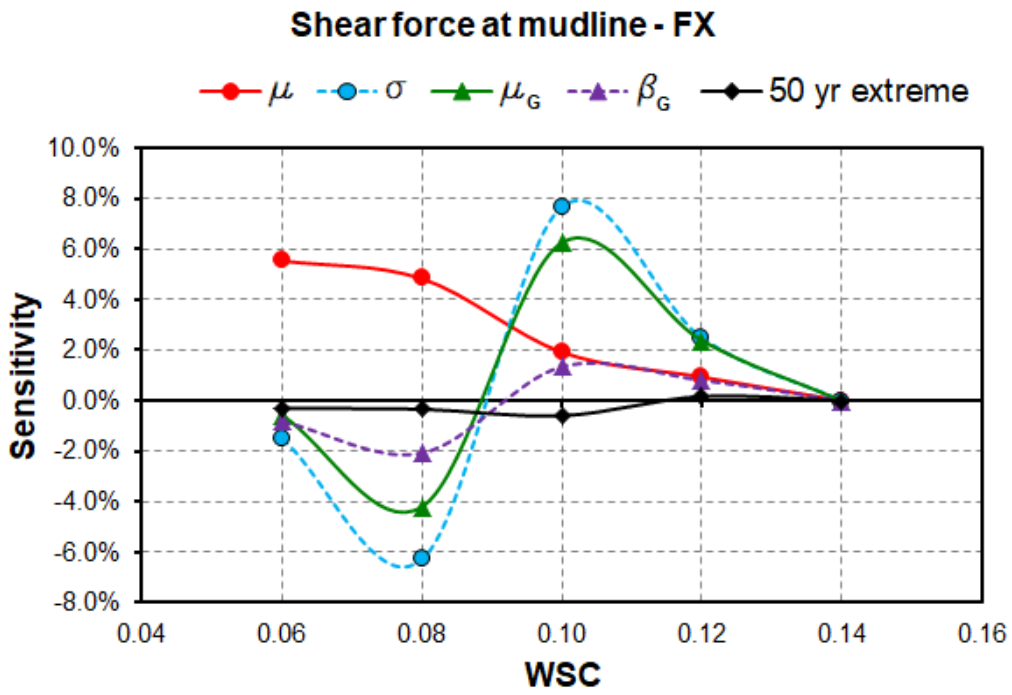

Figure 3.11: Sensitivity of statistical parameters (mean, standard deviation, Gumbel parameters) and 50yr extrapolated extreme for F_X to wind shear coefficient (WSC), values of sensitivity are referred to WSC=0.14.

Regarding the fore-aft bending moment (M_Y), a clear trend is observed in **Fig. 3.12**. Although there is a twist for $\boldsymbol{\sigma}$ and $\boldsymbol{\beta_G}$ between WSC values of 0.08 and 0.10, this can be related to the fact that new ECs for WSC values of 0.06 and 0.08 were identified in the last phase of MECM (see **Table 3.7**). The sensitivity of the 50-yr extreme of M_Y to WSC shows a linear trend, and it reaches a minimum of -3% for a WSC=0.06 in comparison to the value obtained for WSC=0.14. The reason behind these low levels of sensitivity could be attributed to the fact that the variation of WSC only adds loads in the level of kN to the wind turbine, and this variation is restricted to the rotor nacelle assembly. In contrast, the long term extremes are in the order of MN, and then the effect of the load variation due to wind shear could be considered negligible for these responses.

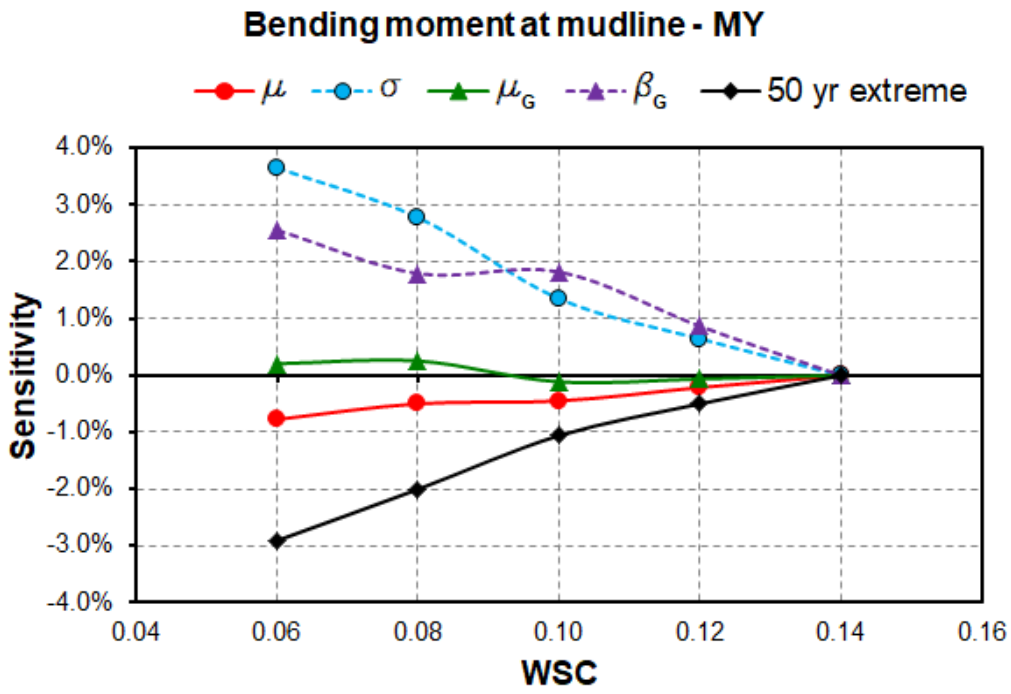

Figure 3.12: Sensitivity of statistical parameters (mean, standard deviation, Gumbel parameters) and 50yr extrapolated extreme for M_Y to wind shear coefficient (WSC), values of sensitivity are referred to WSC=0.14.

As a concluding point, some k values are summarized in **Table 3.8** for the ECs identified by MECM as most important. As it is known, for extreme extrapolation, many stochastic simulations are required but, the mean and standard deviations can be accurately determined with fewer realizations.

Therefore, these K values can become a useful tool for estimating long-term extremes with the only estimation of the mean and standard deviation of a response. These k values are expected to serve as a value of comparison for other types of offshore wind turbines.

Table 3.8: k-values corresponding to Gumbel parameters and 50yr extreme responses for ECs identified as most important by MECM for F_X and M_Y.

	WSC [-]	k_{μ_G}	k_{β_G}	$k_{50\text{-yr Extreme}}$
F_X	0.06	3.43	-0.33	7.74
	0.08	3.45	-0.35	8.13
	0.10	3.43	-0.27	7.08
	0.12	3.45	-0.28	7.51
	0.14	3.44	-0.28	7.69
M_Y	0.06	4.33	-3.49	12.31
	0.08	4.36	-3.54	12.56
	0.10	4.38	-3.59	12.90
	0.12	4.41	-3.63	13.08
	0.14	4.43	-3.67	13.24

CHAPTER IV. IMPACT OF SIMULATION LENGTH AND FLEXIBLE FOUNDATION ON LONG-TERM RESPONSE EXTRAPOLATION OF A BOTTOM-FIXED WIND TURBINE

4.1 INTRODUCTION

In the last few decades, attention to renewable energy sources has been increasing. One of the energy sources that has captured more interest and managed to become one of the most promising is wind energy since it is environmentally friendly, socially justifiable and the resource is ample. Also, its rapid evolution has led to a continuous decrease in the investment needed and operational costs [76]. There are many advantages to embracing the use of wind energy to meet a country's energy needs. However, the main one is the great potential it has to reduce environmental emissions and to help against the serious problem of global warming. The Intergovernmental Panel on Climate Change (IPCC) has found that human activities have caused a rise in global temperature of between 0.8°C and 1.2°C compared to pre-industrial levels. If current trends continue, the 1.5°C barrier is expected to be exceeded between 2030 and 2052 [77]. To ensure sustainable development, how energy is produced becomes strategic. It is imperative to reduce atmospheric emissions to slow down the process of global warming. Thus, the extensive deployment of wind farms will play an important role in achieving this important goal in the near future.

Currently, wind energy is considered a mature and fully commercialized technology that, in some countries, can work free of subsidies, and capable of competing successfully against fossil and nuclear fuels [1]. One of the other major advantages of wind energy is that it helps to diversify and enhance energy security. This aspect is highly valued by countries that have a strong hydropower and gas component in their energy matrix. As a specific example of this trend, in the USA, it is expected that the contribution of wind energy to the electricity supply

reaches 20% by 2030 [78], in 2013 this share was 4.5% [79]. At the global level, it is expected that the contribution from wind energy to world power requirements will reach 18% by 2050 [80].

Among all the available technologies for electricity generation from wind, the most popular and robust are by far wind turbines. Lately, the offshore environment has captured special attention given the significant and vast levels of untapped wind resources. In this domain, Europe, in particular the UK, Denmark, and Germany, has taken a leading role. Until 2019, 5047 wind turbines have been connected to the grid in 110 offshore wind farms among 12 European countries (including sites with turbines partially connected to the grid) making a total of 22 GW. The most popular substructure is still the monopile with a share of 81% of all the installed projects. The average capacity of each turbine for the offshore environment has increased by 16% each year since 2014, and the average nominal capacity installed by 2019 was 7.8 MW [3].

As it can be noticed, there is a growing interest in the development of offshore wind energy plants. However, the main problem that persists in the industry is the Levelized Cost of Energy (LCOE), which in some cases is still high compared to other conventional technologies [81]. In an offshore wind energy project, there are a variety of factors that will impact the LCOE such as individual quality of wind, turbine capacity, project size, expected project lifetime, distance to shore, and water depth [2]. An appropriate balance between these factors will allow a lower LCOE; however, the individual capacity of the turbine draws special attention. Manufacturers are continually pushing established power capacities to new levels [4], [5] as larger turbines provide increased capacity per foundation, and this provides the benefit of access to economies of scale [82]. Similarly, a major component in the investment cost is the foundation which can account for up to 25% of the total investment cost of the project [6]. Taking these two points into consideration, it can be inferred that a significant cost reduction can be achieved by using very large turbines with the most economically available foundation that fully satisfies the reliability requirements of the project.

For offshore wind energy exploitation, there are two types of supporting structures, bottom-fixed and floating, the latter has the highest investment costs

and its technology is still in the testing stages. Fixed foundations have been preferred by most projects currently in operation, especially the relatively low-cost monopile foundation, more details are given in [39]. Due to the prevalence of this type of foundation, there is still interest in optimizing its design process to reduce costs, and at the same time be able to support larger turbines. This objective can be achieved through a more detailed understanding of the uncertainties present in the design phase of the project. In this context, Damiani [10] presented the results of a workshop attended by representatives from academia and industry in the field of wind energy. The meeting explored the uncertainty on the wind engineering design processes and its impact on structural reliability of wind installations. It has been stated that the objective of the new future developments must be focused on technological innovations which can help to reduce the LCOE. For this purpose, a better understanding of the operational environment and the quantification of key uncertainties could lead to changes in current design processes. There is a need to refine guidelines to lower LCOE with reduced uncertainty, low probabilities of failure, and without having an excess of material or over-conservative design. One of the five major sources of uncertainty identified by this study is associated with direct impacts on turbine loads with an emphasis on extreme events and uncertainty in the operational load extrapolation. Control of the uncertainty level in the probabilistic models is expected to produce good and robust predictions of extrapolated loads associated with target recurrence periods [12].

Wind energy could be considered to be still in the early stage, and then experimental or real-world data is not often available. Due to this situation, wind engineering design usually relies on sophisticated numerical models and simulations [83]. In the past, those models were mainly based on deterministic formulations but, lastly, they have been gradually replaced by probabilistic approaches due to the ability to treat with uncertainties. On wind energy systems many uncertainties can be found; there are uncertainties in the aerodynamic characteristics of the turbine; in the material properties, structures and foundations; and in the characteristics of many of the subsystems of a wind turbine [84].

Despite the benefits of a probabilistic approach, there are some inherent problems when it is strongly associated with computational simulations. Reaching statistical significance in the analysis requires the simulation of several events, and if extreme conditions are involved, this requirement is even greater since the probability of occurrence is very small. This situation often requires very large computing resources, which are often not available. It also involves very time-consuming activities that can make it prohibitive to perform. To alleviate this issue it is often necessary to use simplified computational models or perform short-term simulations which can later be extrapolated based on statistical theory and thus obtain answers about long-term processes. In this context, concepts such as independence, statistical extrapolation acquire more significance and importance. There are still doubts about the minimum amount of stochastic realizations needed to achieve high accuracy in statistical inferences [12], or if a simulation length of 10 minutes for the short-term is enough to ensure statistical independence in case of combined wind and wave loading [85].

This chapter seeks to contribute to the understanding of two types of uncertainty in offshore wind turbine design: the statistical uncertainty and the modelling uncertainty. The study is focused on exploring the errors incurred when using simulations shorter than one hour for the 50yr long-term response extrapolation. Simulation lengths of 10, 20, and 30 minutes are evaluated and compared against the 1hr and 50yr extreme value. The Global Maxima Method (GMM) is used to estimate the short-term probability distributions based on 100 stochastic realizations for each environmental condition. Simulations are carried on the NREL 5 MW with a monopile foundation. The important relevant environmental conditions are found by using the Modified Environmental Contour Method (MECM). This approach has shown that it could estimate long-term loads with acceptable accuracy and efficiency. This work also explores the effects of considering the improved apparent fixity soil model to evaluate its influence on the long-term loads of a fixed bottom turbine.

4.2 UNCERTAINTY IN WIND ENERGY

Offshore structures are continuously exposed to harsh environmental conditions. These conditions have stochastic behaviour by nature since many of their characteristics evolve randomly. In this context, probabilistic models are necessary to incorporate this behaviour into the structural design [86]. Due to the stochastic nature of these conditions, it is necessary to consider more advanced approaches than the deterministic to assess and ensure the desired reliability level, i.e. a probabilistic approach. In this regard, it is essential to talk about uncertainties and how to manage them rationally to properly assess the safety of structural designs.

Uncertainty will often be present in any given scenario and it is difficult to make appropriate decisions without considering them in the design process. Many parameters for structural design are rarely known with great confidence, and they must be taken as random variables when a stochastic approach is considered [87]. Depending on the field of study and the source being consulted, there are different ways of classifying sources of uncertainty [88], [89] but, in general, at least three types of uncertainty are recognized in structural reliability theory: physical uncertainty, statistical uncertainty, and model uncertainty [87].

- **Physical uncertainty** is related to the problem of knowing with enough confidence the real values of physical quantities and measurements such as loads, material properties, and dimensions.

- **Statistical uncertainty** concerns the deviations arising from the estimation of parameters of probability distributions caused by insufficient sample size or insufficient observations, it mainly arises as a result of lack of information, and very large samples are often needed to reduce this uncertainty to a proper level.

- **Model uncertainty** concerns the mathematical models used to represent a physical phenomenon. This uncertainty is associated with simplifications, assumptions, other effects (e.g. non-linearities) and interactions with other variables not initially considered in the model employed.

Reliability-based designs rely on statistical theory and consequently, it is necessary to have large amounts of data to manage the levels of uncertainty. However, the offshore wind industry is still considered to be at an early stage and real data is often not available, or at least not in the required volume. As a result, it is necessary to use advanced computational models that represent real-world physical phenomena as accurately as possible. These models must not only replicate isolated phenomena but, also the interaction between them. However, this exposes another problem, statistical uncertainty. To bypass this uncertainty, many simulations are needed. However, this also supposes a greater computational effort that in many cases can be problematic if very long simulations are required. Therefore, a relevant aspect in a simulation-based probabilistic analysis is the simulation length necessary to reach an acceptable level of long-term responses.

A problem that requires a very long simulation time can be decomposed in stochastic processes with reduced simulation time if certain conditions could be met, and thus, the corresponding parameters of the original process can be determined with the help of an extrapolation method. However, using reduced time simulations will introduce new statistical uncertainties [90] into the estimated parameters. Then, it is important to carefully assess this reduction to determine the appropriate simulation length. Choosing a very short time can greatly decrease the computational effort, but it will cause the results to have an important error level in statistical estimations. In contrast, longer simulations could require more calculation time, but the result will be closer to the true parameter value of the stochastic process. This aspect is even more important for Offshore Renewable Energy (ORE) devices due to the interaction of wind and wave loading.

For onshore applications, a minimum simulation length of 10 minutes has been considered adequate. This criteria allows capturing load effects and turbulence fluctuations due to the spectral gap between 10-min and 1h in the van der Hoven [91], [92] wind spectrum. This allows keeping the assumption of statistical stationary and independence as valid. On the other side, previous experiences on the offshore oil/gas industry have shown that for floating structures longer simulation lengths are required to capture low-frequency responses, load

effects, and also extreme loads. For this purpose, simulations between 3 and 6 hours are common practice. However, if combined loading of wind and wave is considered, the assumption of stochastic independence for periods longer than one hour cannot be considered entirely true, especially for the wind spectrum.

Bottom fixed offshore wind turbines (OWT) are in the middle of two concepts. An OWT cannot be considered a floating structure to justify the use of very long simulations as it is less sensitive to low-frequency events, and some of its degrees of freedom are restricted. It will be influenced by wave loading and then, it is expected that simulations of more than 10 minutes will be required to reduce the uncertainty in the statistical extrapolation procedure. Later, in this document it will be seen that there have been some studies addressing this aspect, many of them focused on floating wind turbines but, only a few on bottom-fixed OWT.

Another aspect of uncertainty associated with an OWT is the model uncertainty regarding the soil-structure interaction. For bottom-fixed turbines, this issue is particularly relevant as there are large and direct connections between the substructure and the seabed. The work required to bypass this type of uncertainty is not easy. It is necessary to use more complete models that reflect with great precision the physical phenomena. However, using very complex models can increase the computational effort required to complete the simulations. Thus, the same problem that was observed with statistical uncertainty arises again. Therefore, it is necessary to use a model that allows finding a trade-off between simplicity and accuracy to reflect the soil-structure interaction. Later, a soil model that meets these requirements will be presented in this document, i. e. the improved apparent fixity soil model.

The study of uncertainties, also known as Uncertainty Quantification (UQ), is almost a very new field of study in the offshore wind energy discipline, although it has been applied to various branches of engineering for a long time. There is a growing interest in the topic. However, there is a limited formal application of uncertainty quantification in offshore wind engineering design and analysis processes, possibly due to the inherent complexity of the models that describe wind turbine behaviour and the environment in which it operates [84].

In the context of this paper, the determination of long-term extreme responses is essential in the design phase of offshore wind structures when a reliability-based design is addressed. The ultimate goal is to estimate loads as accurately as possible with appropriate levels of reliability but minimizing computational effort. For this reason, it is very important to understand the nature of uncertainties in the future development of wind energy.

4.3 ENVIRONMENTAL CONTOUR METHOD: TRADITIONAL AND MODIFIED

The determination of the responses which correspond to a target return period is of great interest for the evaluation of the reliability of a structural system. In general terms, the reliability can be defined by Eq. (4.1), based on the probability of failure $\mathbf{P_f}$ and the generic-limit state **g(x)**. Similarly, the probability of failure can be defined in terms of a return period **N** by Eq. (4.2). Here **md** represents the expected number of d-hour sea states per year.

$$\mathrm{R} = \mathrm{P}[\mathrm{g}(\mathrm{x}) > 0] = 1 - \mathrm{P_f} \tag{4.1}$$

$$\mathrm{P_f} = \frac{1}{\mathrm{N} \cdot \mathrm{md}} \tag{4.2}$$

On the other hand, the long-term extreme response of a system subjected to environmental loads is generally defined in terms of an integration of its short-term components, Eq. (4.3). In this equation, $\mathbf{f_S(s)}$ represents the joint probability distribution of the environmental variables involved in the specific problem under analysis, Eq. (4.4), and $\mathbf{F_X(\xi)}$ is the probability that **X** is less than or equal to **ξ**, **LT** and **ST** mean short-term and long-term, respectively.

$$\mathrm{F_X^{LT}}(\xi) = \int \mathrm{F_{X|S}^{ST}}(\xi|\mathrm{s})\mathrm{f_S}(\mathrm{s})\mathrm{ds} \tag{4.3}$$

$$\int \mathrm{f_S}(\mathrm{s})\mathrm{ds} = 1 \tag{4.4}$$

Additionally, the environmental variables typically considered for normal offshore structures are two, the wave height ($\mathbf{H_S}$) and the peak spectral period ($\mathbf{T_P}$). However, for offshore energy structures, wind speed ($\mathbf{U_W}$) is also an important environmental variable. In the latter case, the joint probability distribution $\mathbf{f_S(s)}$ is simplified to the expression shown in Eq. (4.5).

$$f_S(s) \rightarrow f_{Uw,Hs,Tp}(u,h,t) = f_{Uw}(u) \cdot f_{Hs|Uw}(h|u) \cdot f_{Tp|Uw,Hs}(t|u,h) \quad (4.5)$$

Considering Eqs. (4.1)-(4.3), the probability of occurrence of a long-term extreme response can be related to the return period, Eq. (4.6).

$$F_X^{LT}(\xi) = 1 - \frac{1}{N \cdot md} \quad (4.6)$$

If the cumulative probability distribution of the extreme long-term extreme response is explicitly known, Eq. (4.6) allows directly finding the value of the response whose return period is **N**. The method to calculate the required cumulative probability distribution is the Full Long-Term Analysis (FLTA) which consists of performing the direct integration of Eq. (4.3). Although this method provides the most accurate results, it is computationally expensive to perform. It is not an efficient method since it includes all environmental conditions in the calculation and requires several simulations to have a proper fit for the short-term conditional distributions.

For this purpose, Haver et al. [29] proposed the Environmental Contour Method (ECM). It is mainly based on the inverse First Order Reliability Method (IFORM) but, without considering the variability of the extreme response. This method allows, via the mathematical transformation of Rosenblatt [93], decoupling environmental parameters from the response, and thus to estimate the environmental parameters associated with a specific return period e. g. 50 years. In this way, an important reduction in the number of environmental conditions to be evaluated is achieved. In general terms, the method can be summarized by Eq. (4.7). In this expression, it is assumed that the short term period is one hour. Then, the long-term extreme is given by the value of the short-term extreme evaluated for the most relevant environmental condition $\{u_N, h_N, t_N\}$ with return period N identified by the ECM.

$$F_{X_{1hr,Nyr}}(\xi) \approx F^{ST}_{X_{1hr}|U_W,H_S,T_P}(\xi|u_N,h_N,t_N) \quad (4.7)$$

To apply the traditional ECM, it is needed to define the reliability index $\boldsymbol{\beta_S}$, Eq. (4.8). This parameter represents the radius of a hypersphere in a non-physical space. $\boldsymbol{\Phi}$ represents the standard normal cumulative probability function. If only 3

physical random variables (U_W, H_S, and T_P) are considered in the true physical space then the transformed hyperspace is reduced to a three-dimensional space with variables {U_1, U_2, U_3}. These new variables are independent, uncorrelated, have zero mean, and unit standard deviation. Since they belong to a sphere then they fulfil the relationship by Eq. (4.9).

$$\beta_s = \Phi^{-1}(1 - P_f) \tag{4.8}$$

$$\beta_s^2 = U_1^2 + U_2^2 + U_3^2 \tag{4.9}$$

The surface generated by Eq. (4.9) in the non-physical space can be discretized, and the corresponding points in the physical space {U_W=u, H_S=h, T_P=t} can be found by solving the relationships given by Eqs. (4.10)-(4.12). This method is useful to generate the random environmental variables directly in the non-physical space from the joint probability distribution and the target return period with relative simplicity. By using the inverse transformation, a set of environmental conditions is obtained which must then be evaluated.

$$\Phi(U_1) = F_{Uw}(u) \tag{4.10}$$

$$\Phi(U_2) = F_{Hs|Uw}(h|u) \tag{4.11}$$

$$\Phi(U_3) = F_{Tp|Uw,Hs}(t|u,h) \tag{4.12}$$

For a given environmental condition, short-term extreme values of the response are used to fit an empirical probability distribution to find the most probable extreme value. The combination which gives the maximum extreme response among all the set is known as the “design point”, and the response value for this condition is considered the long-term extreme response (N-yr response). However, since the ECM omits the response variability at the beginning, it is necessary to correct the calculated extreme value. This correction is made by applying an empirical fractile level higher than 50%. Values between 70% and 90% are usual for practical applications [94]. The main benefit of this method is that it greatly reduces the effort to estimate the long-term extreme responses by just identifying the critical environmental conditions independently of the structural response. Due to this advantage, it has been widely used in the offshore industry and is a useful method when its assumptions are fulfilled. It has been applied for

floating offshore wind turbines [95]–[98], wave energy devices [99], and combined concepts [30], [100], [101].

Although the traditional ECM is a widely used method in the offshore industry, it does not perform well on systems that have survival strategies based on an active control system. In this context, the main assumption of the ECM regarding the monotonic relationship between responses and environmental parameters is violated. These control systems ensure that as soon as an environmental parameter exceeds a given threshold value, the responses are drastically reduced so that the device can protect itself from catastrophic failure. This non-linear behaviour causes the ECM to perform poorly, and it underestimates the long-term extreme responses. This is the case with wind turbines, once the cut-out wind speed is exceeded; the blade pitch is adjusted to minimize aerodynamic thrust loads. Similar behaviour has been observed in wave energy converters, but in this case, the survival mode is activated by the wave height [30]. As a consequence, the long-term extreme responses are mainly governed by environmental conditions within the operational range and with a higher probability of occurrence. These problems have been documented in the literature [31], [74], [102]–[107].

To bypass the problem that the ECM has, when it is applied to an ORE device, Li et al. [31] proposed the Modified Environmental Contour Method (MECM). This method is based on the ECM, but it adds additional steps to find the true "design point". The MECM is based on the widely accepted assumption that the long-term probability distribution of a response can be extrapolated from the short-term distribution as short-term extreme values are considered statistically independent in a short-term period e. g. one hour. Then, the 50yr 1hr extreme CDF can be written as Eq. (4.13). This equation implies that the 50yr extreme response can be found by estimating an extreme response with a lower return period $\mathbf{N_0}$. This procedure helps to bypass the non-linearity on the limits of the operational range of the wind turbine. Since the return period, $\mathbf{N_0}$ will be lower than 50 years, it is necessary to apply an extrapolation to the probability distribution between brackets to estimate the corresponding value of the response at 50 years level. This extrapolation is achieved by applying the exponent $\mathbf{50/N_0}$. The

expression between brackets can be found by applying the traditional ECM, Eq. (4.7), then it becomes Eq. (4.14) but, considering the return period N_0. In this case, the extreme response is calculated using one-hour short-term extreme distribution.

$$F_{X_{1hr,50yr}}(\xi) = \left[F_{X_{1hr,N_0yr}}\right]^{50/N_0} \tag{4.13}$$

$$F_{X_{1hr,50yr}}(\xi) = \left[F^{ST}_{X_{1hr|U_W,H_S,T_P}}(\xi|u_{N_0}, h_{N_0}, t_{N_0})\right]^{50/N_0} \tag{4.14}$$

Consequently, the MECM mainly focuses on finding the return period N_0 in which the maximum long-term extreme response is achieved. To reach this goal, many inner environmental contours corresponding to wind speeds within the operational range of the turbine need to be tested. For each of these conditions, the extreme long-term response needs to be calculated. The condition that provides the greatest response among all the conditions tested will be the most important environmental condition. The return period that corresponds to this important condition will be the return period required N_0. As it can be noticed, the MECM is a more complex method than the ECM. It requires more environmental contours to be tested, however; the effort is significantly less than applying the FLTA. The results of the MECM can also be useful to identify relevant environmental conditions to include in a reduced long-term analysis (RLTA).

Li et al. [31] provided a specific procedure to apply the MECM to bottom-fixed offshore wind turbines under the combined action of wind and wave. First, it is necessary to establish multiple operational wind speeds with N_K–yr return period and their corresponding most probable sea states $u_{N_K}, h_{N_K}, t_{N_K}$. It is important to remember that the random variable u is the mean wind speed measured at 10 m, and the operational wind speeds U_W are those given at the hub height. Then, it is necessary to use the wind power-law, Eq. (4.15), to relate both parameters, here α is the wind shear coefficient, and H_{HUB} is the height of the hub over the still water level. If we consider Eqs. (4.2), (4.8), (4.9), and (4.10), then the expression that relates each wind speed to its respective return period is given by Eq. (4.16).

$$U_{W_K} = u_{N_K}\left(\frac{H_{HUB}}{10\ m}\right)^{\alpha} \tag{4.15}$$

$$F_{Uw}(u_{N_K}) = 1 - \frac{1}{N_K \cdot md} \tag{4.16}$$

In the next step of the MECM, it is necessary to use each combination of environmental conditions $(u_{N_K}, h_{N_K}, t_{N_K})$ established in the previous step and perform several short-term simulations to fit an empirical probability distribution based on extreme values, then apply load extrapolation, and finally calculate the most probable value of the 50yr extreme response for the simulated conditions, $Mo_{X_{1hr,50yr}}(u_{N_K}, h_{N_K}, t_{N_K})$. For each operational speed, there will be a return period N_K and a most probable value of the 50yr extreme response M_{OX} associated with it. Then the N_0 will be the one that corresponds to the largest $Mo_{X_{1hr,50yr}}(u_{N_K}, h_{N_K}, t_{N_K})$. In the last part of the MECM, it is necessary to generate an environmental counter surface with a return period N_0 previously identified, and to seek for the environmental condition that produces the largest 50yr extreme response with a procedure similar to that previously described. The MECM has been successfully applied to bottom-fixed OWT [31], [85], floating structures [104], and combined energy concepts [30], [105], [106]. In every case, it has been concluded that the MECM performs very well and it gives predictions closer to those obtained with the FLTA.

4.4 STATISTICAL EXTRAPOLATION FROM SHORT-TERM DISTRIBUTIONS

As wind turbine technology evolves to achieve higher power, their sizes and weights are also growing to unprecedented levels. An offshore wind turbine will experience various load conditions during its service life given the characteristic severity of the environmental conditions of this type of zone. In this context, extreme loads are of particular interest at the design stage. It aims to ensure that certain reliability minimum levels are met and thus, prevent unexpected failure events. Relevant standards in the offshore industry recommend considering a 50yr recurrence period in the estimation of long-term extreme loads [35], [61]. However, it is not often feasible to measure or simulate load conditions over very long periods. Then, it is necessary to rely on well-founded statistical procedures to perform load extrapolation [60] which allow the estimation of rare extreme values (low probability of occurrence) from frequent events (high probability of occurrence) [108].

There are several approaches to apply statistical extrapolation to determine the extreme responses of an offshore wind turbine [62]–[64]. They have been used for many years in the wind industry [109]–[112]. In this research, the Global Maxima Method (GMM) is used to obtain a short-term probability distribution. Extreme values obtained from coupled simulations are fitted to a Gumbel distribution, Eq. (4.17), where X is the analysed response, $\boldsymbol{\beta_G}$ is the shape parameter, and $\boldsymbol{\mu_G}$ is the location parameter, and at the same time, the most probable value of the probability distribution $\mathbf{Mo}_X$, also known as the mode.

$$F(X) = \exp\left(-\exp\left(-\frac{(X-\mu_G)}{\beta_G}\right)\right) \tag{4.17}$$

An important part of a successful statistical extrapolation is ensuring the independence condition. Statistical independence is a simple concept, but its relevance is high. This condition ensures that the joint probability distribution of events can be found by multiplication of the marginal probability distribution of the single events. A way to describe independence is that if the occurrence of event A has no statistical impact on the occurrence of event B, then events A and B are statically independent [113].

In the formulation of the MECM for bottom-fixed wind turbines, the 50yr long-term responses are extrapolated from 1hr short-term extremes, Eq. (4.14). At the same time, the 1hr extreme statistics could be extrapolated from simulations with a reduced time; as long as this reduced simulation length can still ensure statistical independence. In the wind industry, it has been assumed for many years that 10 minutes is enough to guarantee statistical independence [12]. It has been proved to work well for onshore wind turbines, although this assumption is currently considered conservative [85] for the offshore environment. This duration is based on the criteria of the spectral gap of wind variation in the van der Hoven spectrum. So the wind process is considered stationary at this time scale. Similarly, it is a common practice in the offshore industry to consider simulation lengths between 3 to 6 hours for floating structures. The reason behind this is the spectral gap of low-frequency waves and the natural low frequencies of floating structures [65].

In the case of offshore wind turbines, there is not much consensus about what simulation length is appropriate to ensure the stationary character of the wind speed, and at the same time, to capture the effects associated with low-frequency waves. For bottom-fixed OWT, there have been some studies about the impact of using simulation lengths other than 10 minutes. Hübler et al. [67] point out that different simulation lengths do not produce any change concerning the ultimate loads. Whereas Zwick et al. [114] argue that there is an appreciable impact. In the case of floating turbines, there are also discrepancies among the studies. Pillai et al. [68] state that a length of simulation greater than 10 minutes will have an impact on the responses of the floating structures. In contrast, Stewart et al. [65] and Haid et al. [66] point out that 10 minutes is long enough to capture all the important effects. Despite the discrepancies between investigations, the simulation length of 10 minutes is still the standard applied in the industry [74], [85], [115], [116].

The present study focuses on bottom-fixed monopile offshore wind turbines. These types of structures obviously cannot be considered as floating bodies to justify the use of long simulations. However, it can be expected that there will be some influence of wave loading. Therefore, a simulation length of 10-minute could be suitable for an onshore wind turbine but, not for a monopile wind turbine under combined loading. As previously stated, for MECM it is necessary to have the 1hr extreme probability distribution for the extrapolation of 50yr extreme responses. This can be achieved by running one-hour simulations or by using shorter simulations and then applying an extrapolation to arrive at one hour level. For this purpose, extreme values extracted from 10-min, 20-min, 30-min, and one-hour simulations will be used to compare the deviations in the most probable values of probability distributions. After extrapolation, the most probable value of the Gumbel distribution is given by Eq. (4.18). In this equation, N_0 is the return period of the environmental condition (EC) tested. The parameter '**r**' will depend on the length of simulation from which we have extracted the extremes for fitting purposes. The value of r is 1, 2, 3, or 6 if the extremes for Gumbel fitting come from 1hr, 30-min, 20-min or 10-min simulations, respectively.

$$\mathrm{Mo_X} = \mu_G + \beta_G \cdot \ln(r \cdot 50/N_0) \tag{4.18}$$

4.5 NUMERICAL MODEL

For the development of this research, the NREL 5 MW wind turbine model supported by a monopile foundation is considered, this is a model widely used in the literature and its details can be found in [32]. The NREL 5 MW is a variable speed and collective pitch wind turbine with rated, cut-in and cut-out wind speed of 11.4, 3 and 25 m/s, respectively. The hub is 90 m above the mean sea level, and it has a rotor and hub diameter of 126 m and 3m, respectively. The coupled simulations are performed using FAST [70].

In the first part of the work, it is necessary to generate the inflow wind profiles for each wind speed to be evaluated, and considering various random seeds, this is done with the help of TurbSim [36]. The Kaimal turbulence spectral model is used, with a characteristic and turbulence type of “B” and “NTM”, respectively. The wind power-law is used to extrapolate wind speeds along the tower and rotor height. For the generation of the stochastic wind field, the coherence model given by IEC 61400-1 (3rd ed.), and a time step of 0.05s are considered. For every wind speed, there will be an associated sea state and then, it is necessary to set the values for the wave height (H_S), peak spectral period (T_P), and the cut-off frequencies of the wave spectrum. Wave profiles are generated internally in FAST with HydroDyn [71] using the JONSWAP spectrum with a peak-shape parameter of 3.3. Heading wave direction is set to 0°, and the water depth is 20 m. The analysis time considered for incident wave calculations is 3630s.

The diameter and thickness of the monopile are 6m and 0.06m, respectively. An important part of achieving accurate dynamic responses when considering wave loading is to properly set the Morison coefficients for drag (C_D), added mass (C_A), and pressure (C_P). The usual ranges for these values are: $1.5 \leq C_P + C_A \leq 2$, and $0.6 \leq C_D \leq 1.2$, according to [37]. For this work, the coefficients have been taken as $C_D=0.9$, $C_A=0.75$, $C_P=1$, for a detailed explanation about the selection of these values the reader is referred to [72] which is also supported by [117]. Other input parameters have been left as they were defined in the NREL 5MW baseline. The offshore site used in this study is the one presented by Li et al. [34] as “Site 15”. The models and coefficients of the joint probability distribution are summarized in **Table 4.1**.

Table 4.1: Probability models for the joint probability distribution at “Site 15” [34].

Variable	Distribution	Formulation
U_W	Weibull	$f_{U_W}(u) = \frac{\alpha_U}{\beta_U}\left(\frac{u}{\beta_U}\right)^{\alpha_U - 1} exp\left[-\left(\frac{u}{\beta_U}\right)^{\alpha_U}\right]$
$H_S \mid T_P$	Weibull	$f_{H_S \mid U_W}(h \mid u) = \frac{\alpha_{HC}}{\beta_{HC}}\left(\frac{h}{\beta_{HC}}\right)^{\alpha_{HC} - 1} exp\left[-\left(\frac{h}{\beta_{HC}}\right)^{\alpha_{HC}}\right]$
$T_P \mid U_W, H_S$	Log-normal	$f_{T_P \mid U_W, H_S}(t \mid u, h) = \frac{1}{\sqrt{2\pi}\sigma_{ln(T_P)} t} exp\left(-\frac{1}{2}\left(\frac{\ln(t) - \mu_{ln(T_P)}}{\sigma_{ln(T_P)}}\right)\right)$

Many codes available for the simulation of wind turbines often ignore the soil-structure interaction. Even the software used for this work, FAST, has a rigid connection to the seabed by default. This condition generates inaccuracies and uncertainties in the calculation of dynamic structural responses [115]. The simplest model to take into account the soil-structure interaction is the apparent fixity model (AF). Unfortunately, there are some problems with this method since it is usual that only the diagonal terms of the stiffness matrix of the fictive beam are matched, without taking into account the cross-coupling stiffness between the horizontal and rotational degree of freedoms. Then, the translational and rotational displacements at the seabed cannot be reproduced with accuracy. Løken et al. [115] managed to solve this problem by considering a second fictive beam with different properties. This method is known as the Improved Apparent Fixity (IAF) Method. A scheme of these two fictive beams with three nodes can be seen in **Fig. 4.1** where the lowest node ($N_{1)}$ has a fully rigid condition. A summary of their main properties is summarized in **Table 4.2**. The advantage of this model is that it is still simple and it can be properly implemented on the SubDyn module of FAST.

Additionally, the capture of rare events with small probabilities of occurrence requires a considerable amount of simulations to achieve a good level of accuracy. In contrast, this involves a cost of time and computing resources that are often prohibitive. Studies suggest that between 80 [31], [69], [85], and 120 [105] simulations are sufficient to ensure that the stochasticity of combined wind and wave loading conditions is captured. For this research, for any environmental condition to be tested, 100 simulations with different random seeds will be performed. Finally, all these models and workflows are implemented in a Python

script to generate the output files from FAST, see Appendix III. The post-processing for Gumbel fitting is made with WAFO [38]. The method used by WAFO to estimate the parameters of the Gumbel distribution for each tested case is the maximum likelihood estimates (MLE) instead of the classical least-squares method which has been pointed out as not performing well for Gumbel fitting purposes [118].

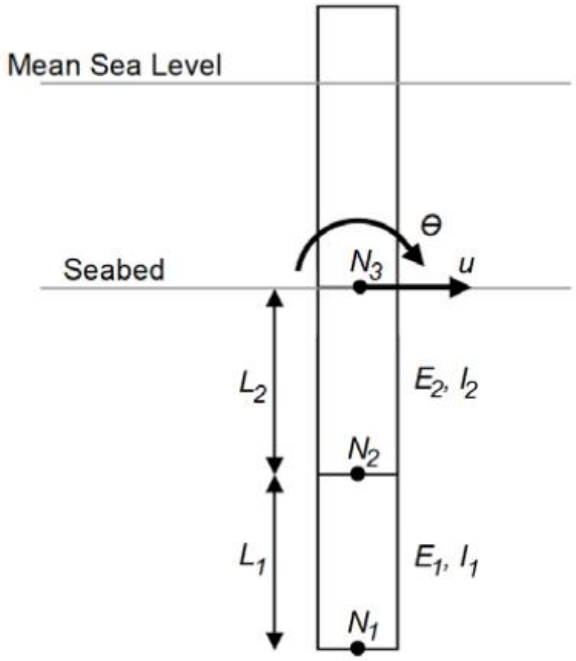

Figure 4.1: Schematic representation of the two fictitious beams considered in the IAF method [115].

Table 4.2: Properties of the two apparently fictitious beams [115].

Beam	L [m]	D [m]	Thickness [m]	I [m^4]	E [N/m^2]
1	19.88	6.00	0.06	5.089	1.743x10E12
2	5.00	6.00	0.06	5.089	1.388x10E11

4.6 RESULTS

The results of the analysis for the fore-aft shear force (FASF) and fore-aft bending moment (FABM) at mudline are presented below. First, the effect of the simulation length on the extrapolation will be analysed, both for the extrapolated

loads at a level of 1 hour and 50 years. In the case of 1hr extrapolation, there is no effect of the return period of each wind speed in the extrapolated load, factor $50/N_0$ in Eq. (4.18). However, when applying the 50-year extrapolation this factor does have an influence. A rigid soil model is considered in all cases.

In a later section, the results obtained from the comparison between the responses using the rigid soil model and the improved apparent fixity (IAF) soil model are discussed. In this case, 1hr simulations are used. In each case, both the trends of the values and the relative errors are shown. In both sections of the results, the relative error is plotted. For the case of simulation length analysis, the relative error is taken from Eq. (4.19), and for the case of the study of the effect of soil flexibility, the relative error is given by Eq. (4.20).

$$\mathrm{R.E.} = \left(\frac{\mathrm{X_{i-min}} - \mathrm{X_{1hr}}}{\mathrm{X_{1hr}}}\right) \times 100\% \; ; \; \mathrm{i} = \{10, 20, 30\} \tag{4.19}$$

$$\mathrm{R.E.} = \left(\frac{\mathrm{X_{IAF}} - \mathrm{X_{Rigid}}}{\mathrm{X_{Rigid}}}\right) \times 100\% \tag{4.20}$$

4.6.1. Effects of simulation length

First, the trend of the most probable values extrapolated from extreme values obtained from 10-min, 20-min, and 30-min simulations will be analysed. All these values have been extrapolated to the level of 1hr. The trend for the FASF is shown in **Fig. 4.2**; it can be also observed the most probable value obtained from one-hour simulations fitting. As it can be seen, the difference between the extrapolated most probable values is small in comparison to the trend obtained with the one-hour simulations (black line with diamonds). In the case of the FABM, **Fig. 4.3**, a slightly greater variation is observed. In this case, the extrapolation obtained from 30-min simulations is the one that best agrees with the one-hour simulations trend.

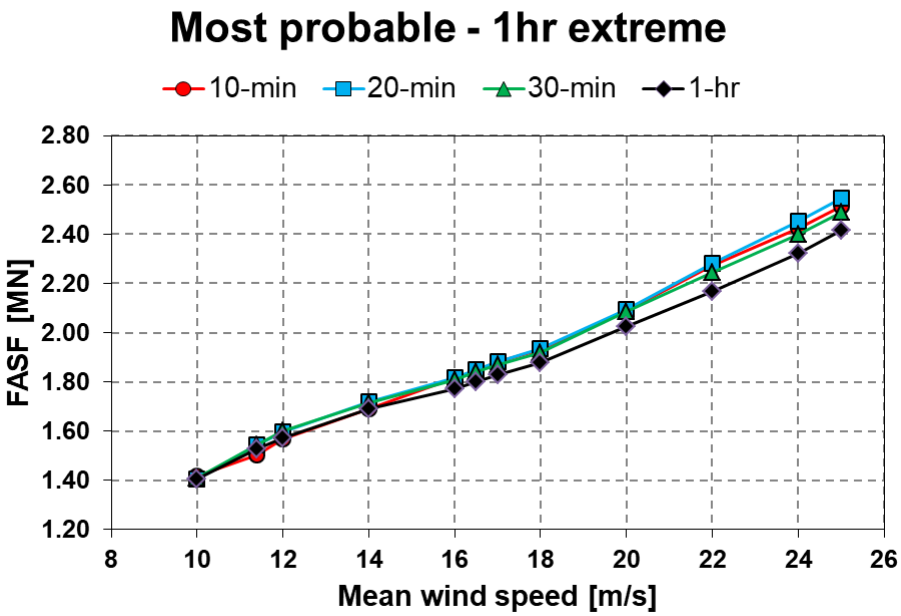

Figure 4.2: Most probable value from 10-min (red circles), 20-min (blue squares), 30-min (green triangles) simulations extrapolated to a 1hr level, and most probable value for FASF from 1hr (black diamonds) simulations versus mean wind speed.

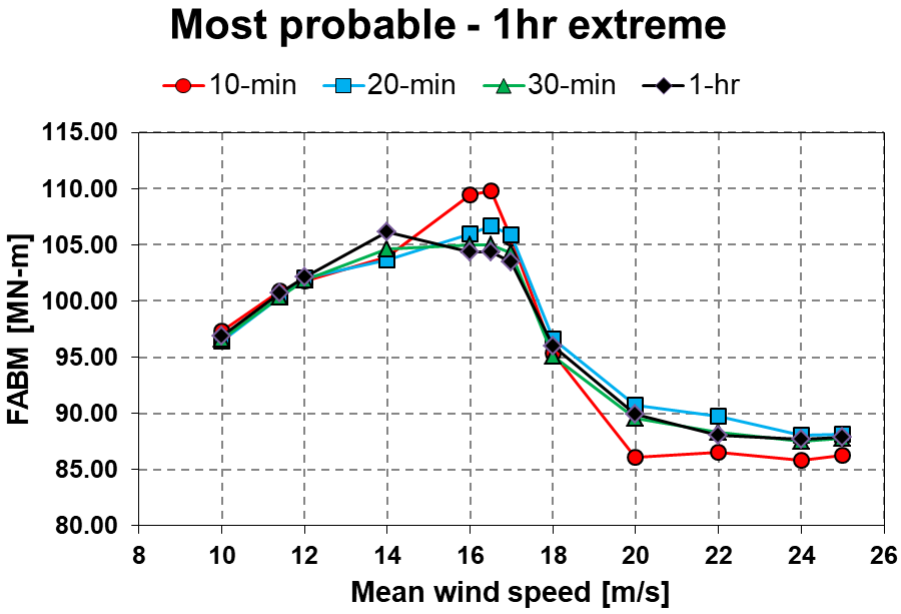

Figure 4.3: Most probable value from 10-min (red circles), 20-min (blue squares), 30-min (green triangles) simulations extrapolated to a 1hr level, and most probable value for FABM from 1hr (black diamonds) simulations versus mean wind speed.

Figs. 4.4 and **4.5** show the relative errors obtained for the FASF and FASBM respectively. In these figures, the most probable values of the extremes obtained from 10-min, 20-min, and 30-min simulations extrapolated to a 1hr level are compared to the most probable value obtained from 1hr simulations. In the case of the FASF, the relative error varies between -2% and 6% whereas this variation ranges from -6% to +6% for the FABM depending on the wind speed considered. In both cases, it is observed that the 30-min simulation offers lower levels of relative error. From **Figs. 4.2**-**4.5**, it can be seen that when the characteristics of extreme values obtained with shorter simulations are extrapolated to the level of one hour there is not a great difference with respect to 1-hour simulations.

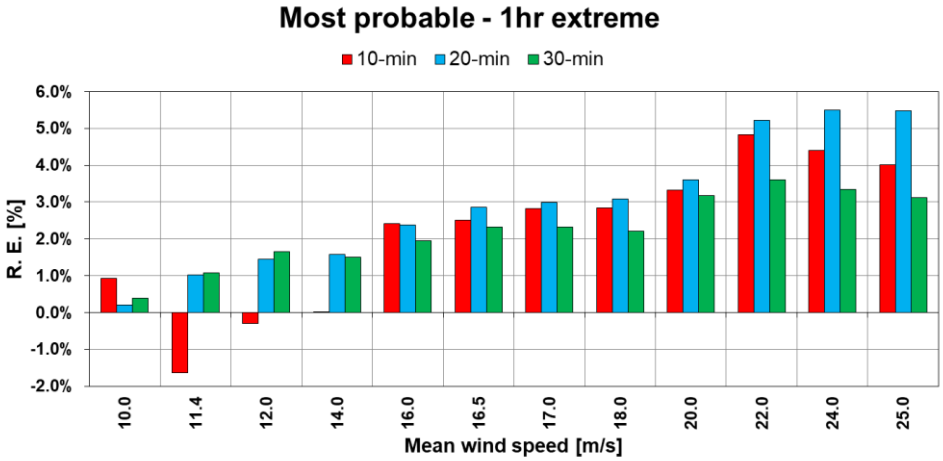

Figure 4.4: Relative errors of the most probable values extrapolated to a 1hr level with respect to most probable values of FASF from 1hr simulations.

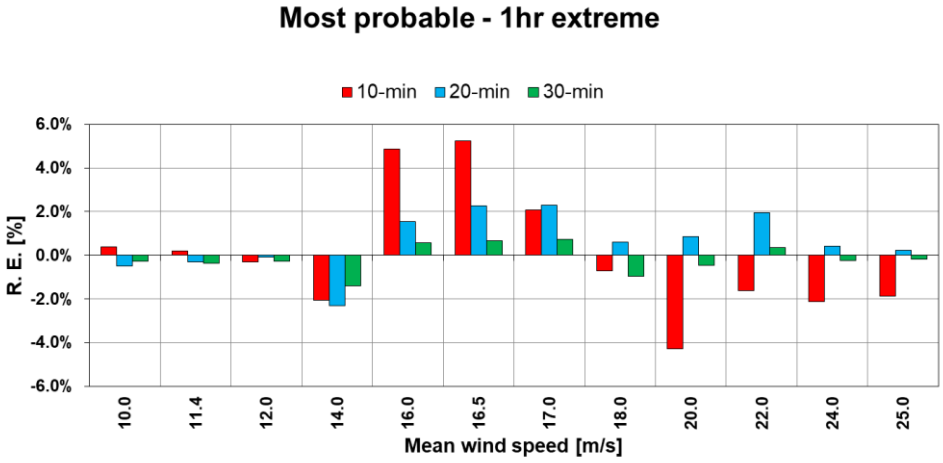

Figure 4.5: Relative errors of the most probable values extrapolated to a 1hr level with respect to most probable values of FABM from 1hr simulations.

Now it will be explored what happens when the extrapolation is done at a level of 50 years. In this case, the factor $50/N_0$ will influence the responses as it is different for each wind value. In **Fig. 4.6**, it can be noticed that the divergence for FASF becomes greater; being the extrapolation obtained from the 30 minutes simulations the one that comes closest to the value obtained from 1hr simulations. In the case of the FABM, **Fig. 4.7**, all extrapolations show a significant deviation from the 1hr case, but the extrapolation obtained from 10-min has the largest difference. It can also be seen that both the 20-min and 30-min extrapolations perform almost the same. Also, it is observed that the critical environmental condition for 10 minutes simulations moves from 16.5 m/s to 17 m/s for the case of 20-min and 30-min simulations.

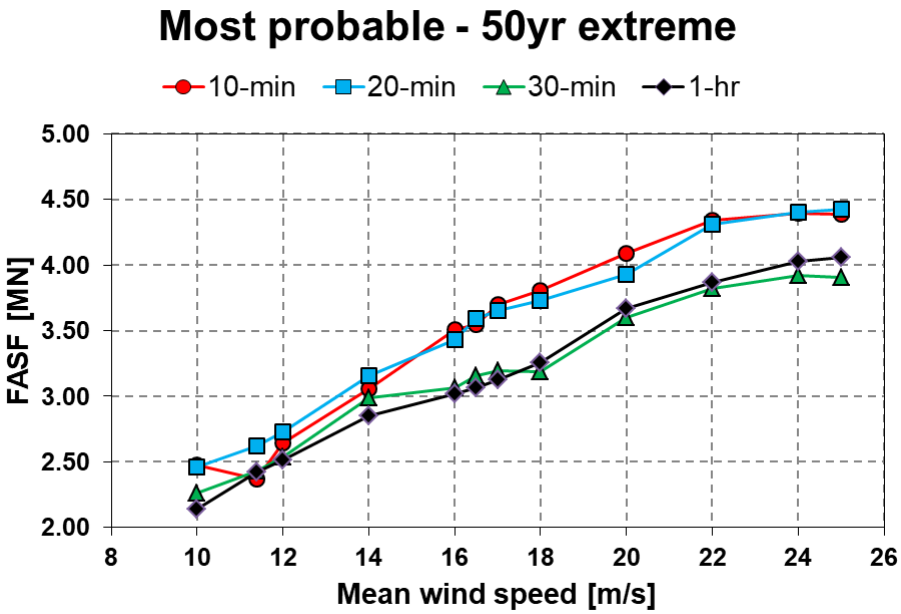

Figure 4.6: Most probable value from 10-min (red circles), 20-min (blue squares), 30-min (green triangles), and 1hr (black diamonds) extrapolated to a 50yr level from simulations versus mean wind speed for FASF.

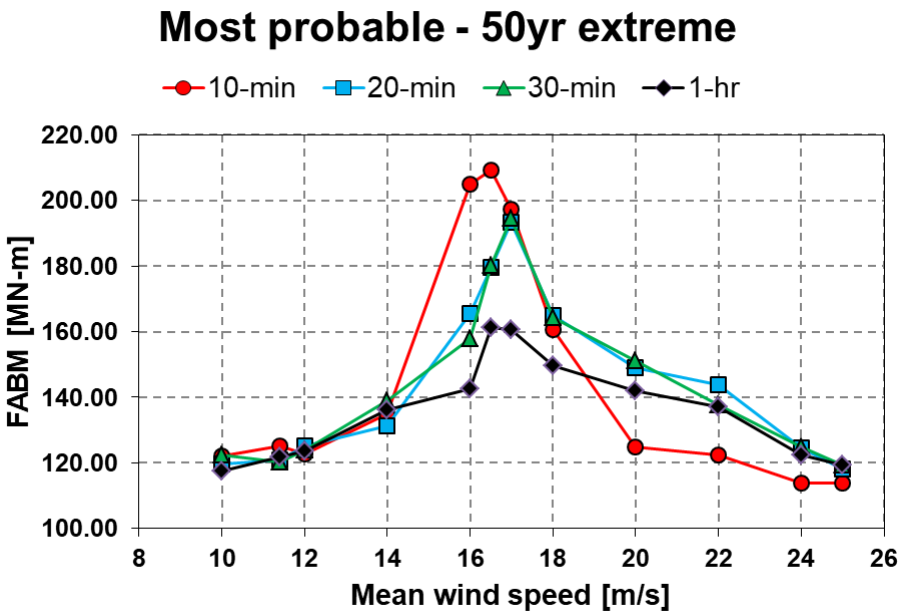

Figure 4.7: Most probable value from 10-min (red circles), 20-min (blue squares), 30-min (green triangles), and 1hr (black diamonds) extrapolated to a 50yr level from simulations versus mean wind speed for FABM.

These differences are better understood when the relative errors are plotted. In the case of the FASF, **Fig. 4.8**, the relative error is higher for the 10-min and 20-min cases, and the error for the extrapolation obtained from the 30-min varies in the range of +-5%. In the case of the FABM **Fig. 4.9**, it is observed that both 20-min and 30-min perform similarly, but using 10-min gives the highest relative error. In the 20-min and 30-min cases, the error varies between +20% (for critical wind speed) and -10% (for higher speeds and near the cut-out wind speed).

4.6.2. Effects of flexible soil

In this section, the effects of considering the soil flexibility through the IAF soil model on load extrapolation will be explored. For this analysis, 1hr simulations will be used and extrapolation will be applied to 50-year levels. In **Figs. 4.10** and **4.11,** it can be observed the trend of the most probable values of the extreme responses in one hour for FASF and FSBM, respectively. As it can be noticed, the difference between both curves is small. Similarly, in **Fig. 4.12** the relative errors for the FASF and the FABM are observed. In this case, the comparisons are made between the response obtained considering the IAF and the response obtained

with the rigid foundation. So, it is observed an increase of up to about 3% for the FASF, and about 2% for the FABM when considering soil flexibility.

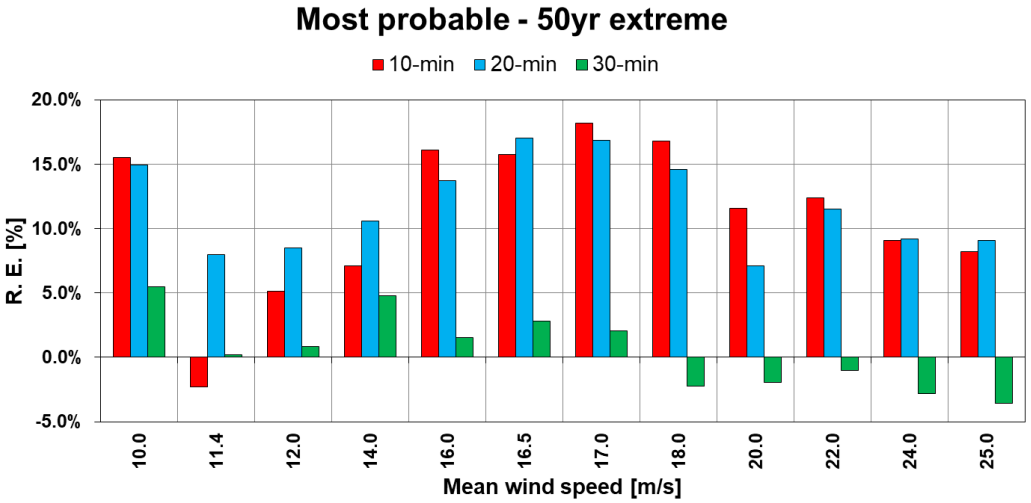

Figure 4.8: Relative errors of the most probable values extrapolated to 50yr level with respect to most probable values extrapolated from 1hr simulations for the FASF.

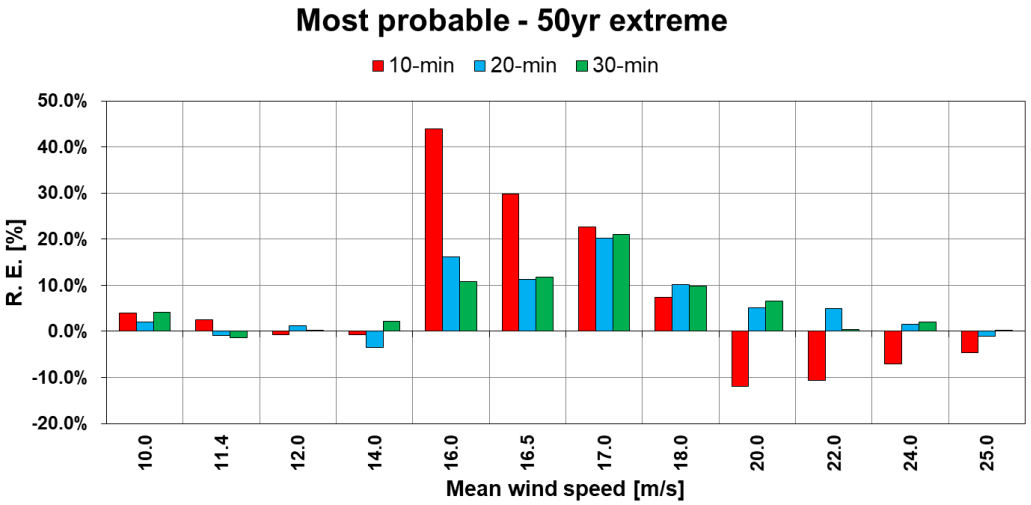

Figure 4.9: Relative errors of the most probable values extrapolated to 50yr level with respect to most probable values extrapolated from 1hr simulations for the FABM.

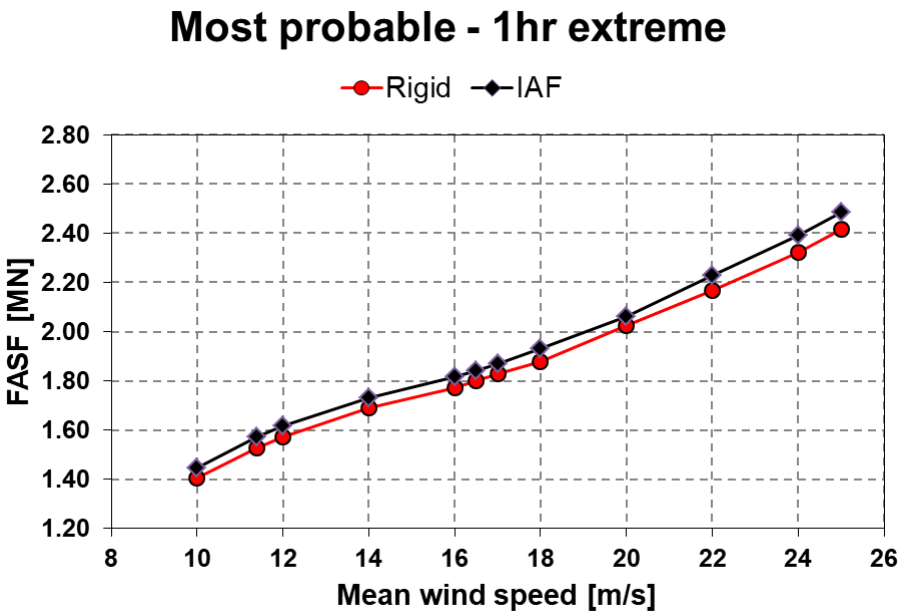

Figure 4.10: Most probable value of extreme response for FASF from 1hr simulations considering rigid foundation (red circles) and IAF foundation (black diamonds) versus mean wind speed.

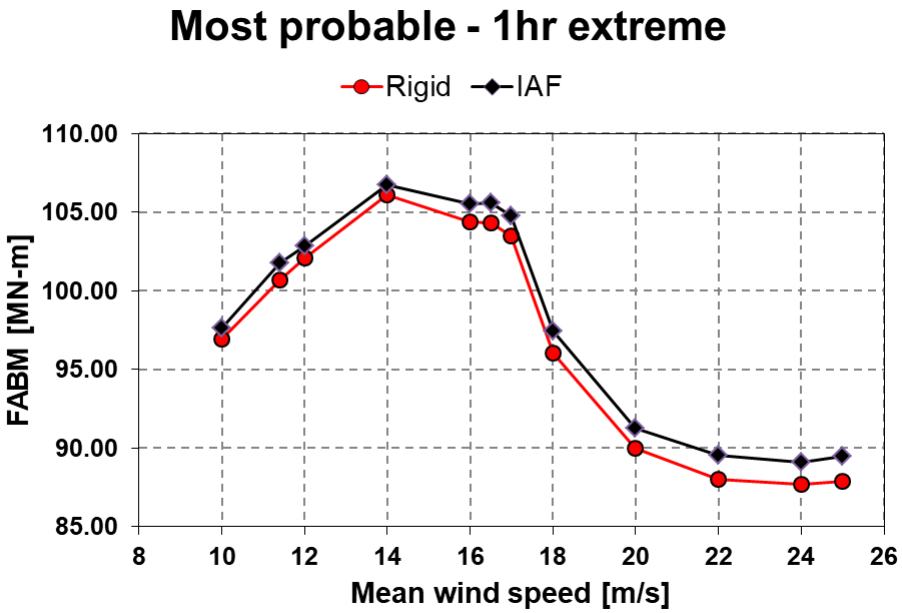

Figure 4.11: Most probable value of extreme response for FABM from 1hr simulations considering rigid foundation (red circles) and IAF foundation (black diamonds) versus mean wind speed.

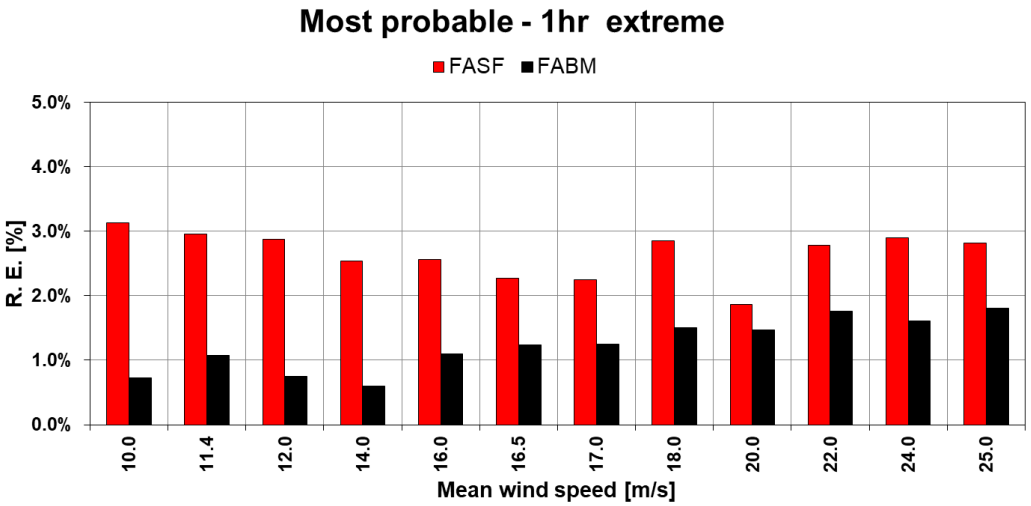

Figure 4.12: Relative error of 1hr extreme response for FASF (Red) and FABM (black) when a flexible soil model is considered.

In **Fig. 4.13**, it can be seen that there is no great variation in the values of FAASF when the extrapolation to a 50yr level is applied. In contrast, the FABM experiences some variations, **Fig. 4.14**. The critical environmental condition moves slightly from the 16.5 m/s speed to 18 m/s. Also, the most likely value after extrapolation increases. This behaviour can be seen more clearly in **Fig. 4.15**. The FASF has maximum deviations close to 4%, and the FABM reaches up to 10% for 18 m/s where the critical mean wind speed is found.

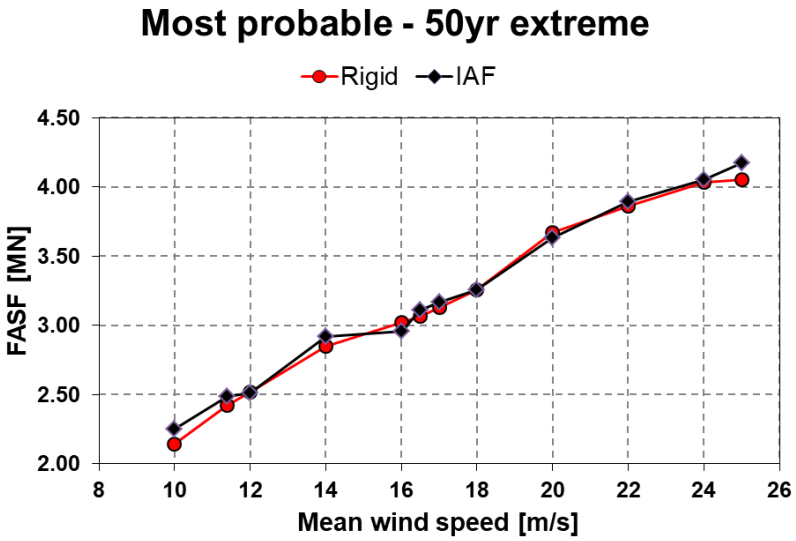

Figure 4.13: Most probable value of extreme response for FASF extrapolated to 50yr level considering rigid foundation (red circles) and IAF foundation (black diamonds) versus mean wind speed.

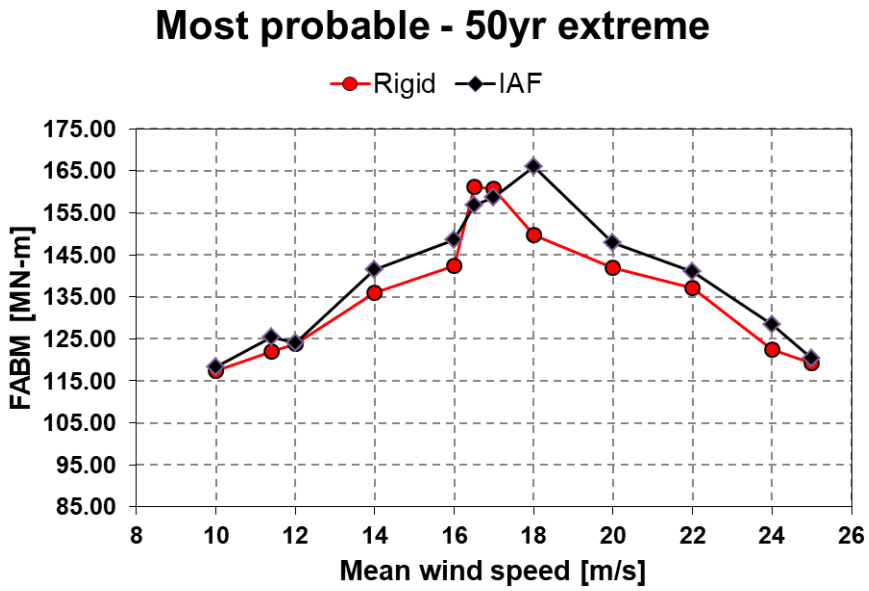

Figure 4.14: Most probable value of extreme response for FASF extrapolated to 50yr level considering rigid foundation (red circles) and IAF foundation (black diamonds) versus mean wind speed.

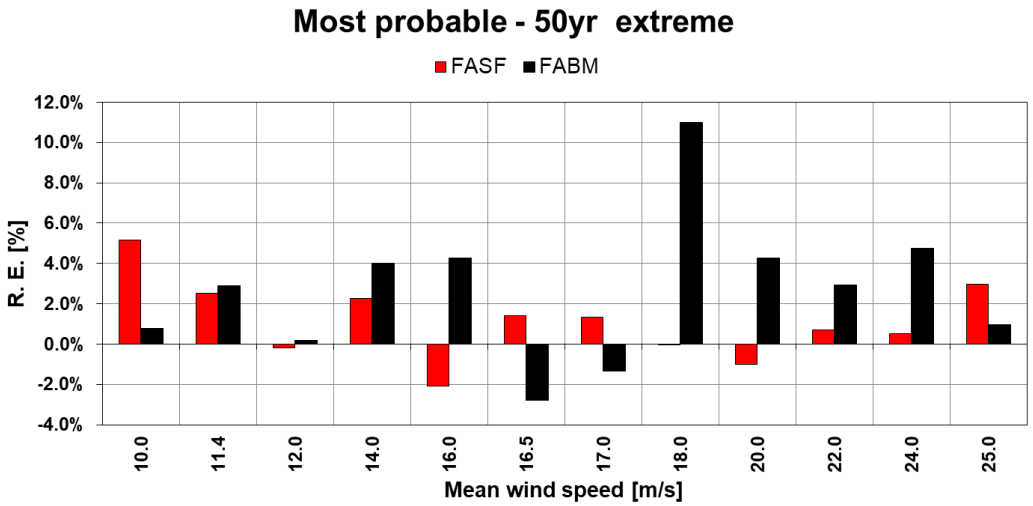

Figure 4.15: Relative error of extreme response extrapolated to 50yr level for FASF (Red) and FABM (black) when a flexible soil model is considered.

CHAPTER V. SUMMARY AND CONCLUSIONS

5.1 SUMMARY OF RESEARCH OBJECTIVES

The main objective (**RO**) of this work has been focused on the study of the uncertainties on the responses of a bottom-fixed offshore wind turbine (NREL 5MW). This has been done through the development of three papers that have dealt with the three main types of uncertainty present in a structural design based on a stochastic approach. The input parameters, on which attention has been centred, have been: wave parameters, wind shear, simulation length and the incorporation of soil flexibility.

In the first part, a study of the effects of uncertainties on wave parameters was carried out. In this case, the selected parameters were the wave height (H_S) and the wave period (T_P). The Environmental Contour Method was used to select appropriate sea states corresponding to relevant wind speeds, the rated and the cut-out, with a return period of 50 years. Subsequently, percentages of variation (uncertainties) were progressively applied and used in coupled aero-hydro-servo-elastic simulations. The propagation of the uncertainty in the dynamic responses was measured through the standard deviations of the time series. For this purpose, sensitivity coefficients were defined based on the results of the simulations, and then, adjusted to linear and quadratic models depending on the input uncertainty level. This study was directly linked to the accomplishment of the first specific objective (**SO1**), and it has been developed in chapter 2.

In chapter 3, the uncertainty of wind shear and its influence on long-term extreme responses was studied. To meet the specific objective 2 (**SO2**), some gaps in the literature were identified and it was determined that the value recommended by the international standards may differ from the actual shear values that can be found in offshore locations. To evaluate the influence of this parameter, progressive variations of the wind shear coefficient were applied in the calculation of the wind fields through the power-law. This relationship was also

useful to correlate wind speeds at different heights. The Modified Environmental Contour Method (MECM) was employed to find the governing environmental conditions instead of the traditional ECM. It was necessary to use the MECM as the traditional method does not consider structures that have an active control system. To obtain stability of the statistical parameters, 100 stochastic realizations were made for each environmental condition considered. Based on the results of the simulations, a fitting procedure of the extreme values was made to estimate the short-term probability distributions using the Global Maxima Method (GMM). Finally, after applying a statistical extrapolation procedure, the most probable values of the long-term extreme responses were calculated.

In chapter 4 it was sought to fulfil the specific objectives 3 and 4 (**SO3** & **SO4**). In that part of the research, it was aimed to contribute to the understanding of the uncertainties in a bottom-fixed monopile wind turbine. Two types of uncertainty were addressed: statistical uncertainty and model uncertainty. The first one was addressed by exploring the influence of simulation length and its effect on the extrapolation of short and long-term responses. After a literature review, it was established that there is no consensus regarding the effective length of simulation applicable to structures under combined load. It was deemed appropriate to explore its influence on dynamic responses. For this purpose, simulations of 10, 20 and 30 minutes were carried out. Then, short-term probability distributions were fitted from the results. The short-term probability distributions were extrapolated to a 1-hour level and compared against the results obtained from full 1-hour simulations. Model uncertainty was the second type of uncertainty addressed in chapter 4. In this case, the influence of soil flexibility was studied. The soil model used in this part of the thesis was the improved apparent fixity (IAF) soil model which is based on the inclusion of two fictitious beams below the mudline. The results of this model were compared against simulations using the usual rigid foundation soil model. In both cases, the results used for the adjustment of the short-term probability distributions came from one-hour simulations. As in the previous chapter, the MECM was used to estimate the governing environmental conditions and determine long-term responses.

5.2 CONCLUSIONS

In the following subsections, the conclusions derived from the work done in this thesis are summarized.

5.2.1. Conclusions from paper 1

Chapter 2, which was focused on wave parameters, leads us to the following conclusions:

1. By systematically introducing uncertainties in the wave parameters (input), and evaluating the results by comparing the standard deviations of the stochastic responses, it was found that there is a relationship between the sensitivity of the outputs that can be well represented as a function of the uncertainties in wave parameters (δ, ε).

2. When the sensitivity indexes were modelled as a function of the input uncertainties, it was observed a linear behaviour when there was only uncertainty in the wave height (H_S). However, when uncertainty was introduced in the wave period (T_P), or both parameters, the effect in the response exhibited a second-order relationship. In all cases, the goodness of the regression function was measured by the coefficient of determination (r^2), reaching values above 95%.

3. After performing a regression analysis to link sensitivity index with the uncertainties in the input parameters by functions, it was found that the coefficients of the regression functions were fitted with adequate precision using a third-order interpolation polynomial. In most cases, the coefficient of determination for the regression polynomial function was above 90%

4. From the analysis of the regression polynomial coefficients, it was observed that several of them had very small values close to zero. Therefore, it could be established that their contribution to the respective calculation of the sensitivity index can be negligible. Especially, in the cases in which the coefficients corresponded to independent or first-order terms. These coefficients can safely be set to zero if a subsequent polynomial regression analysis is performed.

5. To calculate the contribution of the wave loads on the wind turbine, the Morison coefficients are an important aspect. From the analysis carried out, it was found that the added mass coefficient (C_A) has more influence in the dynamic responses than the drag coefficient (C_D), especially for the fore-aft shear force.

5.2.2. Conclusions from paper 2

The effects of variable wind shear were explored in chapter 3, and the following conclusions can be drawn from this study:

6. After performing multiple simulations and fitting extreme values to a Gumbel-type distribution for cases where only wind and wave loads were applied individually, it was found that 50yr long-term extreme responses are driven by different environmental factors. In the case of the fore-aft shear force (F_X), waves are the environmental factor that governs its behaviour. Also, it produces a sustained growth over the range of wind speeds in the operational region. In the case of the fore-aft bending moment (M_Y), it was observed a peak within the operational range, indicating that this response is mainly governed by the wind.

7. Based on the analysis of several scenarios under variable wind shear coefficient in combination with the Modified Environmental Contour Method, it was observed that the WSC influenced the identification of critical wind speed for F_X but not for M_Y. In the case of the fore-aft shear force, the wind shear caused that the critical wind speed to move from a value of 20 m/s for the lower limit (WSC=0.06) to 23 m/s for the upper limit (WSC=0.14), while in the case of the bending moment, the critical wind speed (16.5 m/s) remains unchanged regardless of the WSC value.

8. Several WSC were used as input data to perform stochastic simulations in FAST, the extreme values obtained from the generated time series permitted to obtain short-term probability distributions. By applying the Modified Environmental Contour Method and statistical extrapolation it was possible to evaluate the influence of the WSC on 50yr long term extreme responses. It was found that the long-term extreme responses associated

with monopile (F_X, M_Y) have low sensitivity with respect to WSC. Values show that sensitivity of F_X to varying wind shear values is around 0% whereas the sensitivity of M_Y reaches a value of up to -3% with respect to the reference (WSC=0.14).

5.2.3. Conclusions from paper 3

In the last chapter, the simulation length and the influence of considering the flexibility of the soil were discussed. In this regard, the following conclusions are obtained:

9. After a review of the literature on the applicability of a 10-minute simulation length to structures under combined load, it was identified the need to explore the effects of lengths other than that currently employed. In this regard, it was concluded that a 10-minute simulation can estimate the distribution of one-hour extreme responses with adequate accuracy, but it is not sufficient for long-term responses with a return period of 50 years. In the case of F_X, at least a 30-minute simulation is needed, and in the case of M_Y, similar accuracies are achieved with 20-minute and 30-minute.

10. The consideration of a completely rigid foundation is an assumption widely accepted within the studies carried out in the field of wind turbines since it allows highly simplifying the complex models and then reducing the overall computing time. However, as more accurate and reliable results are required, it becomes necessary to consider the flexibility of the soil. From the results, it was found that the inclusion of this aspect on the simulations does not have much impact on the one-hour extreme response. However, when a return period of 50 years is considered, the critical condition found with the MECM for M_Y is shifted from 16.5 m/s (rigid case) to a new value of 18 m/s (flexible case), and the extreme response increases by 2.96%. In the case of F_X, the inclusion of soil does not produce a significant variation in the long-term extreme response.

5.3 SUGGESTIONS FOR FUTURE RESEARCH

Based on the knowledge gained during the development of this thesis, the literature reviewed, and the analyses made, the following aspects can be recommended for further studies aligned with the objectives of the present thesis:

- Monopiles are the most widely used structure today; however, their use is restricted to shallow waters. In this context, the non-linearities of waves have considerable influence. To capture the effects of this phenomenon, it is important to include higher-order wave kinematics e.g. Stokes 5^{th} order waves, Stream function wave theory, and others. It is also essential to use higher-order loading models to capture the effects that nonlinear wave kinematics can induce on the structure e.g. FNV, Rainey, M&M, and others.

- Soil-structure interaction is a very important subject when an offshore wind turbine is analysed. This becomes more relevant when bottom-fixed turbines are addressed. In this study, the rigid and the IAF model were evaluated and compared. However, it is necessary to evaluate the effects of including more complete and advanced soil models e.g. coupled springs, distributed springs, among others. This inclusion will allow obtaining more reliable results regarding the structural dynamic responses.

- In this work, the effects of each type of uncertainty have been evaluated separately. However, the study of a combined effect will be important to understand how these uncertainties are interrelated and their respective influence on the dynamic responses of interest.

- The phenomena of ringing and springing associated with the excitation of the structure are very important in the calculation of dynamic responses. The evaluation of the effects that these phenomena can produce on the aero-hydro-servo-elastic simulations must be taken very carefully as they can cause extreme loads to increase considerably.

- Traditionally the environmental variables considered within the joint probability distributions have been wind speed, wave height and period. All other variables are treated as deterministic values. However, as the investigation advances it has been seen that this consideration is not fully

valid. Therefore, the inclusion of more environmental variables in the joint probability distributions and their influence on the environmental contour method as well as the dynamic responses should be explored. These include the turbulence intensity, wind veer, wind shear, coherence spectrum parameters, and many others.

- In this thesis, the wind turbine was only studied in an operational situation. However, offshore wind turbines experience different modes of operation during their lifetime. Therefore it is important to study the propagation of uncertainty on the dynamic responses under different working conditions e.g. parked, idling, in installation, with faults, and others.

- To ensure the structural integrity of an offshore wind turbine, several criteria must be met. This thesis was mainly focused on extreme long-term loads. However, fatigue analysis is also an important aspect in the verification of the criteria fulfilment that ensures the reliability of the structure. These types of analysis should be studied in more detail in future research.

- In the wind energy industry, manufacturers and investors are increasingly looking for larger turbines. This leads inevitably to new challenges, and then, the uncertainties acquire higher relevance. In this work, the NREL 5 MW turbine was used as a reference. However, currently, the commercially available turbines already exceed 8 MW, and there are already plans to build wind turbines up to 14 MW [5]. It is evident that this wind turbine size will be the reference for the offshore industry in the future. Therefore, the study of the 14 MW wind turbine becomes relevant for future research. The National Renewable Energy Laboratory (NREL) has recently released the FAST simulation model for a 15 MW wind turbine [119], so further research is expected to be carried out using this model for the near future.

LIST OF REFERENCES

[1] GWEC, ‘Global wind report 2019’, 2019. Accessed: Jun. 24, 2020. [Online]. Available: https://gwec.net/global-wind-report-2019/.

[2] C. Ng and L. Ran, *Offshore Wind Farms: Technologies, Design and Operation*, 1st ed. Woodhead Publishing, 2016.

[3] Wind Europe, ‘Offshore Wind in Europe: Key trends and statistics 2019’, 2019. Accessed: Jun. 24, 2020. [Online]. Available: https://windeurope.org/about-wind/statistics/offshore/european-offshore-wind-industry-key-trends-statistics-2019/.

[4] GE Renewable Energy, ‘The world’s most powerful offshore wind turbine: Haliade-X 12 MW offshore wind turbine platform’, 2020. https://www.ge.com/renewableenergy/wind-energy/offshore-wind/haliade-x-offshore-turbine (accessed Jun. 24, 2020).

[5] Siemens Gamesa Renewable Energy, ‘Powered by change: Siemens Gamesa launches 14 MW offshore Direct Drive turbine with 222-meter rotor’. https://www.siemensgamesa.com/en-int/newsroom/2020/05/200519-siemens-gamesa-turbine-14-222-dd (accessed Jun. 24, 2020).

[6] International Energy Agency, ‘Offshore Wind Outlook 2019: World Energy Outlook Special Report’, 2019. Accessed: Jun. 24, 2020. [Online]. Available: https://www.iea.org/reports/offshore-wind-outlook-2019.

[7] A. N. Robertson, K. Shaler, L. Sethuraman, and J. Jonkman, ‘Sensitivity analysis of the effect of wind characteristics and turbine properties on wind turbine loads’, *Wind Energy Sci.*, vol. 4, pp. 479–513, 2019, doi: 10.5194/wes-4-479-2019.

[8] T. J. Sullivan, *Introduction to Uncertainty Quantification*, 1st ed. Springer, 2015.

[9] National Research Council, *Assessing the reliability of complex models: mathematical and statistical foundations of verification, validation, and uncertainty quantification*. National Academies Press, 2012.

[10] R. R. Damiani, 'Uncertainty and Risk Assessment in the Design Process for Wind', 2018. doi: 10.2172/1421379.

[11] Z. Jiang, W. Hu, W. Dong, Z. Gao, and Z. Ren, 'Structural reliability analysis of wind turbines: A review', *Energies*, vol. 10, no. 12, p. 2099, 2017, doi: 10.3390/en10122099.

[12] J. Fogle, P. Agarwal, and L. Manuel, 'Towards an improved understanding of statistical extrapolation for wind turbine extreme loads', *Wind Energy*, vol. 11, pp. 613–635, 2008, doi: 10.1002/we.303.

[13] OSINERGMIN, 'Renewable Energy Auctions'. https://www.osinergmin.gob.pe/empresas/energias-renovables/subastas (accessed Jun. 26, 2020).

[14] OSINERGMIN, 'Power Generation Projects in Peru'. https://www.osinergmin.gob.pe/empresas/electricidad (accessed Jun. 24, 2020).

[15] OSINERGMIN, 'Technical sheet of the wind power plant "MARCONA"'. https://www.osinergmin.gob.pe/seccion/centro_documental/electricidad/Documentos/PROYECTOS GFE/Acordeón/Generación/1.7.1.pdf (accessed Jun. 24, 2020).

[16] OSINERGMIN, 'Technical sheet of the wind power plant "TRES HERMANAS"'. https://www.osinergmin.gob.pe/seccion/centro_documental/electricidad/Documentos/PROYECTOS GFE/Acordeón/Generación/1.7.4.pdf (accessed Jun. 24, 2020).

[17] OSINERGMIN, ‘Technical sheet of the wind power plant “WAYRA I”’. https://www.osinergmin.gob.pe/seccion/centro_documental/electricidad/Documentos/PROYECTOS GFE/Acordeón/Generación/3.5.1.pdf (accessed Jun. 24, 2020).

[18] OSINERGMIN, ‘Technical sheet of the wind power plant “CUPISNIQUE”’. https://www.osinergmin.gob.pe/seccion/centro_documental/electricidad/Documentos/PROYECTOS GFE/Acordeón/Generación/1.7.2.pdf (accessed Jun. 24, 2020).

[19] OSINERGMIN, ‘Technical sheet of the wind power plant “TALARA”’. https://www.osinergmin.gob.pe/seccion/centro_documental/electricidad/Documentos/PROYECTOS GFE/Acordeón/Generación/1.7.3.pdf (accessed Jun. 24, 2020).

[20] OSINERGMIN, ‘Technical sheet of the wind power plant “DUNA”’. https://www.osinergmin.gob.pe/seccion/centro_documental/electricidad/Documentos/PROYECTOS GFE/Acordeón/Generación/3.5.3.pdf (accessed Jun. 24, 2020).

[21] OSINERGMIN, ‘Technical sheet of the wind power plant “HUAMBOS”’. https://www.osinergmin.gob.pe/seccion/centro_documental/electricidad/Documentos/PROYECTOS GFE/Acordeón/Generación/3.5.2.pdf (accessed Jun. 24, 2020).

[22] OSINERGMIN, ‘La industria de la energía renovable en el Perú: 10 años de contribuciones a la mitigación del cambio climático’, Lima, 2017. Accessed: Jun. 24, 2020. [Online]. Available: https://www.osinergmin.gob.pe/seccion/centro_documental/Institucional/Estudios_Economicos/Libros/Osinergmin-Energia-Renovable-Peru-10anios.pdf.

[23] A. Saltelli *et al.*, *Global Sensitivity Analysis. The Primer*, vol. 1, no. John Wiley & Sons, 2008.

[24] R. C. Smith, *Uncertainty quantification: theory, implementation, and applications*. SIAM, 2013.

[25] J. M. Rinker, ‘Calculating the sensitivity of wind turbine loads to wind inputs using response surfaces’, *J. Phys. Conf. Ser.*, vol. 753, no. 3, p. 32057, 2016, doi: 10.1088/1742-6596/753/3/032057.

[26] M. Karimirad and E. E. Bachynski, ‘Sensitivity Analysis of Limited Actuation for Real-time Hybrid Model Testing of 5MW Bottom-fixed Offshore Wind Turbine’, *Energy Procedia*, vol. 137, pp. 14–25, 2017, doi: 10.1016/j.egypro.2017.10.331.

[27] J.-T. Horn, J. R. Krokstad, and J. Amdahl, ‘Long-term fatigue damage sensitivity to wave directionality in extra-large monopile foundations’, *Proc. Inst. Mech. Eng. Part M J. Eng. Marit. Environ.*, vol. 232, no. 1, pp. 37–49, 2018, doi: 10.1177/1475090217727136.

[28] A. N. Robertson, L. Sethuraman, J. M. Jonkman, and J. Quick, ‘Assessment of wind parameter sensitivity on extreme and fatigue wind turbine loads’, *2018 Wind Energy Symp.*, 2018, doi: 10.2514/6.2018-1728.

[29] S. Haver and S. R. Winterstein, ‘Environmental contour lines: A method for estimating long term extremes by a short term analysis’, *Trans. - Soc. Nav. Archit. Mar. Eng.*, 2008, [Online]. Available: https://www.researchgate.net/profile/Steven_Winterstein/publication/242315833_Environmental_Contour_Lines_A_Method_for_Estimating_Long_Term_Extremes_by_a_Short_Term_Analysis/links/5e84b9144585150839b33618/Environmental-Contour-Lines-A-Method-for-Estimatin.

[30] Q. Li, C. Michailides, Z. Gao, and T. Moan, ‘A comparative study of different methods for predicting the long-term extreme structural responses of the combined wind and wave energy concept semisubmersible wind energy and flap-type wave energy converter’, *Proc. Inst. Mech. Eng. Part M J. Eng. Marit. Environ.*, vol. 232, no. 1, pp. 85–96, 2018, doi: 10.1177/1475090217726886.

[31] Q. Li, Z. Gao, and T. Moan, ‘Modified environmental contour method for predicting long-term extreme responses of bottom-fixed offshore wind turbines’, *Mar. Struct.*, vol. 48, pp. 15–32, 2016, doi: 10.1016/j.marstruc.2016.03.003.

[32] J. Jonkman, S. Butterfield, W. Musial, and G. Scott, ‘Definition of a 5-MW reference wind turbine for offshore system development’, OSTI, 2009. doi: 10.2172/947422.

[33] B. Barahona, J. M. Jonkman, R. Damiani, A. Robertson, and G. Hayman, ‘Verification of the New FAST v8 Capabilities for the Modeling of Fixed-Bottom Offshore Wind Turbines’, *33rd Wind Energy Symp.*, 2015, doi: 10.2514/6.2015-1205.

[34] L. Li, Z. Gao, and T. Moan, ‘Joint Environmental Data at Five European Offshore Sites for Design of Combined Wind and Wave Energy Devices’, *Proc. Int. Conf. Offshore Mech. Arct. Eng. OMAE*, 2013, doi: 10.1115/omae2013-10156.

[35] International Electrotechnical Commission, ‘IEC 61400-3:2009. Wind turbines - Part 3: Design requirements for offshore wind turbines’. International Electrotechnical Commission, 2009, Accessed: Jun. 24, 2020. [Online]. Available: https://webstore.iec.ch/publication/5446.

[36] B. J. Jonkman, ‘Turbsim User’s Guide: Version 1.50’, 2009. doi: 10.2172/965520.

[37] M. Karimirad, *Offshore Energy Structures: For Wind Power, Wave Energy and Hybrid Marine Platforms*, vol. 1. Springer, 2014.

[38] WAFO Group, ‘WAFO - A Matlab Toolbox for Analysis of Random Waves and Loads - A Tutorial’, Sweden, 2000. Accessed: Jun. 24, 2020. [Online]. Available: http://www.maths.lth.se/matstat/wafo.

[39] X. Wang, X. Zeng, J. Li, X. Yang, and H. Wang, ‘A review on recent advancements of substructures for offshore wind turbines’, *Energy Convers. Manag.*, vol. 158, pp. 103–119, 2018, doi: 10.1016/j.enconman.2017.12.061.

[40] I. Abdallah, A. Natarajan, and J. D. Sørensen, ‘Influence of the control system on wind turbine loads during power production in extreme turbulence: Structural reliability’, *Renew. Energy*, vol. 87, pp. 464–477, 2016, doi: 10.1016/j.renene.2015.10.044.

[41] C. E. Clark and B. DuPont, ‘Reliability-based design optimization in offshore renewable energy systems’, *Renew. Sustain. Energy Rev.*, vol. 97, pp. 390–400, 2018, doi: 10.1016/j.rser.2018.08.030.

[42] M. Leimeister and A. Kolios, ‘A review of reliability-based methods for risk analysis and their application in the offshore wind industry’, *Renew. Sustain. Energy Rev.*, vol. 91, pp. 1065–1076, 2018, doi: 10.1016/j.rser.2018.04.004.

[43] International Electrotechnical Commission, ‘IEC 61400-1:2005. Wind turbines - Part 1: Design requirements’. International Electrotechnical Commission, 2005, Accessed: Jun. 24, 2020. [Online]. Available: https://webstore.iec.ch/publication/5426.

[44] B. Ernst and J. R. Seume, ‘Investigation of site-specific wind field parameters and their effect on loads of offshore wind turbines’, *Energies*, vol. 5, no. 10, pp. 3835–3855, 2012, doi: 10.3390/en5103835.

[45] B. Kim, J. Jin, O. Bitkina, and K. Kang, ‘Ultimate load characteristics of NREL 5-MW offshore wind turbines with different substructures’, *Int. J. Energy Res.*, vol. 40, no. 5, pp. 639–650, 2015, doi: 10.1002/er.3430.

[46] R. M. M. Slot, L. Svenningsen, J. D. Sørensen, and M. L. Thøgersen, ‘Importance of shear in site assessment of wind turbine fatigue loads’, *J. Sol. Energy Eng.*, vol. 140, no. 4, 2018, doi: 10.1115/1.4039748.

[47] X. Chen, Z. Jiang, Q. Li, and Y. Li, ‘Effect of wind turbulence on extreme load analysis of an offshore wind turbine’, *Proc. Int. Conf. Offshore Mech. Arct. Eng. OMAE*, 2019, doi: 10.1115/OMAE2019-95634.

[48] E. Berge, Ø. Byrkjedal, Y. Ydersbond, D. Kindler, and A. S. Kjeller Vindteknikk, ‘Modelling of offshore wind resources. Comparison of a meso-scale model and measurements from FINO 1 and North Sea oil rigs’, *Eur. Wind Energy Conf.*, 2009, [Online]. Available: https://www.researchgate.net/publication/228586135_Modelling_of_offshore_wind_resources_Comparison_of_a_meso-scale_model_and_measurements_from_FINO_1_and_North_Sea_oil_rigs.

[49] M. Brower, *Wind resource assessment: a practical guide to developing a wind project*. John Wiley & Sons, 2012.

[50] T. R. Camp *et al.*, ‘Design Methods for Offshore Wind Turbines at Exposed Sites Final. Final Report of the OWTES Project’, 2003.

[51] A. Peña Diaz *et al.*, ‘Offshore vertical wind shear: Final report on NORSEWInD’s work task 3.1’, DTU Wind Energy, 2012. [Online]. Available: https://orbit.dtu.dk/en/publications/offshore-vertical-wind-shear-final-report-on-norsewinds-work-task.

[52] A. M. Viselli, G. Z. Forristall, B. R. Pearce, and H. J. Dagher, ‘Estimation of extreme wave and wind design parameters for offshore wind turbines in the Gulf of Maine using a POT method’, *Ocean Eng.*, vol. 104, pp. 649–658, 2015, doi: 10.1016/j.oceaneng.2015.04.086.

[53] O. Krogsæter and J. Reuder, ‘Validation of boundary layer parameterization schemes in the weather research and forecasting model under the aspect of offshore wind energy applications—Part I: Average wind speed and wind shear’, *Wind Energy*, vol. 18, no. 5, pp. 769–782, 2014, doi: 10.1002/we.1727.

[54] D. Corrigan, S. Li, and D. H. Matthiesen, ‘Computational fluid dynamics modeling of the structural influences on offshore wind measurements at the Cleveland water intake crib in Lake Erie’, *Wind Eng.*, vol. 40, no. 3, pp. 283–292, 2016, doi: 10.1177/0309524x16647855.

[55] Z. R. Shu, Q. S. Li, Y. C. He, and P. W. Chan, ‘Observations of offshore wind characteristics by Doppler-LiDAR for wind energy applications’, *Appl. Energy*, vol. 169, pp. 150–163, 2016, doi: 10.1016/j.apenergy.2016.01.135.

[56] G. Gualtieri, ‘Surface turbulence intensity as a predictor of extrapolated wind resource to the turbine hub height: method’s test at an offshore site’, *Renew. Energy*, vol. 111, pp. 175–186, 2017, doi: 10.1016/j.renene.2017.03.095.

[57] A. Albani and M. Z. Ibrahim, ‘Wind energy potential and power law indexes assessment for selected near-coastal sites in Malaysia’, *Energies*, vol. 10, no. 3, p. 307, 2017, doi: 10.3390/en10030307.

[58] E. Gonzalez, L. Valldecabres, H. Seyr, and J. J. Melero, ‘On the effects of environmental conditions on wind turbine performance: An offshore case study’, *J. Phys. Conf. Ser.*, vol. 1356, no. 1, p. 12043, 2019, doi: 10.1088/1742-6596/1356/1/012043.

[59] J. Li and X. B. Yu, ‘Onshore and offshore wind energy potential assessment near Lake Erie shoreline: a spatial and temporal analysis’, *Energy*, vol. 147, pp. 1092–1107, 2018, doi: 10.1016/j.energy.2018.01.118.

[60] Y. Ding, *Data Science for Wind Energy*. New York: Chapman and Hall/CRC, 2019.

[61] DNV GL AS, ‘Recommended practice. DNVGL-RP-C205. Environmental conditions and environmental loads’. 2017, Accessed: Jun. 24, 2020. [Online]. Available: https://oilgas.standards.dnvgl.com/download/dnvgl-rp-c205-environmental-conditions-and-environmental-loads.

[62] H. S. Toft, J. D. Sørensen, and D. Veldkamp, ‘Assessment of load extrapolation methods for wind turbines’, *J. Sol. energy Eng.*, vol. 133, no. 2, 2011, doi: 10.1115/1.4003416.

[63] J. Wang, H. Chen, Y. Li, Y. Wu, and Y. Zhang, ‘A Review of the Extrapolation Method in Load Spectrum Compiling.’, *Stroj. Vestnik/Journal Mech. Eng.*, vol. 62, no. 1, pp. 60–75, 2016, doi: 10.5545/sv-jme.2015.2905.

[64] P. Graf, R. Damiani, K. Dykes, and J. M. Jonkman, ‘Advances in the assessment of wind turbine operating extreme loads via more efficient calculation approaches’, 2017, doi: 10.2514/6.2017-0680.

[65] G. Stewart, M. Lackner, L. Haid, D. Matha, J. Jonkman, and A. Robertson, ‘Assessing fatigue and ultimate load uncertainty in floating offshore wind turbines due to varying simulation length’, *11th Int. Conf. Struct. Saf. Reliab.*, pp. 239–246, 2013, doi: 10.1201/b16387.

[66] L. Haid, G. Stewart, J. Jonkman, A. Robertson, M. Lackner, and D. Matha, ‘Simulation-length requirements in the loads analysis of offshore floating wind turbines’, *Proc. Int. Conf. Offshore Mech. Arct. Eng. OMAE*, 2013, doi: 10.1115/OMAE2013-11397.

[67] C. Hübler, C. G. Gebhardt, and R. Rolfes, ‘Development of a comprehensive data basis of scattering environmental conditions and simulation constraints for offshore wind turbines’, *Wind Energy Sci.*, vol. 2, pp. 491–505, 2017, doi: 10.5194/wes-2-491-2017.

[68] A. C. Pillai, P. R. Thies, and L. Johanning, ‘Impact of Simulation Duration for Offshore Floating Wind Turbine Analysis Using a Coupled FAST-OrcaFlex Model’, *Proc. Int. Conf. Offshore Mech. Arct. Eng. OMAE*, 2019, doi: 10.1115/omae2019-95159.

[69] J.-T. Horn and S. R. Winterstein, ‘Extreme response estimation of offshore wind turbines with an extended contour-line method’, *J. Phys. Conf. Ser.*, vol. 1104, p. 12031, 2018, doi: 10.1088/1742-6596/1104/1/012031.

[70] J. M. Jonkman and M. L. Buhl Jr, ‘FAST User’s Guide - Updated August 2005’, 2005. doi: 10.2172/15020796.

[71] J. Jonkman, A. Robertson, and G. Hayman, ‘HydroDyn User’s Guide and Theory Manual (draft version)’, 2014.

[72] D. Barreto, A. Moghtadaei, M. Karimirad, and A. Ortega, ‘Sensitivity Analysis of a Bottom Fixed Offshore Wind Turbine Using the Environmental Contour Method’, *Proc. Int. Conf. Offshore Mech. Arct. Eng. OMAE*, 2019, doi: 10.1115/OMAE2019-95390.

[73] M. Karimirad and T. Moan, ‘Feasibility of the application of a spar-type wind turbine at a moderate water depth’, *Energy Procedia*, vol. 24, pp. 340–350, 2012, doi: 10.1016/j.egypro.2012.06.117.

[74] P. Agarwal and L. Manuel, ‘Simulation of offshore wind turbine response for long-term extreme load prediction’, *Eng. Struct.*, vol. 31, no. 10, pp. 2236–2246, 2009, doi: 10.1016/j.engstruct.2009.04.002.

[75] A. Morató, S. Sriramula, N. Krishnan, and J. Nichols, ‘Ultimate loads and response analysis of a monopile supported offshore wind turbine using fully coupled simulation’, *Renew. Energy*, vol. 101, pp. 126–143, 2017, doi: 10.1016/j.renene.2016.08.056.

[76] S. Aguilar Vargas, G. R. Telles Esteves, P. Medina Maçaira, B. Quaresma Bastos, F. L. Cyrino Oliveira, and R. Castro Souza, ‘Wind power generation: A review and a research agenda’, *J. Clean. Prod.*, vol. 218, pp. 850–870, 2019, doi: 10.1016/j.jclepro.2019.02.015.

[77] IPCC, ‘Global Warming of 1.5 ^{o}C’, IPCC, 2018. Accessed: Jun. 24, 2020. [Online]. Available: https://www.ipcc.ch/sr15/.

[78] U.S. Department of Energy, ‘20% Wind Energy by 2030 Increasing Wind Energy’s Contribution to U.S. Electricity Supply’, U. S. Department of Energy, 2008. Accessed: Jun. 24, 2020. [Online]. Available: https://www.nrel.gov/docs/fy09osti/42864.pdf.

[79] U.S. Department of Energy, ‘Wind Vision: A New Era for Wind Power in the United States’, 2015. Accessed: Jun. 24, 2020. [Online]. Available: http://energy.gov/sites/prod/files/WindVision_Report_final.pdf.

[80] International Energy Agency, ‘Technology Roadmap: Wind Energy’, 2013. Accessed: Jun. 24, 2020. [Online]. Available: https://webstore.iea.org/technology-roadmap-wind-energy-2013.

[81] REN21, ‘RENEWABLES 2019: GLOBAL STATUS REPORT’, 2019. Accessed: Jun. 24, 2020. [Online]. Available: https://www.ren21.net/gsr-2019/.

[82] J. Aldersey-Williams, I. D. Broadbent, and P. A. Strachan, ‘Better estimates of LCOE from audited accounts – A new methodology with examples from United Kingdom offshore wind and CCGT’, *Energy Policy*, vol. 128, pp. 25–35, 2019, doi: 10.1016/j.enpol.2018.12.044.

[83] A. M. Page, V. Næss, J. B. De Vaal, G. R. Eiksund, and T. A. Nygaard, ‘Impact of foundation modelling in offshore wind turbines: Comparison between simulations and field data’, *Mar. Struct.*, vol. 64, pp. 379–400, 2019, doi: 10.1016/j.marstruc.2018.11.010.

[84] P. Bortolotti, H. Canet, C. L. Bottasso, and J. Loganathan, ‘Performance of non-intrusive uncertainty quantification in the aeroservoelastic simulation of wind turbines’, *Wind Energy Sci.*, vol. 4, no. 3, pp. 397–406, 2019, doi: 10.5194/wes-4-397-2019.

[85] X. Chen, Z. Jiang, Q. Li, Y. Li, and N. Ren, ‘Extended Environmental Contour Methods for Long-Term Extreme Response Analysis of Offshore Wind Turbines’, *J. Offshore Mech. Arct. Eng.*, vol. 142, no. 5, 2020, doi: 10.1115/1.4046772.

[86] S. Ghahramani, *Fundamentals of Probability: With Stochastic Processes*, 4th ed. New York: Chapman and Hall/CRC, 2018.

[87] P. Thoft-Christensen and M. J. Baker, *Structural Reliability Theory and Its Applications*. Springer, 1982.

[88] M. C. Kennedy and A. O'Hagan, 'Bayesian calibration of computer models', *J. R. Stat. Soc. Ser. B (Statistical Methodol.*, vol. 63, no. 3, pp. 425–464, 2001, doi: 10.1111/1467-9868.00294.

[89] H. G. Matthies, 'Quantifying uncertainty: modern computational representation of probability and applications', in *Extreme Man-Made and Natural Hazards in Dynamics of Structures*, Springer, 2007, pp. 105–135.

[90] L. V. S. Sagrilo, Z. Gao, A. Naess, and E. C. P. Lima, 'A straightforward approach for using single time domain simulations to assess characteristic extreme responses', *Ocean Eng.*, vol. 38, no. 13, pp. 1464–1471, 2011, doi: 10.1016/j.oceaneng.2011.07.003.

[91] I. Van der Hoven, 'Power spectrum of horizontal wind speed in the frequency range from 0.0007 to 900 cycles per hour', *J. Meteorol.*, vol. 14, no. 2, pp. 160–164, 1957, doi: https://doi.org/10.1175/1520-0469(1957)014<0160:psohws>2.0.co;2.

[92] M. A. Escalante Soberanis and W. Mérida, 'Regarding the influence of the Van der Hoven spectrum on wind energy applications in the meteorological mesoscale and microscale', *Renew. Energy*, vol. 81, pp. 286–292, 2015, doi: 10.1016/j.renene.2015.03.048.

[93] M. Rosenblatt, 'Remarks on a multivariate transformation', *Ann. Math. Stat.*, vol. 23, no. 3, pp. 470–472, 1952, doi: 10.1214/aoms/1177729394.

[94] S. R. Winterstein, T. C. Ude, C. A. Cornell, P. Bjerager, and S. Haver, 'ENVIRONMENTAL PARAMETERS FOR EXTREME RESPONSE: INVERSE FORM WITH OMISSION FACTORS', *Proc. Int. Conf. Struct. Saf. Reliab.*, 1993, [Online]. Available: https://www.researchgate.net/publication/288935223_Environmental_parameters_for_extreme_response_inverse_FORM_with_omission_factors.

[95] M. Karimirad and T. Moan, 'Extreme dynamic structural response analysis of catenary moored spar wind turbine in harsh environmental conditions', *J. Offshore Mech. Arct. Eng.*, vol. 133, no. 4, 2011, doi: 10.1115/1.4003393.

[96] D. Karmakar, H. Bagbanci, and C. Guedes Soares, ‘Long-term extreme load prediction of spar and semisubmersible floating wind turbines using the environmental contour method’, *J. Offshore Mech. Arct. Eng.*, vol. 138, no. 2, 2016, doi: 10.1115/1.4032099.

[97] J. Liu, E. Thomas, A. Goyal, and L. Manuel, ‘Design loads for a large wind turbine supported by a semi-submersible floating platform’, *Renew. Energy*, vol. 138, pp. 923–936, 2019, doi: 10.1016/j.renene.2019.02.011.

[98] K. Raed, A. P. Teixeira, and C. G. Soares, ‘Uncertainty assessment for the extreme hydrodynamic responses of a wind turbine semi-submersible platform using different environmental contour approaches’, *Ocean Eng.*, vol. 195, p. 106719, 2020, doi: 10.1016/j.oceaneng.2019.106719.

[99] J. Canning, P. Nguyen, L. Manuel, and R. G. Coe, ‘On the long-term reliability analysis of a point absorber wave energy converter’, *Proc. Int. Conf. Offshore Mech. Arct. Eng. OMAE*, 2017, doi: 10.1115/OMAE2017-62141.

[100] M. J. Muliawan, M. Karimirad, Z. Gao, and T. Moan, ‘Extreme responses of a combined spar-type floating wind turbine and floating wave energy converter (STC) system with survival modes’, *Ocean Eng.*, vol. 65, pp. 71–82, 2013, doi: 10.1016/j.oceaneng.2013.03.002.

[101] N. Ren, Z. Gao, T. Moan, and L. Wan, ‘Long-term performance estimation of the Spar–Torus-Combination (STC) system with different survival modes’, *Ocean Eng.*, vol. 108, pp. 716–728, 2015, doi: 10.1016/j.oceaneng.2015.08.013.

[102] K. Saranyasoontorn and L. Manuel, ‘On assessing the accuracy of offshore wind turbine reliability-based design loads from the environmental contour method’, 2004, [Online]. Available: https://www.onepetro.org/conference-paper/ISOPE-I-04-030.

[103] Q. Li, Z. Gao, and T. Moan, ‘Extreme response analysis for a jacket-type offshore wind turbine using environmental contour method’, *11th Int. Conf. Struct. Saf. Reliab.*, pp. 5597–5604, 2013, doi: 10.1201/b16387.

[104] Q. Li, Z. Gao, and T. Moan, ‘Modified environmental contour method to determine the long-term extreme responses of a semi-submersible wind turbine’, *Ocean Eng.*, vol. 142, pp. 563–576, 2017, doi: 10.1016/j.oceaneng.2017.07.038.

[105] L. Li, Z.-M. Yuan, Y. Gao, X. Zhang, and T. Tezdogan, ‘Investigation on long-term extreme response of an integrated offshore renewable energy device with a modified environmental contour method’, *Renew. Energy*, vol. 132, pp. 33–42, 2019, doi: 10.1016/j.renene.2018.07.138.

[106] Q. Li, N. Ren, Z. Gao, and T. Moan, ‘Efficient determination of the long-term extreme responses by the modified environmental contour method for a combined wind turbine and wave energy converter system’, *J. Ocean Eng. Mar. Energy*, vol. 4, no. 2, pp. 123–135, 2018, doi: 10.1007/s40722-018-0111-4.

[107] K. Raed, A. P. Teixeira, and C. G. Soares, ‘Assessment of long-term extreme response of a floating support structure using the environmental contour method’, *Proc. 3rd Int. Conf. Renew. Energies Offshore (RENEW 2018)*, no. October, pp. 685–692, 2018, doi: 10.1201/9780429505324.

[108] T. C. Smith, ‘Validation Approach for Statistical Extrapolation’, in *Contemporary Ideas on Ship Stability*, Springer, 2019, pp. 573–589.

[109] P. Ragan and L. Manuel, ‘Statistical extrapolation methods for estimating wind turbine extreme loads’, *J. Sol. Energy Eng.*, vol. 130, pp. 0310111–03101115, 2008, doi: 10.1115/1.2931501.

[110] S. Lott and P. W. Cheng, ‘Load extrapolations based on measurements from an offshore wind turbine at alpha ventus’, *J. Phys. Conf. Ser.*, vol. 753, no. 7, p. 72004, 2016, doi: 10.1088/1742-6596/753/7/072004.

[111] N. Dimitrov, ‘Comparative analysis of methods for modelling the short-term probability distribution of extreme wind turbine loads’, *Wind Energy*, vol. 19, no. 4, pp. 717–737, 2016, doi: 10.1002/we.1861.

[112] P. Graf, K. Dykes, R. Damiani, J. Jonkman, and P. Veers, ‘Adaptive stratified importance sampling: hybridization of extrapolation and importance sampling Monte Carlo methods for estimation of wind turbine extreme loads’, *Wind Energy Sci.*, vol. 3, pp. 475–487, 2018, doi: 10.5194/wes-3-475-2018.

[113] A. Grami, *Probability, Random Variables, Statistics, and Random Processes: Fundamentals and Applications*. John Wiley & Sons, 2019.

[114] D. Zwick and M. Muskulus, ‘The simulation error caused by input loading variability in offshore wind turbine structural analysis’, *Wind Energy*, vol. 18, no. 8, pp. 1421–1432, 2015, doi: 10.1002/we.1767.

[115] I. B. Løken and A. M. Kaynia, ‘Effect of foundation type and modelling on dynamic response and fatigue of offshore wind turbines’, *Wind Energy*, vol. 22, no. 12, pp. 1667–1683, 2019, doi: 10.1002/we.2394.

[116] E. A. Rendon and L. Manuel, ‘Long-term loads for a monopile-supported offshore wind turbine’, *Wind Energy*, vol. 17, no. 2, pp. 209–223, 2014, doi: 10.1002/we.1569.

[117] E. E. Bachynski, T. Kristiansen, and M. Thys, ‘Experimental and numerical investigations of monopile ringing in irregular finite-depth water waves’, *Appl. Ocean Res.*, vol. 68, pp. 154–170, 2017, doi: 10.1016/j.apor.2017.08.011.

[118] T. Burton, N. Jenkins, D. Sharpe, and E. Bossanyi, *Wind Energy Handbook*, 2nd ed. John Wiley & Sons, 2011.

[119] E. Gaertner *et al.*, ‘IEA Wind TCP Task 37: Definition of the IEA 15-Megawatt Offshore Reference Wind Turbine’, United States, 2020. doi: 10.2172/1603478.

APPENDICES

The scripts employed in the development of this thesis are presented below. Only the main routines are given. However, all the scripts, including the auxiliary files and secondary programs are available in https://github.com/dbarretol/Thesis.

Appendix I: Script used in chapter 2 to create input files for FAST considering variations in wave parameters.

```
#THIS PROGRAM IS FOR HYDRODYN AND FAST INPUT FILES CONSIDERING A SQUARE DOMAIN
#-------------Step 1: Creation of HydroDyn files ---------------------
import os
cwd = os.getcwd()
cwd
os.chdir("./inp_Hydro")
cwd = os.getcwd()
cwd
#====== CHECKING THE NUMBER OF SEA STATES ==================
fileHs="inp_Hs.txt"
fileTp="inp_Tp.txt"
countHs = len(open(fileHs).readlines(  ))
countTp = len(open(fileTp).readlines(  ))
n_SS=int((countHs+countTp)/2)
print("Verificación! #Hs es igual a #Tp?")
if (countHs==countTp):
        print("SI")
else:
        print("NO")

#======== READING OF WAVE HEIGHTS ============================
file = open(fileHs,"r").read()
elementsHs = file.split("\n")
print("--------ALTURAS DE OLA-------")
for i in range(countHs):
        print("Hs[",i,"] =",elementsHs[i],"m")

#======== READING OF WAVE PERIODS =====================
file = open(fileTp,"r").read()
elementsTp = file.split("\n")
print("--------PERIODOS DE OLA-------")
for i in range(countTp):
        print("Tp[",i,"] =",elementsTp[i],"s")
```

```
#========== SUMMARY OF ANALYSED SEA STATES ====================
print("Resumen de Estados de Mar   Hs       Tp")
for i in range(countHs):
       print("Estado de mar ",i,":        ",elementsHs[i],"   ,  ",elementsTp[i])
print("Cant. de alturas:",countHs,"\nCant. de periodos:",countTp,"\nCant. de Estados
de Mar:",n_SS)

#--------- SUPPLEMENTARY TEXT FOR HYDRODYN INPUTS -----------------------
with open("Hydrotxt_1.txt","r") as f:      csup = f.read()
with open("Hydrotxt_2.txt","r") as f:      cinf = f.read()
htext1="   WaveHs         - Significant wave height of incident waves (meters) [used
only when WaveMod=1, 2, or 3]"
htext2="   WaveTp         - Peak-spectral period of incident waves       (sec) [used
only when WaveMod=1 or 2]"

#======DATA FOR VARIATION OF Hs AND Tp=========================
var_coef=[0,1,5,10,15]
var_Qty=len(var_coef)
coef_Hs=list()
coef_Tp=list()
for j in range(var_Qty):
              coef_Hs.append(round(1+var_coef[j]/100,4))
              coef_Tp.append(round(1+var_coef[j]/100,4))
for s in range(n_SS):
       for ih in range(var_Qty):
              for it in range(var_Qty):
                     ah=float(elementsHs[s])
                     bh=float(coef_Hs[ih])
                     tempHs="{0:.3f}".format(ah*bh)
                     at=float(elementsTp[s])
                     bt=float(coef_Tp[it])
                     tempTp="{0:.3f}".format(at*bt)
                                  # Sea State          Coef Var Hs/Tp
                     namehydro="SS"+str(s)+"_Hs"+str("{0:.0f}".format((coef_Hs[ih]-
1)*100))+"_Tp"+str("{0:.0f}".format((coef_Tp[it]-1)*100))+".dat"
                     contenthydro=csup+"\n         "+str(tempHs)+htext1+"\n
"+str(tempTp)+htext2+"\n"+cinf
                     hydrofile=open(namehydro,"w+")
                     hydrofile.write(contenthydro)
              f.close()
os.chdir("../")
cwd=os.getcwd()
```

```
#======== CREATION OF CONTAINER FILE FOR TITLES =================
namefiledat="Out_ListHydroDats.txt"
f=open(namefiledat,"w+")
for file in os.listdir("./inp_Hydro"):
              if file.endswith(".dat"):
                     x=os.path.join(file,"\n")
                     f.write(x)
f.close()

#========= DELETION OF '\' FROM THE FILE NAMES ================
n_lines = len(open(namefiledat).readlines(  ))
file = (open(namefiledat,"r").read())
ListHydroNm = file.split("\n")
real_ListHydroNm=list()
for i in range(n_lines):
       real_ListHydroNm.append((ListHydroNm[i])[:-1])
g=open(namefiledat,"w+")
for k in range(len(real_ListHydroNm)):
       g.write(real_ListHydroNm[k]+"\n")
g.close()

#--------- SUPPLEMENTARY TEXT FOR FAST INPUTS ------------------------
with open("fstext_1.txt","r") as f: csup = f.read()
with open("fstext_2.txt","r") as f: cinf = f.read()
ctext1="    HydroFile       - Name of file containing hydrodynamic input parameters
(quoted string)"

#======= Creation of *.fst files for FAST ===============
for m in range(len(real_ListHydroNm)):
       namefast=(real_ListHydroNm[m])[:-4]+".fst"
       content=csup+"\n"+'"inp_Hydro'+'/'+real_ListHydroNm[m]+'"
'+ctext1+"\n"+cinf
       fastfile=open(namefast,"w+")
       fastfile.write(content)
fastfile.close()
```

Appendix II: Script used in chapter 2 to automate the execution of FAST.

```
#THIS PROGRAM OPENS FAST AND PASSES THE INPUT FILES IN GROUPS
import os
import time
import math
winproc="FAST_Win32.exe"
tmp=os.popen("tasklist").read()

#========= CREATION OF THE COMMANDS TO CALL FAST IN EACH CASE ==========
file=open("Out_ListHydroDats.txt",'r').read()
elements=file.split("\n")
new_elements=list()
for i in range(len(elements)):
	if not elements[i]:
		pass
	else:
		new_elements.append("start cmd.exe /c  FAST_Win32.exe "+(elements[i])[:-
4]+".fst")

#=========================================================================
#     EXECUTING FAST COMMANDS IN
#     'n' GROUP PACKAGES WITH 's' ELEMENTS
#=========================================================================
print("Cuantos casos a la vez quieres correr en FAST?")
s_elements=int(input())
n_group=math.ceil(len(new_elements)/s_elements)
print("Hay un total de ",len(new_elements)," llamados a FAST, si se toman:
",s_elements," por grupo, entonces habrian: ",n_group," grupos")
commands_Fast=list()
for  r in range(n_group):
	commands_Fast.append(" &
".join(new_elements[(r*(s_elements)):((r+1)*(s_elements))]))

#==================== FAST EXECUTION ==============================
c=0
while(c<=n_group):
	if(winproc in tmp):
		print(winproc," sigue activo")
		time.sleep(30)
		tmp=os.popen("tasklist").read()
	else:
		print("FAST inactivo, lanzando grupo:",c)
		os.system(commands_Fast[c])
```

```
                time.sleep(10)
                tmp=os.popen("tasklist").read()
                c=c+1
while(winproc in tmp):
        print(winproc," sigue activo")
        time.sleep(30)
        tmp=os.popen("tasklist").read()
print("FAST terminó satisfactoriamente")
```

Appendix III: Script used in chapter 3 and 4 to generate input files for FAST.

```
#This script generates inputs file with the data
import pandas as pd
from scipy import stats
from datetime import datetime
import os, math
WD_Master=os.getcwd()
currdate=datetime.now().strftime("%d-%m-%Y_%I-%M-%S_%p")

#---------------Fixed Values----------
shear_exp=0.14
H=90
md=8766               # 365.25*24/1hr
au, bu=2.299, 8.92    #Weibull Distr. of u_10m
a1,a2,a3=1.755, 0.184, 1    #aHC=a1+a2*u^a3
b1,b2,b3=0.534,0.07,1.435    #bHC=b1+b2*u^b3
th_et,gamma_exp= -0.477, 1
e1,e2,e3= 5.563, 0.798, 1
f1,f2,f3= 3.5, 3.592, 0.735
k1,k2,k3= 0.05, 0.388, -0.321

#----------------FUNCTIONS---------
def read_data(column):     #To get the data from an excel file
    tmp=pd.read_excel(r'./Data/Data.xlsx',usecols=column)
    tmp1=tmp.dropna()
    n_tmp1=int(tmp1.count())
    outvar=list()
    for i in range(n_tmp1):
        outvar.append(float(tmp1.iloc[i]))
    return outvar
def uten(UHH):   #To convert the Hub-Height Wind Speed to 10m level of reference
    return float(UHH)/(H/10)**shear_exp
def FUW(u):   #To calculate the cumulative distribution value
    return 1-math.exp(-1*(u/bu)**au)
def get_N(u):  #To get the return period of the wind speed
    return 1/((1-FUW(u))*md)
```

```
#-----------------Initial Steps-----------------
Uw=read_data('A')
Seed_Uw=read_data('B')
Seed_Wv=read_data('C')
u=list()
for i in range(len(Uw)):
    u.append(uten(Uw[i]))
N=list()
for j in range(len(u)):
    N.append(get_N(u[j]))
del i,j

#------------Calculation of the most probable sea state----------

#Parameters for Hs
aHC=list()
bHC=list()
for i in range(len(u)):
    aHC.append(a1+a2*(u[i])**a3)
    bHC.append(b1+b2*(u[i])**b3)
Hs=list()
for j in range(len(u)):
    Hs.append(bHC[j]*(math.log(1-0.5)*-1)**(1/aHC[j]))
del i,j

#Parameters for Tp
Tp=list()
for j in range(len(u)):
    vTp_h=k1+k2*math.exp(Hs[j]*k3)
    Tp_h=e1+e2*(Hs[j])**e3
    u_h=f1+f2*(Hs[j])**f3
    mu_Tp=Tp_h*(1+th_et*((u[j]-u_h)/u_h)**gamma_exp)
    sigma_Tp=vTp_h*mu_Tp
    sigma_lnTp=(math.log(vTp_h**2+1))**0.5
    mu_lnTp=math.log(mu_Tp/(1+vTp_h**2)**0.5)
    Tp.append(stats.lognorm(sigma_lnTp,scale=math.exp(mu_lnTp)).ppf(0.5))

#Saving values
os.chdir(WD_Master)
os.chdir('./Data/')
Results_title="Results Joint Probability (shear="+str(shear_exp)+") "+currdate+".txt"
Results_file=open(Results_title,'w+')
Results_file.write("Uw[m/s] \t u[m/s] \t N[-] \t Hs[m] \t Tp[m] \n")
for i in range(len(Uw)):
```

```
txt=str(Uw[i])+'\t'+str("{0:.3f}".format(u[i]))+'\t'+str("{0:.8f}".format(N[i]))+'\t'+st
r("{0:.3f}".format(Hs[i]))+'\t'+str("{0:.3f}".format(Tp[i]))+'\n'
    Results_file.write(txt)
Results_file.close()
del txt, Results_title, sigma_lnTp, mu_lnTp, aHC, bHC,  N
del a1, a2, a3, b1, b2, b3
del j, i, Tp_h, e1, e2, e3, f1, f2, f3, k1, k2, k3, mu_Tp, sigma_Tp
del th_et, u_h, vTp_h, gamma_exp

#--------------Creation of *.inp input files for TurbSim---------------
os.chdir(WD_Master)
os.chdir('./5MW_Baseline/InflowWind/TS')
WD_TS=os.getcwd()
with open('TS1.dbarretol') as f: ts_1=f.read()
with open('TS2.dbarretol') as f: ts_2=f.read()
with open('TS3.dbarretol') as f: ts_3=f.read()
with open('TS4.dbarretol') as f: ts_4=f.read()
var_tstitle=list()
for i in range(len(Seed_Uw)):
    for j in range(len(Uw)):
        TS_title="Uw"+str(j)+"_SeedUw"+str(i)
        var_tstitle.append(TS_title)
        TS_content=ts_1+str(int(Seed_Uw[i]))+ts_2+str(Uw[j])+ts_3+str(shear_exp)+ts_4
        TS_file=open(TS_title+".inp",'w+')
        TS_file.write(TS_content)
        TS_file.close()
del ts_1, ts_2, ts_3, ts_4, TS_title, TS_content, i, j

#-------Creation of *.dat input files for InflowWind----------------
os.chdir(WD_Master)
os.chdir('./5MW_Baseline/InflowWind')
WD_IF=os.getcwd()
with open('IF1.dbarretol') as f: if_1=f.read()
with open('IF2.dbarretol') as f: if_2=f.read()
for i in range(len(var_tstitle)):
    IF_content=if_1+var_tstitle[i]+".bts"+if_2
    IF_file=open(var_tstitle[i]+'.dat','w+')
    IF_file.write(IF_content)
    IF_file.close()
del i, IF_content, if_1, if_2

#-------Creation of *.dat input files for HydroDyn---------------
os.chdir(WD_Master)
os.chdir('./5MW_Baseline/HydroData')
WD_HYD=os.getcwd()
```

```
with open('HD1.dbarretol') as f: hd_1=f.read()
with open('HD2.dbarretol') as f: hd_2=f.read()
with open('HD3.dbarretol') as f: hd_3=f.read()
with open('HD4.dbarretol') as f: hd_4=f.read()
with open('HD5.dbarretol') as f: hd_5=f.read()
with open('HD6.dbarretol') as f: hd_6=f.read()
with open('HD7.dbarretol') as f: hd_7=f.read()
var_hdtitle=list()
for ss in range(len(Uw)):
    for i in range(len(Seed_Wv)):
        hd_title="SS"+str(ss)+"_SeedWv"+str(i)
        var_hdtitle.append(hd_title)
        lowcoff=0.25*(2*math.pi/Tp[ss])
        hicoff=5.1*(2*math.pi/Tp[ss])
        seedwv2=Seed_Wv[i]+10
        hd_cnt1=hd_1+str("{0:.3f}".format(Hs[ss]))+hd_2+str("{0:.3f}".format(Tp[ss]))
        hd_cnt2=hd_3+str("{0:.3f}".format(lowcoff))+hd_4+str("{0:.3f}".format(hicoff))
        hd_cnt3=hd_5+str(int(Seed_Wv[i]))+hd_6+str(int(seedwv2))+hd_7
        HD_file=open(hd_title+".dat",'w+')
        HD_file.write(hd_cnt1+hd_cnt2+hd_cnt3)
        HD_file.close()
del seedwv2, hicoff, lowcoff, i, ss
del hd_1, hd_2, hd_3, hd_4, hd_5, hd_6, hd_7
del hd_cnt1, hd_cnt2, hd_cnt3, hd_title

#----------Creation of *.fst input files for FAST 8----------
os.chdir(WD_Master)
with open('FST1.dbarretol') as f: fst_1=f.read()
with open('FST1_d.dbarretol') as f: fst_1d=f.read()
with open('FST2.dbarretol') as f: fst_2=f.read()
with open('FST3.dbarretol') as f: fst_3=f.read()
for k in range(len(Uw)):
    if(Uw[k]>=19):
        edyn='pitch20'
    else:
        if(Uw[k]>=13):
            edyn='pitch10'
        else:edyn='pitch0'

    for i in range(len(Seed_Uw)):
        for j in range(len(Seed_Wv)):
            iftxt="Uw"+str(k)+"_SeedUw"+str(i)+".dat"
            hdtxt="SS"+str(k)+"_SeedWv"+str(j)+".dat"
            fst_title="EC"+str(k)+"_SeedUw"+str(i)+"_SeedWv"+str(j)+".fst"
            fst_content=fst_1+edyn+fst_1d+iftxt+fst_2+hdtxt+fst_3
```

```
            fst_file=open(fst_title,'w+')
            fst_file.write(fst_content)
            fst_file.close()
del fst_1, fst_2, fst_3, fst_content, fst_title, hdtxt, iftxt
```